東京大学大学院新領域創成科学研究科
複雑理工学専攻

令和 2 年度

修士論文

Development of a VHF receiver for earth observation data broadcast

2020 年 9 月 02 日提出

指導教員　吉川　一朗　教授

張　天旭

Abstract

Since the first technical "earth observation" carried out by Sputnik-1 on earth's ionosphere, numbers of EOS (earth observation satellites) have been utilized to conduct comprehensive observation of earth on multiple aspects. Amongst them, several series of polar orbiting meteorological satellites were launched to provide continuous observation data of earth's surface with moderate resolution. Compared to geosynchronous meteorological satellites, those satellites' with polar orbit could provide many forms of local meteorological data with higher resolution, thus more detailed and localized earth observation data could be acquired from receiving those satellites' broadcast. NOAA-POES series satellite, is a series of polar orbiting meteorological satellite operated by National Oceanic and Atmospheric Administration (NOAA) with a suite of observation equipment onboard. Automatic Picture Transmission as one of many downlink broadcasted by NOAA satellites with FM-AM modulation could be demodulated and frame retrieved with relatively simple procedure due to analog modulation adopted. Thus APT signal has a substantially lower hurdle for public users to receive compared to other signal with digital modulation. Usually NOAA satellites are launched in a tandem manner for continuous operation. However, with the termination of NOAA-POES program on NOAA-19(N') satellite and surprisingly long surviving predecessors, 3 satellites are operating simultaneously on orbit which is a rare occasion. With the easy to receive APT signal broadcasted by NOAA satellites, publics receiving earth observation data of 3 satellites continuously in orbit became possible.

In order to provide simple yet functioning design of APT receiver for public, the work of this thesis is dedicated to design a simple FM demodulating front-end for receiving APT signal broadcasted in VHF band. The receiver is designed with certain compatibility to a usual FM receiver, but several critical changes were made to ensure its performance under weak satellite broadcasted signal and narrow bandwidth.

In this thesis, chapter 1 and 2 are dedicated for background information about APT signal and several sets of information including modulation and frame format of retrieved data. The received signal strength under certain relative positioning of satellite is derived in Chapter3, while Chapter 4 is used to discuss several important design feature in detail. Finally, the performance of oscillation circuit and receiver itself are evaluated in Chapter 5 from perspective of frequency domain, and result of frame retrieval were also reviewed on several trials.

Keywords: NOAA satellites, VHF satellite receiver, Analog circuit design.

Contents

Chapter 1: Preface

Since the successful launch and operation of Tiros-1(Television and Infrared Observation Satellite) in 1960, earth observation satellite has been used intensively in multiple purposes. While various satellite embedded with payloads designed to observe the earth in different aspects (Imagery under different wavelength, Microwave sounding, Synthetic Array Radar etc.), the data collected and transferred is extremely valuable in metrological purposes. The observation itself and following analysis assuredly produces numbers of valuable data, however, the receiving of transmission data itself could be more vital part of whole "Chain" of earth-observation satellite system. In this chapter, a brief introduction of earth observation satellites, and meteorological data currently distributed from those satellites are provided. Then, the introduction of a series of satellites operated by National Oceanic and Atmospheric Administration (NOAA), NOAA-series satellites is introduced. Automatic Picture Transmission (APT), a downlink method adopted by NOAA series satellite is also introduced

1.1: Background of Earth observation satellites and broadcasted signals

Earth observation carried by satellite could be dated back to Sputnik-1 (Kznetsov et al, 2015), where its radiowave emission is monitored for ionosphere observation. Today, earth observation is one of the most common operations carried by both low earth orbit satellites and geostationary satellites. Observation methods are also much more variant compared to pioneers in early ages, including imagery under multiple wavelengths, microwave sounding. In fact, major earth observation satellites represented by TIROS series carry a suite of sensing and communication devices, to provide an immensely wide range of remote sensing with multiple coverage options. To give an instance, sensors/modules onboard a TIROS-N series satellite (Figure 1.1) is listed in Table 1.1. For sensor arrangement refer Figure 2.15a.

Figure1.1: Image of a TIROS-N series weather satellite (Satnews, 2009)

TIROS-N	
Instrument	Description
AMSU	Advanced Microwave Sounding Unit
AVHRR	Advanced Very High Resolution Radiometer
ESA	Earth Sensor Assembly
HRIS	High Resolution Infrared Radiation Sounder
MEPED	Medium Energy Proton/Electron Detector
MHS	Microwave Humidity Sounder
SBUV	Solar Backscatter Ultraviolet Radiometer
TED	Total Energy Detector

Table1.1 Remote sensing instruments onboard TIROS-N satellite (Schwalb, 1978)

Major Polar Orbit Meteorological Satellites		
Satellite	Frequency（MHz）	Modulation
Landsat-8	8200.5	OQPSK
JPSS-1（NOAA20）	7812(HRD)	QPSK
EOS-N (TERRA, AQUA)	8212.5	OQPSK
TIROS-N（NOAA-N）	1698~1707(HRPT)	BPSK
	137.1~137.9(APT)	FM-AM
SUOMI NPP	7812（HRD）	OQPSK
	8212.5（SMD）	
FY-3 Series	8145.95~8175(DPT)	QPSK
	7775~7780(MPT)	QPSK
Elektro-L N	7500(RDAS)	QPSK
Meteor-M N2	8128(HRIT/LRIT/MLTP)	BPSK
	137.1 (LRPT)	QPSK
Meteor-M N2-2	(137.1)Disabled	(OQPSK)Disabled
Sentinel-2	8260	8PSK

Table 1.2: Meteorological Satellite currently broadcasting observed data, frequency and modulation

In order to retrieve observed earth data, different methods of downlink communication into ground station has been adopted. In particular, weather satellite tasked to transmit local observed or stored data into receiving end as soon as possible. From the TV transmission of magnetic tape stored data (recorded by Vid-con) in Tiros-1, the method of data downlink has evolved into a multiple-layer service of different quality data in recent satellites such as EOS series (Terra，Aqua,) and METOP series satellites. Currently transmitted LEO weather/earth observation satellite broadcasts that could be received and decoded with published method are listed in Table 1.2. It is obvious that most of observation result downlink is transmitted in various bands with multiple modulation method. While most of which are digital modulated and transmitted with carrier frequency up to 9 GHz, several downlink has remained on a relatively lower band around 130MHz. Those transmissions are, to some extent, reminiscent of earlier age attempt of transmitting observation data. One major representative is NOAA series satellite emitted APT (Automatic Picture Transmission) service.

1.2: NOAA satellites and APT signal

NOAA series satellites are operated by the National Oceanic and Atmospheric Administration of United States as the major line-up of polar orbiting meteorological satellite. Over the operation years of NOAA satellites this series provided a very extensive library of earth observation data including vegetation monitoring, sea ice monitoring and biomass burning data.

A brief timeline of NOAA operated polar orbiting meteorological satellites and major milestones are summarized in Figure 1.2. The operation of NOAA satellites date back to the launch of Improved-TIROS (ITOS) satellite as NOAA-1 (ITOS-B) where expanded amount of observation equipment were carried compare to its predecessor. The basic scheme on “suite” of equipment onboard current NOAA satellites, already shown in Table 1.1, was established with the operation of TIROS-N and NOAA-6. Currently operational satellites, NOAA-15, NOAA-18 and NOAA-19 belongs to the group starting from NOAA-15 (NOAA-KLM series), with advanced version of observation equipment such as AVHRR/3 is equipped.

Usually, NOAA-series satellites, starting from TIROS-N were launched and operated in a serial manner, unlike other satellites that are usually demanded to form constellation. Thus usually no more than 3 NOAA satellites are active at a given time point. However,

during the history of NOAA-series satellites there were several period of time that multiple satellites were in operation status, thanks to earlier launched satellites surviving an excessive amount of years beyond designed life. Detailed operational lifetime of each satellites after TIROS-N and NOAA-6 are covered in Figure 1.3. (NOAA, 2008). The figure comes from a pre-launch report of NOAA-19 thus the operation after year 2008 is not included.

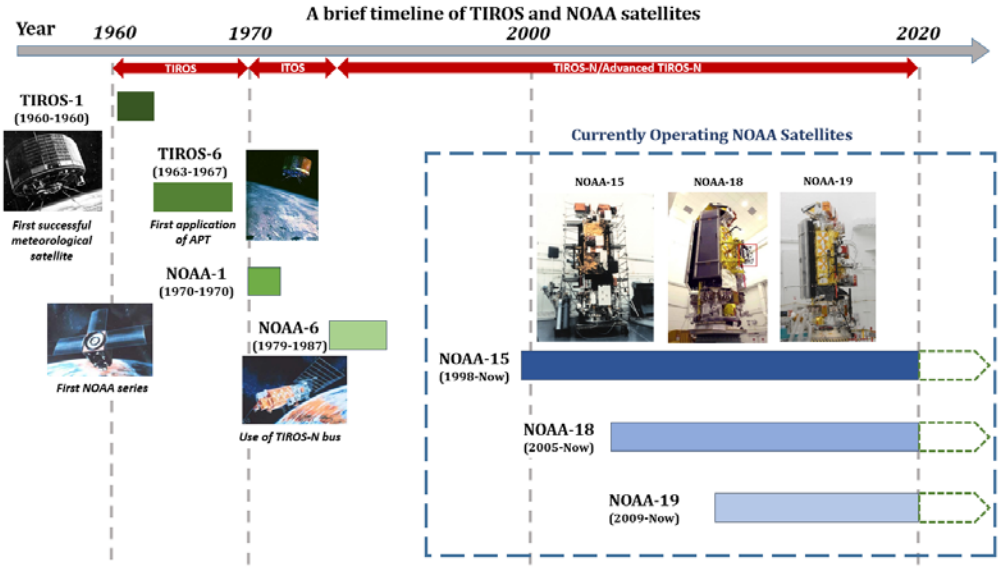

Figure 1.2: A brief history of TIROS series meteorological satellites and currently operating NOAA satellites.

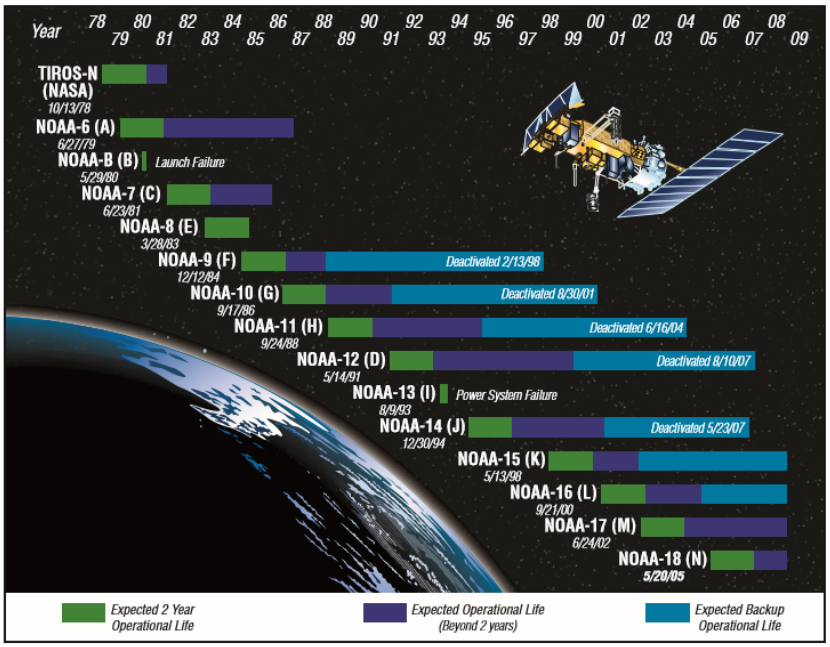

Figure1.3: Operational and extended period of NOAA (TIROS-N) satellites until NOAA-18 (NOAA, 2008)

During most of the operational time of NOAA-14, more than 3 satellites were operational simultaneously. However, after the launch of NOAA-18, maximum of 5 satellites were operational before decommission of NOAA-16 and NOAA-17. Currently, only three satellites, NOAA-15, NOAA-18 and NOAA-19 are operational and broadcasting downlink signal, and the end of NOAA-POES program indicates that no more following satellite will be launched with ability to broadcast downlink signal. In fact NOAA-20 which is operated under JPSS program omitted broadcasting capabilities of currently available downlink before.

Type of Service	Description	Downlink Frequency	Modulation
HRPT (High Resolution Picture Transmission)	Full resolution AVHRR & TIP data, available in a format defined by the ground receiving station.	1698 or 1707MHz	Split Phase PSK (Phase-shift Keying)
APT (Automatic Picture Transmission)	Reduced resolution geometrically corrected analog video from two channel of AVHRR, selected by command.	137.10 MHz (NOAA-19)	FM-256 bit AM
DSB (Direct Sounder Broadcasting)	A VHF beacon to users who don't have S-band reception. Data content: HIRS, SEM, DCS, SBUV	137.50 or 137.62MHz	67deg PSK
CDA (Command Centre Data Acquisition)	Global and Local data (GAC and LAC)	2247.5MHz	PSK

Table1.3: Downlink service broadcasted from currently operating NOAA satellites, their description and characteristics

Among four major downlink service transmitted from currently operating NOAA satellites, Listed in Table 1.3, Automatic Picture Transmission (APT) is the most accessible service due to its simple structure.

Automatic Picture Transmission was first adopted in TIROS-VIII weather satellite (Figure 1.4) as a way of broadcasting real-time scanned image in order to provide local weather information for a given ground station. APT employed a FM-AM double modulation scheme with VHF FM and 2.4 KHz AM subcarrier, which was considered an advanced technique at the time, compared to Analog TV signal beforehand. Before the APT all downlink from TIROS satellite were consisted of magnetic tape recorded video image captured as shown in Figure 1.5. As a fresh experiment of remote sensing downlink the APT was a great success in TIROS-VIII and kept as a default signal transmission method till NOAA-19. Detailed information of APT signal will be discussed in Chapter 2.

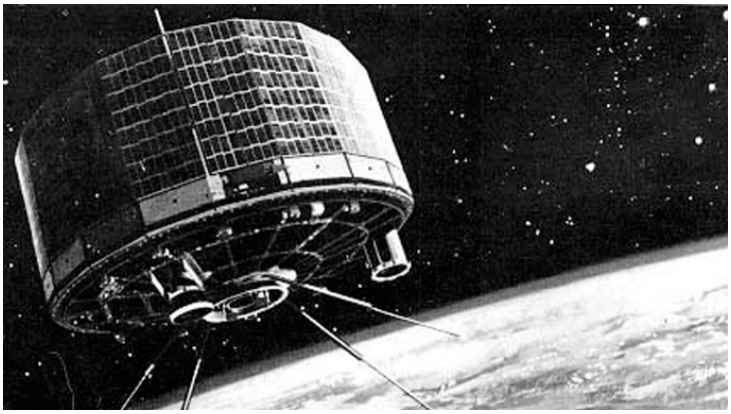

Figure 1.4: Rendered image of a TIROS Satellite (NOAA, 2020)

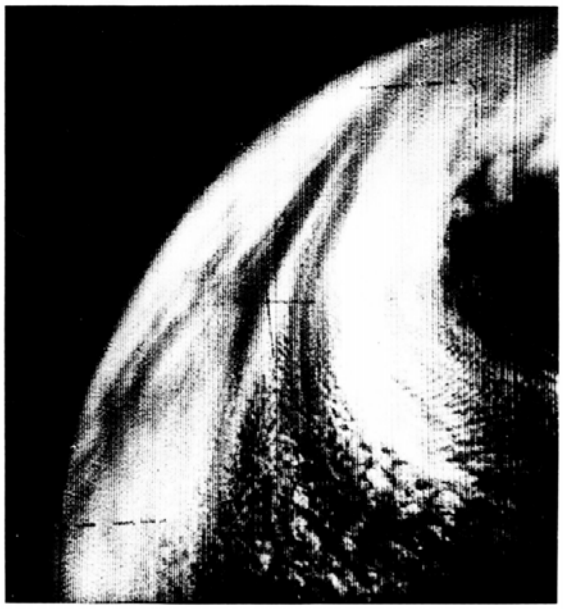

Figure 1.5: Television image of a cyclone captured by Tiros-1 satellite during year 1960. (NOAA, 2020)

With the introduction of NOAA-KLM series satellite and adoption of AVHHR/3 (Advanced Very High Resolution Radiometer, shown in Figure 1.6), APT transmission system started to provide a reduced resolution set of image taken from the AVHRR/3. As it will be discussed in Chapter 2, any two of the AVHRR channels can be chosen by ground command for processing and ultimate output to the APT transmitter. Usually one visible channel is used to provide visible APT imagery during daylight, and one IR channel is used constantly. During the (local) night time, a second IR channel is schedule to replace the visible channel for continuous observation (Robert, 2014)

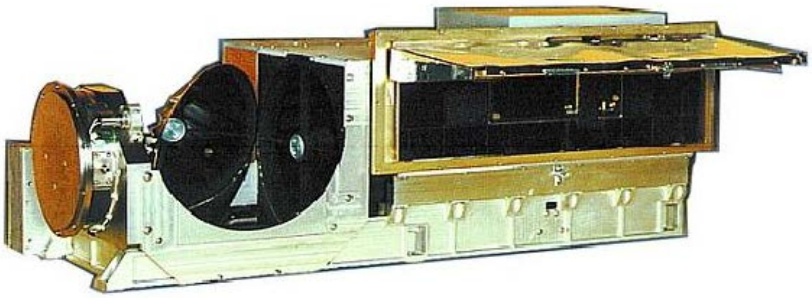

Figure 1.6: Image of AVHRR/3 Radiometer onboard NOAA-15(K) and thereafter (NASA, NOAA 2009)

Before the launch of TIROS-N (NOAA) satellite and adoption of digital communication the APT served as the major method of transmitting local earth image data. As shown in Figure 1.7 receiving APT signal required a substantial amount of instrument and infrastructure, basically isolated from public access. However, after the adoption of HRPT as a main method of providing local earth-observation data and development of receiving devices, APT became the choice for ground stations without sufficient tracking device or high rate digital demodulation/decoding equipment, when trying to obtain earth observation or meteorological data.

With the development of computer technology, analog-to-digital sampling and digital signal processing, the AM subcarrier of APT signal was able to be sampled by PC soundcard for further frame reconstruction. This mean that, given a working VHF FM receiver and a sufficient post processing of subcarrier, theoretically, any user could use their own PC to receive and decode the earth observation data broadcasted from currently operating NOAA satellites. Which is one of the purposes of the work involved in this thesis.

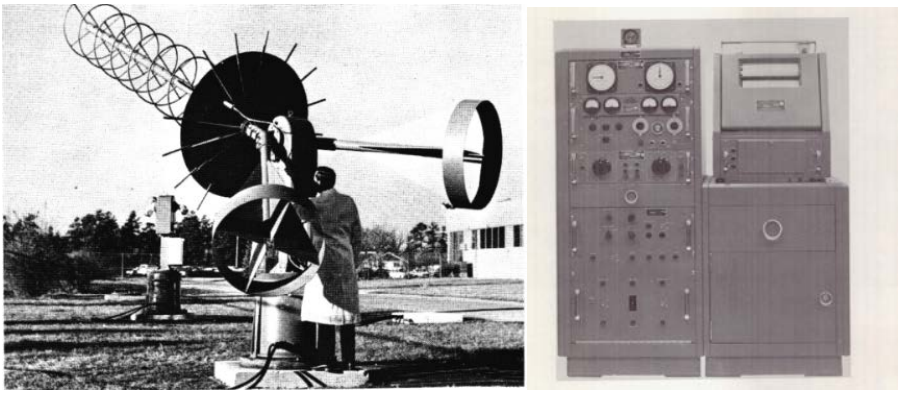

Figure1.7: Helix antenna and decoder for Automatic Picture Transmission system (NASA Facts B-2-64, 1964)

With the development of several software decoder of APT signal including GNU-Radio (especially the development of several software defined radio interface), the frame reconstruction methods finally became available to public users during the last decades.

With regard to the fact that 3 satellites are surviving and broadcasting APT signal simultaneously and the number is only destined to decline, it is sufficient to conclude that now is the last window for constructing a functioning and available APT signal receiver system for public users.

1.3: Purpose of this thesis

The local broadcasting nature of APT signal means that the down-sampled AVHRR data are disposed immediately after the acquisition, thus a vast amount of local earth observation data broadcasted by APT are unavailable if no receivers are active in that area. Distributing the APT receiver could construct a larger receiving base for APT signal, especially for region without access to stored data downlink from NOAA, could lead to a larger collection of earth observation data, which could have been disposed without being retrieved.

Based on the current status of NOAA satellites, a relatively easily constructible design of APT receiver is proposed in order to accomplish the basic proposal of building a larger data collection for APT downlink. The work involved in this thesis is primarily the design a FM front-end receiver with sufficient performance demodulating the FM part of APT signal, and performance evaluation based on manufactured prototype. For the demodulation of AM part, either functioning freeware or GNU radio block created by author could be used, thus AM demodulation and frame reconstruction is not of main focus. As for the derivable, a narrowband FM (NFM) receiver sophisticated to receive VHF signal, based on common design of FM radio receiver, is designed and prototypes were manufactured for evaluation test.

This thesis is written as a part of the documentation summarizing the related property of APT signal, overall satellite telecommunication (telemetry in this case, for we're not transmitting anything into the satellite), design detail of APT receiver and its performance evaluation process including receiving actual APT signal.

Chapter 2 describes the overall property of NOAA-APT signal as a VHF broadcast radiowave. Properties including the band (frequency and related), polarization,

modulation and its subcarrier were introduced and discussed.
In chapter 3, further characteristic of NOAA APT signal is introduced and discussed in detail. APT's frame structure including the telemetry and video image itself is explained as for any satellite downlink signal. Then, as a part of receiver design and evaluation the link budget calculation is done under several assumptions, with a result of evaluated margin of receiving FM signals from NOAA satellites. The antenna used in receiving this signal (as a part of application) is also specified to be a convenient omnidirectional QFH antenna.

Chapter 4 discusses detailed design of FM receiver based on drawn circuit diagram. Principle of several basic components consisting a superheterodyne FM receiverare described in detail. Including: Crystal oscillator, upconverter and overall LO, superheterodyne mixer, ceramic IF filter, and FM demodulation IC.

Process and result of several performance measurement of a completed APT receiver prototype were written in Chapter 5. Frequency measurement with spectrum analyzer of: Local Oscillator, RF amplifier, 1st Mixer, IF filter were discussed with corresponding results.

Chapter 2: APT Signal Characteristics

As it is described in the previous introduction on NOAA APT and its radio-wise characteristics, it is obvious that the receiver has the mast basic requirement as a Very-High-Frequency (VHF) Narrow FM receiver. Likewise, explanation of the NOAA APT transmission itself and related design-details of the receiver is given as part of the technical documentation.

2.1: Basic properties of APT signal

The information of APT signal is provided in table 2.1. The following section will explain the properties introduced in the table

Satellite	NOAA-15	NOAA-18	NOAA-19
Carrier Frequency	137.62MHz	137.1MHz	137.9125MHz
Modulation Type	AM(sub)/FM(Car)	*	*
Power	5Watts EIRP	*	*
Polarization	RHCP	*	*
Bandwidth	45KHz	*	*

Table 1.1: Basic information of NOAA15, 18, 19 APT signal.

In NOAA POES satellite family after NOAA-15, NOAA-16 and 17 disabled all transmission and are decommissioned in early 2010s. NOAA-20 (JPSS-1) and SUOMI-NPP (Another satellite of JPSS) does not carry either AVHRR or APT broadcasting capability on board.

2.1.1Band

As it is shown in Table 2.1 NOAA series satellite transmits the APT signal with the carrier frequency of around 137 MHz, 2.8 meters in wavelength. This frequency of 137MHz belongs to the region of radio-wave. Under the allocated band system it falls into the VHF region, which, by definition, covers the frequency range of 30~300MHz (IEEE, 1984). Figure 2.1 illustrates the position of VHF in wireless-bands under IEEE radar band nomenclature and the position of APT signal in VHF band.

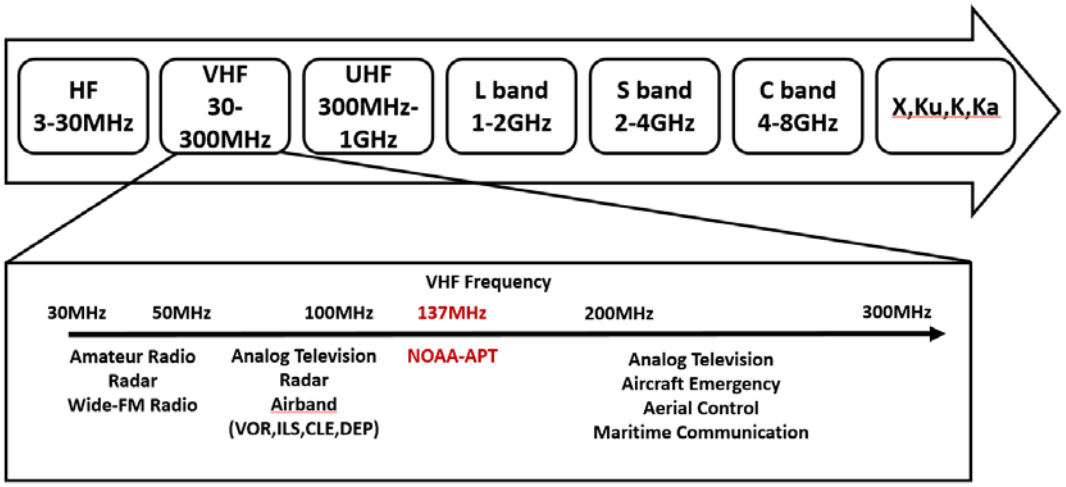

Figure 2.1: Position of VHF band in wireless frequency and position of APT signal in VHF

For additional explanation, the L, S, C and following band stands for the wireless frequencies above 1GHz. Those higher frequency band is mainly used in Mobile Communication, Tracking, Meteorology Radar and Satellite Telecommunication.

For the VHF frequency, due to its characteristics the band is usually used in important infrastructure communications. The VOR, ILS, CLE and DEP stands for VHF Omnidirectional Ranging, Instrumental Landing System, Clearance and Departure in avionics navigation and communication. The DEP communication usually use 120~130MHz band which is relatively close to the APT signal, but with different modulation.

It could be seen in the figure that the APT frequency is located in a rather lower side of the spectrum, due to the fact that the VHF-band is one of the earliest frequencies utilized to conduct actual telecommunication, and APT itself started its first broadcasting in mid-1960s. For the VHF band, multiple type of antenna could be used to receive the electromagnetic wave efficiently assuming the antenna itself is matched to certain frequency. In practice the 137MHz VHF band APT signal is emitted through the VRA antenna onboard NOAA satellite, with a sufficiently high power of 5 watt. Thus no parabolic reflector aperture or feed-horn with satellite tracking system is needed for receiving the 137MHz APT signal. In this project, OFH (Quad-filler helix) antenna is used for receiving the signal due to the polarization of transmitted signal. Detailed description on satellite telecommunication line budget and QFH antenna would be given in Chapter 3.

2.1.2 Polarization:

The polarization is one of the basic characteristics of electro-magnetic wave. Naturally it is also an important characteristic of the communication link to consider when trying to receive any telecommunication signal. Figure 2.2 shows different polarization of radio wave.

There are two major set of polarization in electromagnetic wave (here we're mostly talking about radio wave, with larger wavelength), linear polarization and circular polarization,

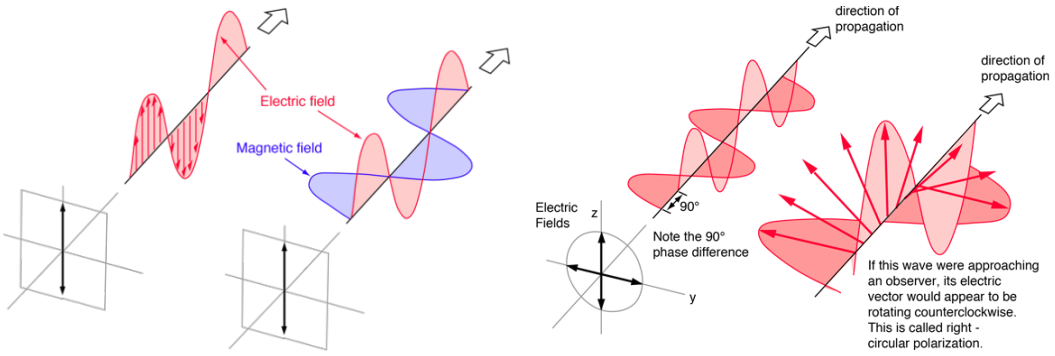

Figure 2.2: Linear polarization and circular polarization of electromagnetic wave (R.nave, 2019)

In Radio wave with linear polarization, the oscillation of E-field is always lined up in a particular plane. Where in Circular polarization the E-field rotates in a particular direction, drawing a circle in the propagation plane (yz plane in Figure 2.2). The polarization of a particular signal is determined by its feeding system and antenna. For lower frequency transmitting antenna the polarization is determined by the antenna shape, where in higher frequency (1GHz~) polarization is determined by the waveguide.

In ground-to-ground usage of radio wave (broadcasting, etc.), linear polarization is usually applied due to the simplified structure of antennae and feed-horn. However, in satellite telecommunications due to the self-spin and excessive relative speed between satellite and ground station, the polarization plane and signal strength could vary drastically under linear polarization, leading to negative effects. In practice, circular polarization predominates most of the satellite telecommunication band due reduced effects in problems caused by satellite spin and relative motion with ground station. In the case of NOAA satellite circular polarization is also used in all signals. NOAA emits APT signal in RHCP which stands for Right Handed Circular Polarization, where the E-

plane rotates clockwise relative to the transmitter. That being said, a decent number of smaller satellite launched recently still utilize linear polarization antenna in certain bands because those adverse effects described above are relative latescent, while geometries are favorable.

As an example, Hodoyoshi-1 (figure 1.3 shows the Nadir-facing panel of Hodoyoshi-1), a Micro-satellite (50Kg level) manufactured by University of Tokyo. There the X-band downlink antenna is a LHCP iso-flux antenna that transmits the earth-observation data at 10Mbit/s speed. 4 UHF telemetry downlink antenna and one command uplink receiving antenna is obviously linear-polarization dipole antenna. The data transmitted from the X-band antenna is currently received by the X-band parabola antenna in Kashiwa-campus. (Kouyama et.al, 2019)

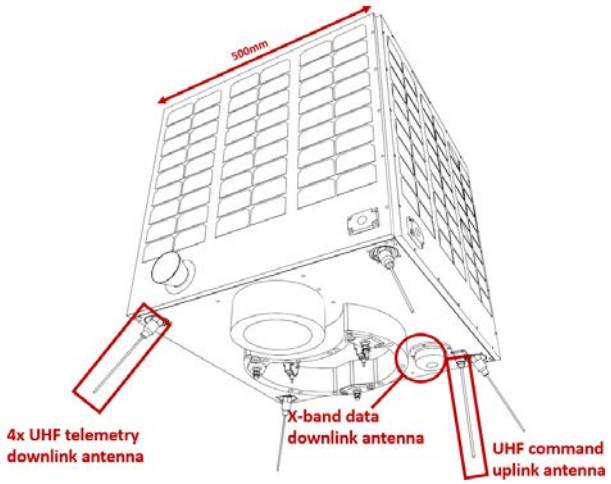

Figure 2.3: Nadir-side panel of Hodoyoshi-1 satellite (Nakasuka, 2012)

2.1.3 Intermediate frequency and subcarrier

Another important thing to mention in this section is the use of intermediate-frequency (IF) and subcarrier.

Intermediate Frequency:

By definition, the intermediate frequency (IF) is a frequency in which carrier frequency is shifted as an intermediate step in transmitting and reception. Its major use sits in telecommunications with frequencies higher than HF (High Frequency, refer to Figure 2.1) for several reasons

One significant reason is that the demodulation/sampling device simply could not directly handle the arbitrarily infinite numbers of carrier wave frequency. Namely it is

impossible for sampling/processing device to directly tune themselves into a specific (GHz level) frequency, let alone having an agile tuning range while doing so.

Suppose there are two C-band communication with arbitrarily selected frequencies (6109MHz and 6003MHz) to be received. Nyquist sampling theorem indicates that sampling frequency higher than 12GHz is required in order to completely sample the wave. This is simply impossible for current ADC could only operate up to megahertz of clock frequency. And trying to directly tune the sampling frequency into those carrier frequencies, 12418MHz and 12006MHz in this case, is out of context based on current technologies. Thus the receiver used in telecommunication are mostly not designed to process (sample, demodulate) the carrier frequency from the beginning, but a series of mixers (or down-converters) are designed inside so that the final frequency is a selected value that is sufficiently low for sampling/processing.

Another reason is that the frequency higher than UHF band usually gets depleted (attenuated in technical term) severely in commonly used transmission line in receiving end (i.e Coax cable), thus a series of bulky waveguide is required to relay the signal form the antenna. Which means that the received signal gets extensively attenuated if trying to relay all the way into receiver itself. In order to avoid those problem, received carrier frequency is often downconverted into a lower IF near antenna in order to transmit the signal without much attenuation into processing units indoor.

The ground station receiving the Hodoyoshi-1 is taken as an example here. From Figure 2.4 it could be seen that the 8.8GHz X-band signal is down-converted into 2GHz right after receiving. Then the 2GHz signal is transmitted indoor for another stage of down-converter where it is converted into 720MHz, at which sampling and demodulation of signal could be done sufficiently. Two local oscillator frequency f1 and f2 is around 6.8GHz and 1280MHz respectively. The down-converting itself is performed through a mixer process of analog superheterodyne.

In the case of NOAA-APT receiver designed in this thesis, the intermediate frequency is selected so that common designs and parts could be employed. In order to utilize mainstream FM radio equipment, the 1st IF of 10.7MHz and 2nd IF of 455 KHz is selected. The downconvertion from 137MHz to 455 KHz is also performed through a set of superheterydyne mixers .Detailed design feature will be provided in Chapter 4.

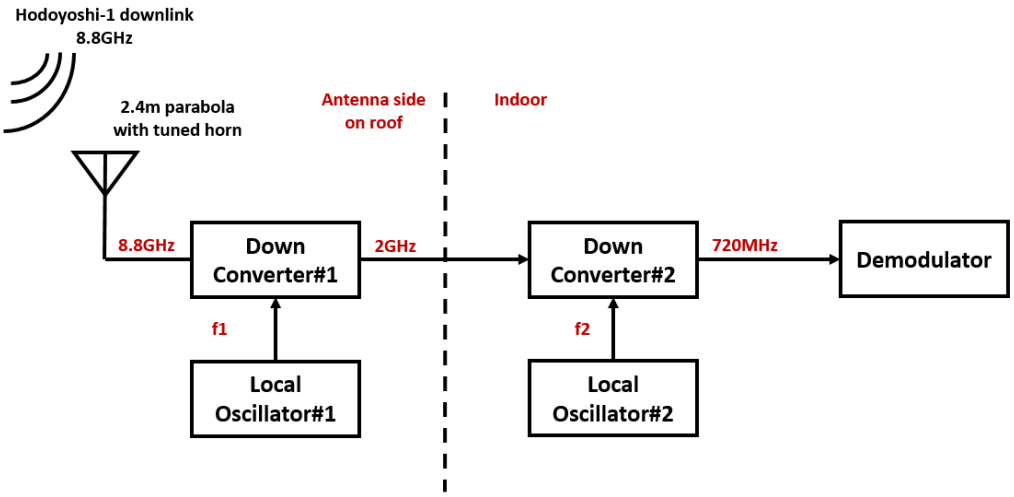

Figure 2.4: simple diagram of Kashiwa-ground station receiving Hodoyoshi-1 satellite

Subcarrier:

Different to the intermediate-frequency the subcarrier in this case stands for sidebands of a carrier radio-wave. In the case of radio broadcasting using amplitude modulation, the subcarrier simply stands for the audio frequency sound modulated into the carrier wave. In amplitude modulation, two identical baseband envelope form two sidebands (Upper sideband and Lower Sideband) and each sideband symmetrically placed around carrier frequency stand for the subcarrier. In the case of NOAA APT signal, the subcarrier is the AM-modulated 2400Hz audio-frequency signal which is the source of characteristic "Beep". It is also the designed output of this designed analog receiver, detail is given in the Chapter 4.

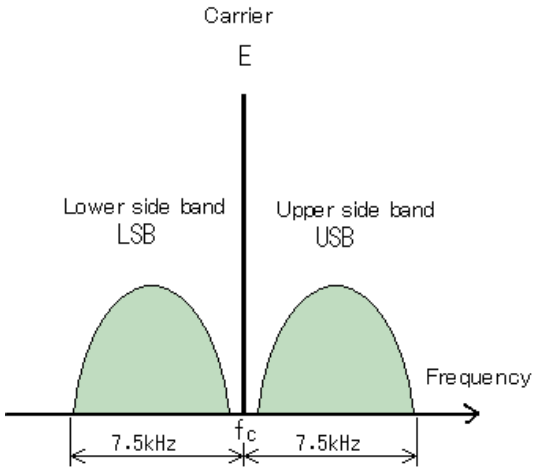

Figure 2.5 the frequency-power plot of a received AM modulated signal with 15 KHz bandwidth. The bulge on each side of carrier frequency E will vary in actual received signal. (Asnatro.net 2019)

2.1.4: Modulation

Modulation is a basic treatment on radio-wave when transferring information is considered. In telecommunication it is defined as “process of varying one or multiple properties of a periodic waveform (carrier wave) with a modulating signal that contain the information to be transmitted”. Which is, combining the base-band signal frequency and a certain frequency of carrier wave in order to transmit intended information through that carrier frequency. After the receiving of transmitted signal, corresponding demodulation process is required to retrieve the intended information. Also the modulation could be conducted in multiple layers depending on the specific usage.

In the case of NOAA-APT signal, two layers of modulation is conducted onto the image/telemetry frame information. The first layer of modulation is a 256-level AM which encodes information into 256 different amplitudes of the subcarrier wave. With 256-levels one could denote that this modulation is intended to transfer 8-bit data, which is also the data format of APT frame. Here the frame data itself is encoded into 2400Hz audio frequency signal, which is the “Subcarrier” discussed in previous chapter. Detail on AM modulation and frame-structure is discussed on Chapter 2.2.

The next layer of modulation is the Frequency-modulation (FM) which encodes the 2400Hz subcarrier into the transmitted 137MHz VHF radio wave. The transmitted signal takes up 34 KHz of bandwidth, which categorizes as NFM transmission. Figure 2.6 illustrates the frequency domain waterfall diagram of NOAA-15 APT transmission signal received on SDR (software defined radio) the central carrier frequency and FM sideband could be observed. Note that the center of spectrum is slightly different from designated transmission frequency of NOAA-15, which is 137.62MHz. This varying frequency difference is caused by the Doppler shift caused by the relative speed between satellite and ground station (Receiver).

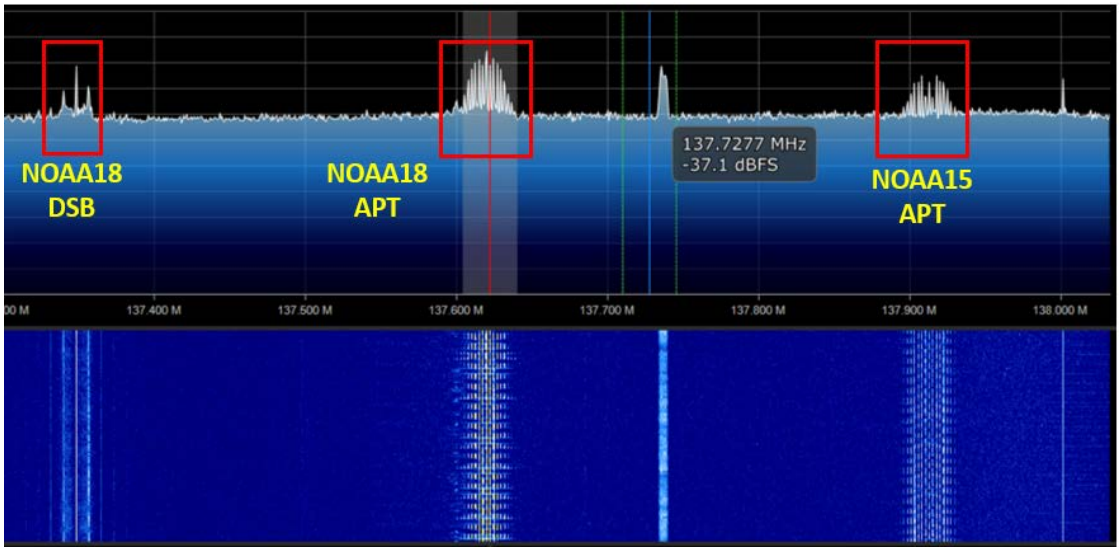

Figure 2.6: The frequency domain FFT plot and waterfall showing three signals captured by SDR (plotted on SDR# software). The DSB beacon, APT of NOAA-18 and APT of NOAA-15 could be seen.

Based on the 2-layer modulation structure of transmitted APT signal, the required demodulation format is also clear. Which is, first receiving and demodulating the 137MHz NFM transmission into 2400Hz subcarrier, and then demodulating the AM modulated subcarrier to obtain the information, as illustrated in figure 2.7. In this project the AM modulated subcarrier is designed to be outputted by the receiver and further sampled/handled in computer software. Thus the receiver is only designed to satisfy operation in the red frame of Figure 2.7. As it is mentioned in the purpose of this receiver, handling of subcarrier and retrieving of image data are not included in the design of this FM receiver.

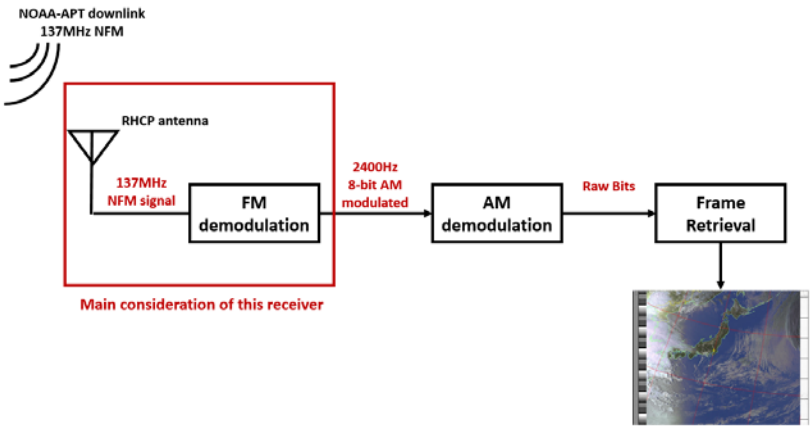

Figure 2.7: Simple diagram of required APT demodulation process.

2.2 Frame format of subcarrier retrieved image

In this section the frame-format of data demodulated from 2400Hz subcarrier, and the format of image itself is explained. As it is mentioned several times above the receiver only demodulates 137MHz NFM carrier and output subcarrier signal. Thus in practice the subcarrier is inputted into computer through soundcard and further processed.

The word "Frame" here stands for certain packet of data transmitted, that includes synchronization features (usually a serial of bits) for indicating the start/end of payload transmission. To provide an indication on relative position of "Frame" in typical wireless communication, an example from CCSDS layer standard is given in Figure 2.8 (Cola and Tomaso, 2010, P57). There the frame is positioned as a unit of synchronization and channel coding sub-layer which is at a lower level in the whole structure. Usually it is the product after demodulation and decoding of error-correction code.

In the case of NOAA-APT, based on its nature of one-way transmission with constant transmitting frequency, the relationship is much simpler than that of CCSDS, where the frame format directly corresponds to the retrieved image. Figure 2.9 (NOAA, 2019) shows a full frame of APT transmission, and Figure 2.10 is the line format of a single video scan line in APT frame.

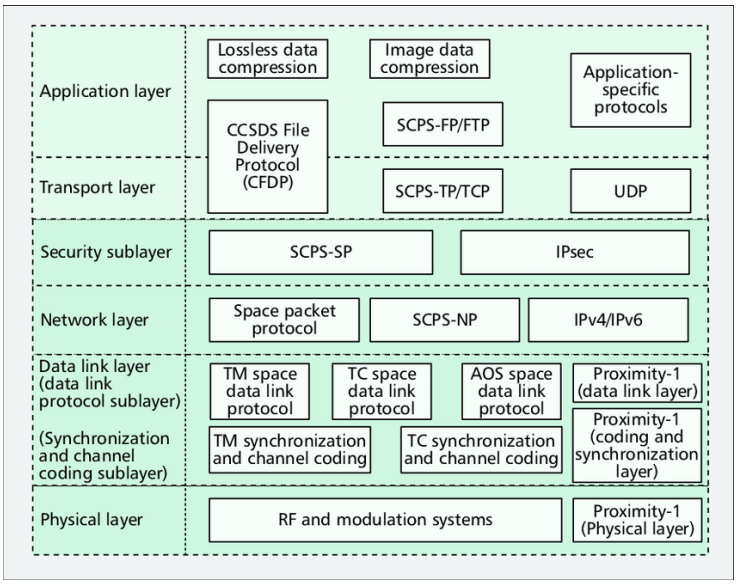

Figure 2.8: CCSDS protocol layer structure in satellite communication. In Data link layer, TM (Telemetry) and TC (Tele command) stands for downlink and uplink respectively. (Cola.T et al. 2019)

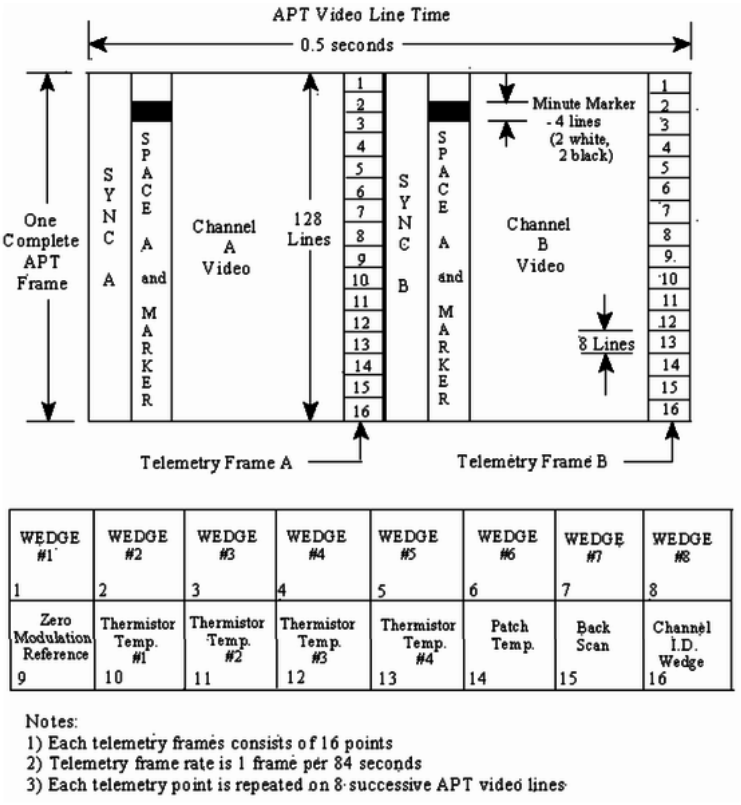

Figure2.9: Full format of one APT transmission frame (NOAA, 2019).

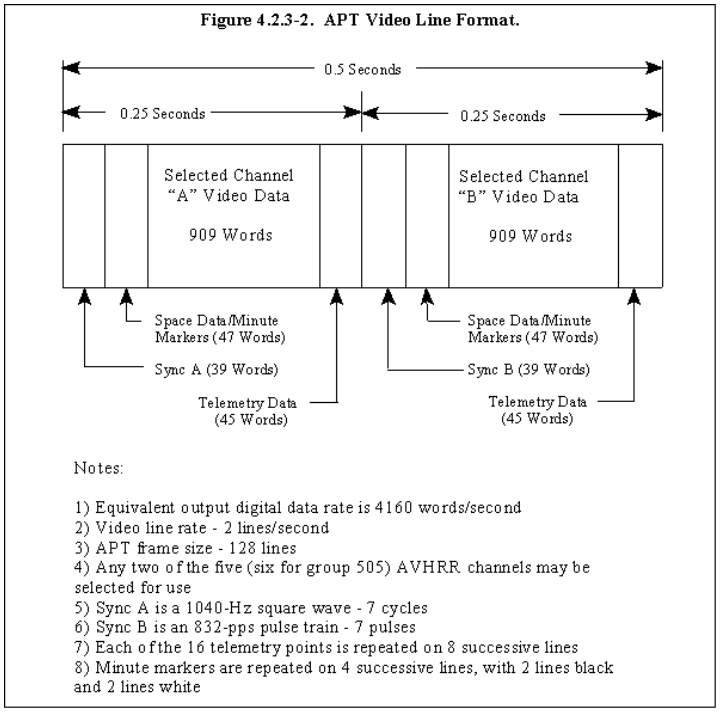

Figure2.10: Format of a full video scan line including Sync, Channel A/B image and telemetry (NOAA,2019)

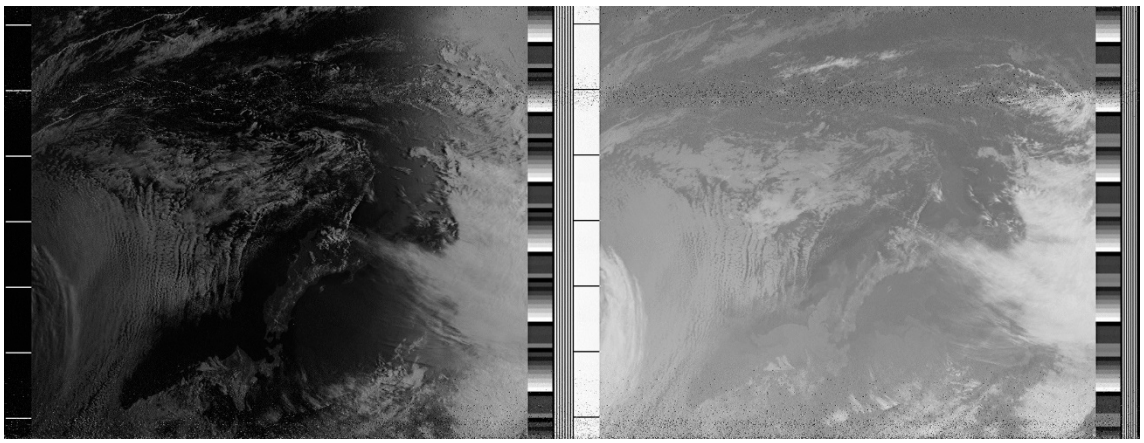

Figure 2.11 retrieved image from NOAA-APT signal. Retrieved in an evening path with 89 deg peak elevation showing cloud near japan.

From the figure it is clear that the broadcasted transmission is made of two channels for the image, synchronization and telemetry information. One complete frame consists of 128 complete horizontal video lines with a scan speed of 2 lines per second. A complete APT Video Line (Which is the horizontal scan line in output image) consists of 2080pixels, while two images from Channel A and Channel B takes up 990 pixels each. One complete APT video line includes two independent channel: Channel A followed by Channel B. Each video channel is consisted by a low resolution image down-sampled from original images taken from AVHRR/3 (1/3 of 360 scan lines per minute of AVHRR/3). As mentioned in Chapter 1.3, two out of six channels of AVHRR/3 is selected for channel A and B. Under local daytime visible image is transmitted in channel 1 and infrared in B.

Each video channel A and B have their own telemetry blocks at the end of their video line, as seen in the figure above. Each telemetry frames consists of 16 points (wedges) while each point is formed by 8 specific channel's telemetry part of a video line. The total height of 128 video lines (which is 16 points, as shown in figure) forms a complete frame. Calculating from the previous 2 lines/second scan rate, the time needed for receiving a complete telemetry frame is 64 seconds. Space and minute marker on the left side of each channel line is used for notation of time while receiving the signal, which is also directly related to the space parameter of captured image. The blank region comes from the pre-scan of AVHRR/3 scanning outside the earth. Time between two successive markers is 60 seconds. Minute markers themselves are repeated on 4 successive lines, with 2 black lines and 2 while lines. For Channel B the image itself is always coming from IR channel of AVHHR (Ch. 4 usually), with white background and black minute markers. On the contrary Channel A image is usually coming from a visible channel, in the case of visible

image the background is black with white minute markers, otherwise it appears like Channel B.

Figure 2.11 shows the retrieved APT image received from NOAA19. One complete frame of Channel A data is cropped and annotated in Figure 2.12. Based on the description above, all the features of frame format described above could be clearly seen, including 16 "wedges" of telemetry and space/time marker. From figure 2.13 it could also be seen that the wedge length and width are 8pixels/45pixels each, corresponding to the description above.

Figure2.12: One complete frame of Channel A. Telemetry, image and space mark are circled out in the image.

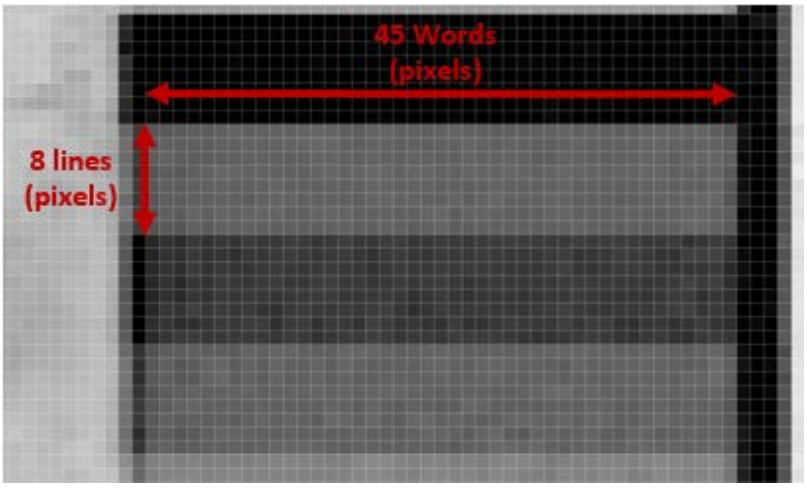

Figure2.13 Magnified image of telemetry section in Figure 2.12

Because the satellite is passing from the south and the frame scanned the video-lines from top to down, the top of image resembles the southbound. Here it could be seen that visible-light image is transmitted in Channel A, for background of minute markers are black. The gradient change of brightness observable on the left side shows the dusk at that local time.

Similar picture transmission method where the demodulated frame is directly retrieved

as telemetry and image information, exists in short-wave facsimile. In fact APT itself could be treated as a satellite transmitted weather-fax to some extent. Those short-wave facsimile is utilized in maritime weather-forecast transmitted through carrier frequency in 3~30MHz. Figure 2.14 shows the waterfall frequency diagram and received weather forecast of JMH by author. (Through the VHF Yagi-antenna in Kashiwa-campus). The received image is dimmer than standard (complete white usually), for the tuned frequency of USB receiver is higher than standard frequency. In fact geosynchronous GOES series satellite employs same weather fax transmission for broadcasting image of half disc. However the image itself is unable to be received in current region.

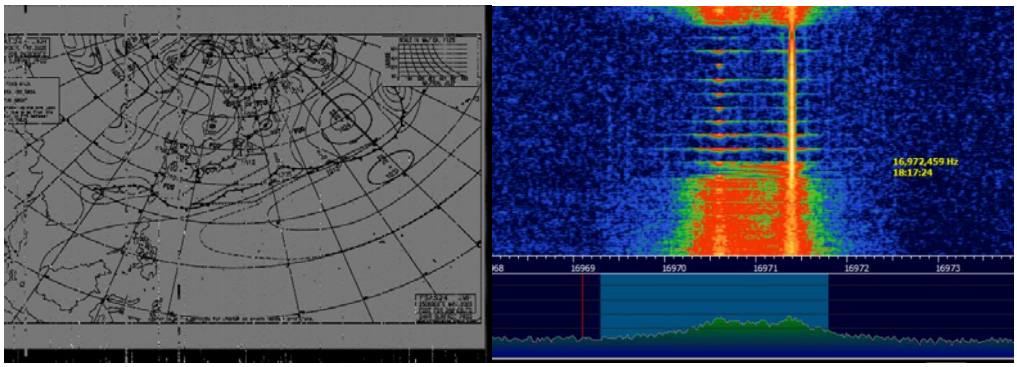

Figure 2.14: Waterfall-frequency diagram and received forecast image of JMH Wefax. The received image is dimmer than usual for characteristics when receiving USB signal.

Chapter 3: Communication link budget estimation

As the characteristics of signal is explained, and basic requirement of an APT receiver is shown (in Table 1.2), the line budget estimation, as one other important aspect when receiving satellite transmitted signal, has to be completed.

The common goal for link budget calculation is to estimate the difference between the sensitivity of receiver and received power at the input, so that the power margin (=difference) could be estimated as an index of link stability. During the course of designing this receiver the sensitivity is obviously unknown. Thus the goal of link budget estimation here is to assess the received power at input. With a sufficiently set, or guessed margin the "Passing mark" of receiver sensitivity is able to be derived for actual receiver evaluation.

Link budget calculation is often performed through the equation 1.3.1 below.

$$M = -S + P_T + G_{TA} - L_T - L_{FS} - Ab_a - L_{pol} - L_{antmis} + GT_s - L_{boltzman} - L_{bitrate} - L_{BER} \quad (3.1)$$

Feature of all the parameter is given in Table 3.1.

Parameter	Feature	Unit
M	Margin	dB
S	Sensitivity	dBm
P_T	Transmitter Power	dBm
G_{TA}	Transmitting antenna gain	dB
L_T	Transmission loss	dB
L_{FS}	Free space loss	dB
Ab_a	Atmospheric absorption	dB
L_{pol}	Polarization loss	dB
L_{antmis}	Antenna Misalignment	dB
GT_s	GT of the antenna	dB/K
$L_{boltzman}$		dBw/K/Hz
$L_{bitrate}$	Bitrate Correction	dB
L_{BER}	Bit Error Rate Correction	dB

Table 2.1: Parameters used in line budget estimation

3.1 Parameters, perquisites and calculation.

3.1.1 Antenna

In equation 1.3.1, two parameters are directly related to the antennae both in transmitting and receiving, transmitting antenna gain G_{TA} and receiving antenna GT_s. Transmitting antenna gain and GT of receiving antenna are used to calculate the radiated power and received power.

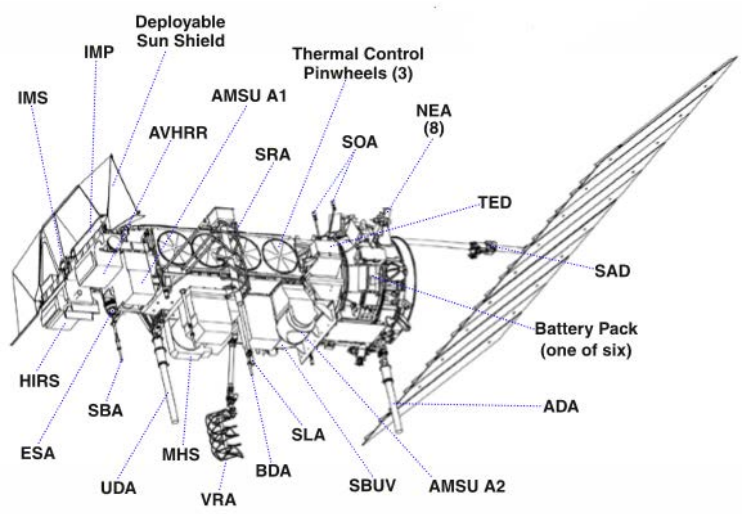

Figure 3.1a: Illustration of major instruments onboard NOAA satellite. The VHF real time antenna (VRA) is used to transmit APT signal. (NOAA, 2004)

The gain of an antenna could be calculated through its geometry and several related parameters. This calculated antenna gain is feasible in both transmitting and receiving thanks to reciprocating law of antenna.

In the case of NOAA-APT the transmitting antenna is already known as QFH (Quadrifilar Helix) antenna, as shown in Figure 3.1a and 3.1b

For the signal receiving antenna used in this project, a QFH antenna is also selected due to its ease of construction and omnidirectional gain pattern. Figure 3.2 shows the image of QFH antenna used for receiving APT signal in Kashiwa Campus.

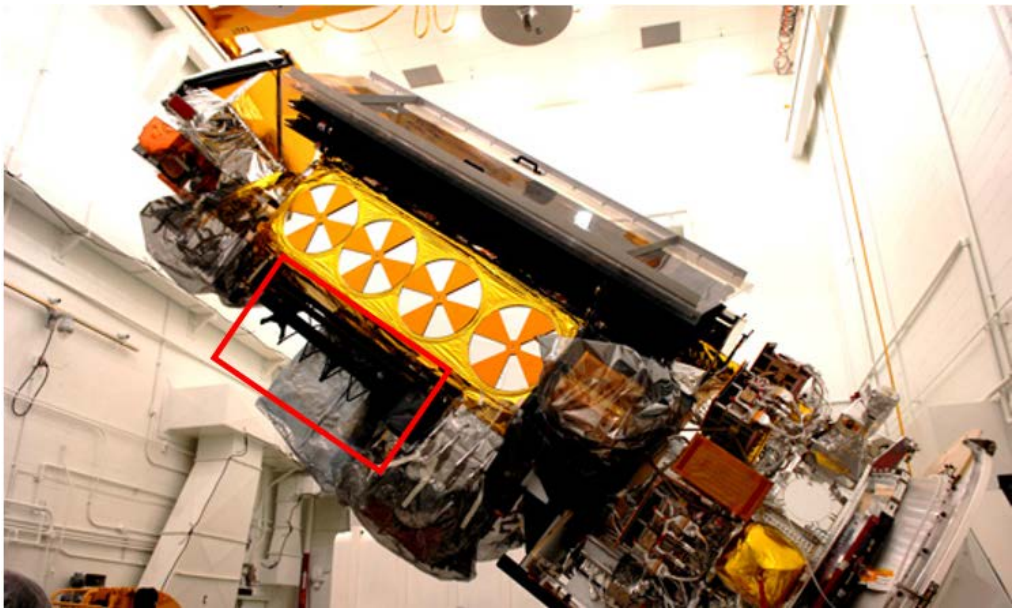

Figure 3.1b: Image of NOAA-19 satellite lifting to vertical before launch. VRA antenna is visible inside red frame (USAF, 2008)

Figure 3.2: QFH antenna used in receiving APT at Kashiwa campus

As the antenna used both in transmitting end and receiving end are specified, the antenna gain could be calculated. Fortunately the QFH antenna has a very helpful characteristic of being omnidirectional in azimuth, which means that its gain on horizontal plane has same values for 2π. The vertical gain of a QFH antenna gain sampled from 3 azimuthal angle is shown in Figure 3.17.

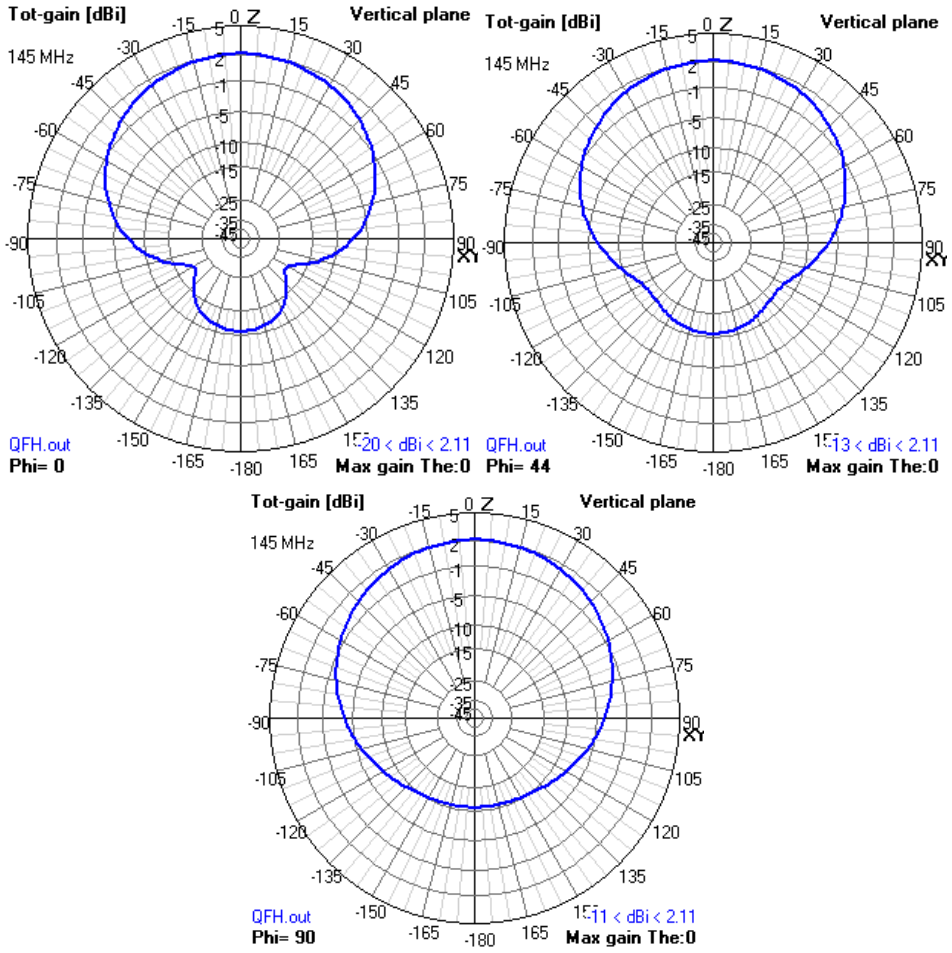

Figure 3.3: Vertical plane antenna pattern relative to elevation angle under azimuthal angle(phi) $0°, 45°, 90°$ of a QFH antenna tuned into 145MHz.
(M. Mascarello& A.Busso, 2011)

It is obvious that, the antenna pattern only has one main-lobe above the horizontal plane, and the pattern above $-90° \sim +90°$ does not change.

Within the interval of $-75° \sim +75°$ which is the practical elevation angle in receiving APT transmission (in Kashiwa Campus) the patter of QFH antenna is close to that of an ideal isotropic antenna. Thus, an assumption could be made for APT signal that, both transmitting and receiving antenna behave closely to an isotropic antenna.

This assumption eases up a bunch of things related to antenna gain calculation, for both the transmitting antenna gain and receiving antenna gain could be assumed 0dBi during the calculation.

3.1.2 Transmitted Power, loss and EIRP

In case of radiowave transmission from satellite, Effective Isotropic Radiated Power (EIRP) represents the equivalent transmitted power at the aperture of antenna onboard satellite, relative to the case when same radiowave gets transmitted by an isotropic antenna.

The EIRP, transmitted power, transmission loss and antenna gain have the relationship of equation 3.2.

$$EIRP = P_T + G_{TA} - L_T \quad (3.2)$$

As the antenna gain is explained in previous chapter, transmitted power and transmission loss is explained below. Usually telemetry downlink data is converted into radio-wave through the transmitter inside satellite and onboard antennae. Figure3.4a shows the system block diagram of high-data rate onboard transmitter of Hodoyoshi-4, another micro-satellite manufactured by University of Tokyo.

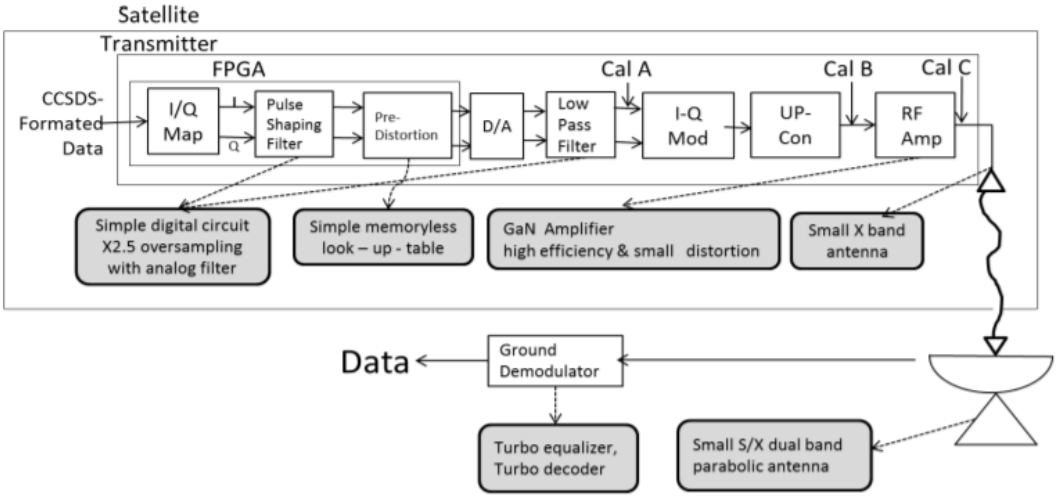

Figure 3.4a: System diagram of transmitter on board Hodoyoshi-4 (Hirobumi et al. 2020)

Just as the case on Hodoyoshi-4, downlink data is packed into a certain format then inputted into the transmitter through data bus. After modulation and amplification (or) frequency conversion the carrier wave is transferred into the antenna. A simplified diagram of this operation is given in Figure 3.4b.

The transmitted power, as shown in figure 1.18b is measured at the output of transmitter with unit of decibel-mill watt (dBm)

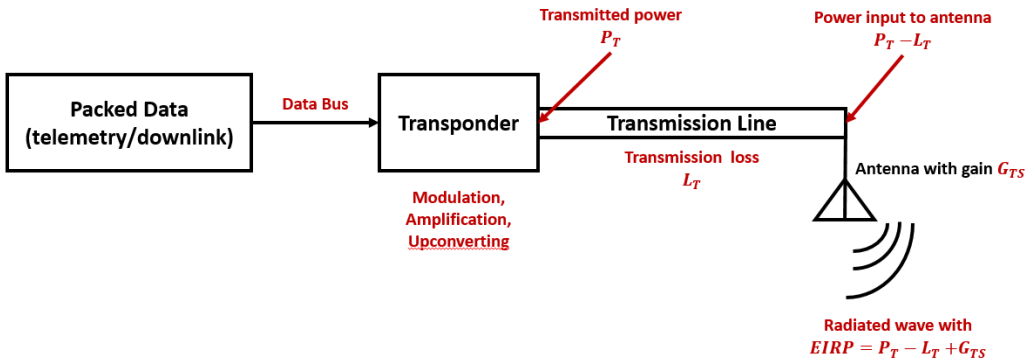

Table 3.4b simplified diagram of satellite data transmission

The transmission loss is the result of several attenuation during the high-frequency signal transmission from transponder to the antenna. Attenuation may happen as imperfection of connector or characteristics of transmission line. The latter one is usually more overt, for coaxial cable with dielectric medium is more often used than waveguide with lower damping. Concrete attenuation of coax cable depends on its dielectric filler material and several other parameters, but usual PE filled attenuation sits in the range of 0.5~2dB/10m (JARL, 2010).

With all the explanation on Transmitting diagram and transmission lost being done, in this NOAA-APT line budget calculation, the transmitting power and inner transmission loss is unknown. Here the EIRP, it is assumed to be the "Transmit Power" in Table 1.1.1, which is 5w in power and 36.9897 dBm. Thus, for the first three right-hand side variables of equation 3.1 we have

$$EIRP = P_T + G_{TA} - L_T = 36.9897 \text{ dbm} \quad (3.3)$$

3.1.3 Propagation loss:

For satellite is orbiting around the earth with height of more than 400Km, and the basic law of reverse-square $1/R^2$ relationship of radio wave intensity versus the distance and existence of atmosphere, it is obvious that the transmitted radio is bound to suffer a significant amount of depletion before reaching the receiving antenna. The total loss of power reaching receiving end relative to the transmitter is denoted by "Propagation loss". Most common form of propagation loss contain L_{FS}: Free space loss Ab_a: Atmospheric Absorption L_{pol}: polarization loss, and antenna misalignment loss: L_{antmis}

The relationship between propagation loss L_{prop} (in dB) and all the factors have the

relationship of equation 3.4:

$$L_{prop} = \ L_{FS} + Ab_a + L_{pol} + L_{antmis} \quad (3.4)$$

The free space loss is simply the loss of radio wave due to its characteristic of spherical propagation. It is calculated by the expression of equation 1.3.3

$$L_{FS} = 10\log\left(\left(\frac{4\pi df}{c}\right)^2\right) dB \quad (3.5)$$

Where d is the distance of transmitter to the receiver antenna f the frequency of transmitted radiowave, and c the light speed in vacuum.

For the line budget estimation, variable d is chosen with consideration of expected feasibility of receiving a signal under certain margin. It is specified under certain satellite orbit radius and elevation angle relative to the ground station. Relationship between those factors are shown in Figure 3.5

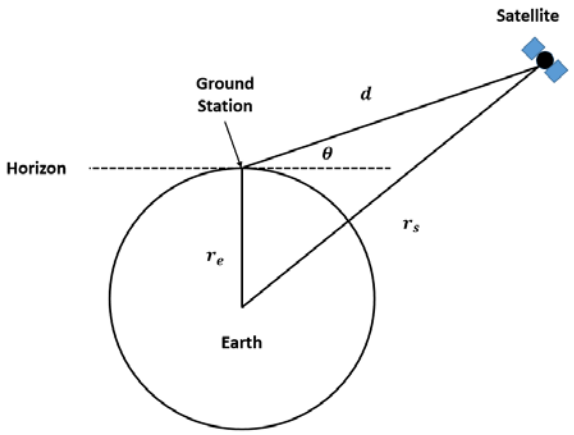

Figure 3.5: Relation between satellite distance d and orbit radius under elevation angle θ

Where r_e is the mean radius of earth, θ elevation angle, d satellite distance and r_s distance of earth center to satellite. From cosine law, it is easy the deduce the expression showing relationship between d and θ, as shown in equation 3.6

$$d = \sqrt{(r_e^2 \sin\theta \ + r_s^2 - \ r_e^2)} \ - r_e \sin\theta \ (3.6)$$

As it is noted in previous section, practical elevation angle where signal receiving is

estimated to be started in 15°. With the satellite-earth center distance of $r_s = 7561km$, the distance could be calculated to be

$$d = 3114km \quad (3.7)$$

Under the frequency of $f = 137MHz$, the free space loss could be calculated from equation 1.3.3 to be

$$L_{FS} = 125\,dB \quad (3.8)$$

The polarization loss occurs under the mismatch of polarization between receiving antenna and the transmitted radiowave. Because antenna with RHCP is used in both transmission and receiving end of APT signal, polarization loss is assumed to be non-existent.

$$L_{pol} = 0dB \quad (3.9)$$

Similar assumption is made on antenna misalign loss L_{antmis}, for this factor is used to describe the misalignment of antenna with high directivity i.e. antenna gain. When using antenna with very narrow main lobe BWHM (-3dB beam width) this misalignment of antenna could be a major problem. However QFH antenna used in receiving NOAA APT is an omnidirectional antenna with close to zero relative gain, thus the misalign loss here is also assumed to be zero.

$$L_{antmis} = 0dB \quad (3.10)$$

The absorption loss is a complicated factor, for different layers of atmosphere provides different characteristic of attenuation under variable conditions. For simplicity here we take an empirical value of 1dB as an assumption for absorption loss. Thus:

$$Ab_a = 1dB \quad (3.11)$$

Hence, from equation (3.4)

$$L_{prop} = \ L_{FS} + Ab_a + L_{pol} + L_{antmis} = 126dB \quad (3.12)$$

3.1.4 G/T, bitrate correction and bit error rate correction (BER).

To conclude first, G/T of receiving antenna, bitrate correction and BER are all equal to zero.

$$\begin{aligned} GT_s &= 0 \\ L_{bitrate} &= 0 \\ L_{BER} &= 0 \end{aligned} \qquad (3.13)$$

For GT_s its value comes from a previous assumption that QFH antenna used in APT receiving perform closely to an omnidirectional antenna, with relative gain of 0dBi.

The other two parameter, $L_{bitrate} = 0$ $L_{BER} = 0$ is assumed to be zero, because the modulated carrier wave is essentially analog FM modulated where no equivalent bit-rate let alone BER exists in this layer of modulation, and in this receiver design we're only concerned in demodulating 137MHz NFM signal into 2.4KHz signal.

3.2 Budget calculation

Based on all the calculation and assumption in previous chapters, we find that the link budget estimation became the observed strength of carrier wave where antenna is standing. This is an obvert result, assuming the receiving antenna does not have directivity and transferring loss from antenna to the receiver is neglected. Thus the received powerP_{res} is calculated through the expression below (equation 1.3.5)

$$P_{res} = \text{EIRP} - L_{prop} \qquad (3.14)$$

We have:

$$P_{res} = -90\text{dBm} \qquad (3.15)$$

As it is described before chapter 1.3.1, certain margin could be set to evaluate the feasibility of receiver. Because all the parameter except sensitivity S in equation 1.3.1 are determined, here if we assume a margin of 30dB, from equation 1.3.1 we could calculate the requires sensitivity of

$$S = P_{res} - \text{M} = -120\text{dBm} \quad (3.16)$$

Note that the goal of budget estimation is still the check of feasibility in signal receiving with sufficient margin.

Chapter 4: Principle and Design of APT receiver

4.1: Preface

We already introduced the characteristics and properties of transmitted APT-signal in Chapter 1.1. From there the design specification of the receiver could be deduced to be a Narrow-FM receiver with 2400Hz beat frequency as the output signal. In Chapter 2, based on the basic receiver design specification, the design details and several principle behind certain features are explained.

Figure 4.1 shows a simple system diagram of an arbitrary VHF FM receiver with a HF (Hearing Frequency, or AF as audio frequency) speaker output.

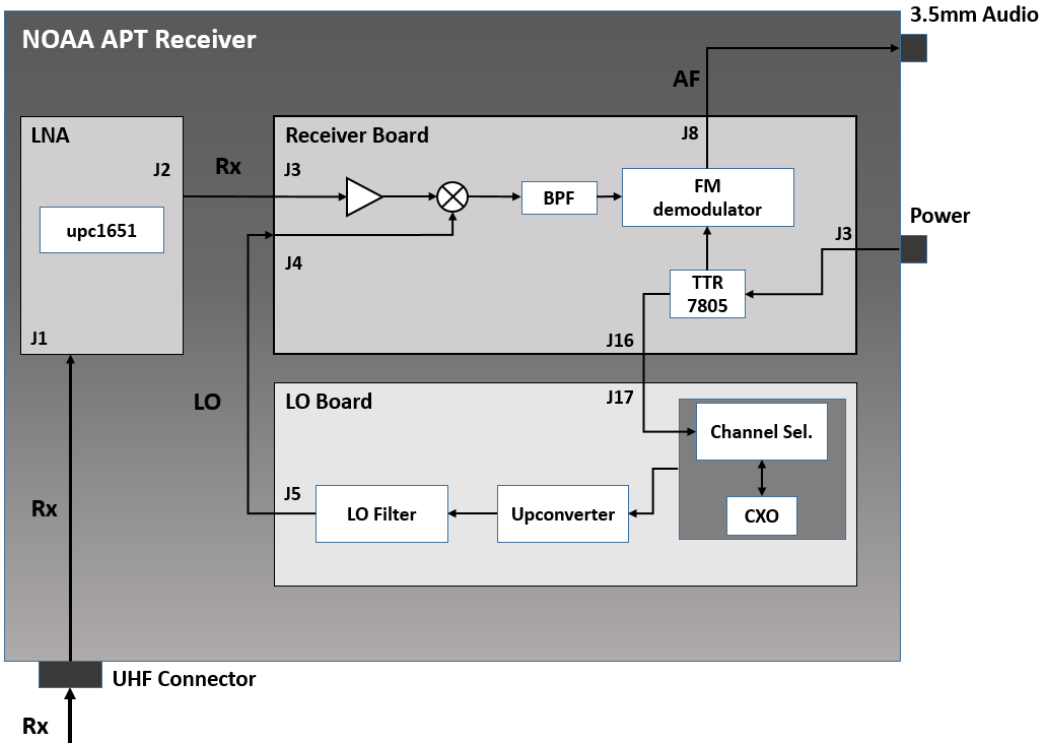

Figure 4.1: Simple system diagram of typical FM receiver

For receiver used in radio-frequency, some core-components has to be present in the design so that the electromagnetic-wave could successfully be picked and sampled by the receiver. Those might vary depending on the frequency requirement and modulation form of transmitted signal. Here in this design, the receiver is designed for FM modulated VHF signal with a narrow bandwidth, and the components are also based on the typical receiver requirements.

In typical analog receiver design RF amplifier is connected to the antenna so that received signal is amplified into a level that mixer& filters could sufficiently process. The signal with frequency equal to carrier frequency f_R is inputted into the mixer to produce

intermediate frequency (Introduced in Chapter 2.2). In FM receiver and most of receivers working over VHF frequency, superheterodyne mixer is applied to down-convert carrier frequency into desired intermediate frequency. In this case local oscillator provides a precise sinusoidal waveform (signal) with frequency f_{LO} as LO input for mixer. The received signal is then downconverted into IF signal with frequency$f_R - f_{LO}$. For major applications more than one number (level) of downconversion is applied.

The downconverted IF signal $f_R - f_{LO}$ goes through a set of filters, for the superheterodyne mixer generates a substantial amount of harmonics. Considering the signal frequency at this stage, LC filter with independent component is applied rather than print-pattern generated used frequently in frequency higher than 1GHz.

Filtered IF is then inputted into FM demodulator (discriminator) in order to generate modulated base-band signal. Here the output baseband is assumed to be HF (audio frequency). Usually the output power of demodulator is not enough for driving a speaker or maintain sufficient level before I/O of other devices. Thus a HF amplifier then amplify the demodulator output so that speaker, or interface with other HF input has sufficient power to be driven.

From the overall description above, it is not hard to conclude that there is a certain stream of from RF to IF and HF conversion. This is because such a structure is widely used in FM receiver to an extent of standardization. And this is also the reason why the APT receiver, lengthily explained in this chapter, is designed in this specific way. Surely NFM signal could easily be converted into its complex envelope by I/Q demodulator, however, for the sake of applicability and ease in assembly a traditional superheterodyne style receiver was chosen.

For detailed explanation of receiving antenna is already done in previous chapter 3.2, it is now taken as a known design feature in this chapter. Other components and their principles will be explained along with the actual design of 137MHz APT receive

4.2: Overall components designed in NOAA-APT receiver.

Based on the analysis of APT signal in previous chapter, a basic set of performance requirement for APT receiver is derived. For convenience, requirements are listed in table 4.1. Similar to the basic system diagram shown in Figure4.1, a more specified system diagram describing the designed NFM receiver is shown in Figure 4.2

Requirements	
Input frequency	137.1 (NOAA19) 137.91(NOAA18) 137.62(NOAA15)
Modulation	Narrow FM
Bandwidth	45KHz
Minimal input level	108dBm
Output	2400Hz HF (Speaker, 3.5mm jacket)

Table 4.1: Basic requirements of APT receiver

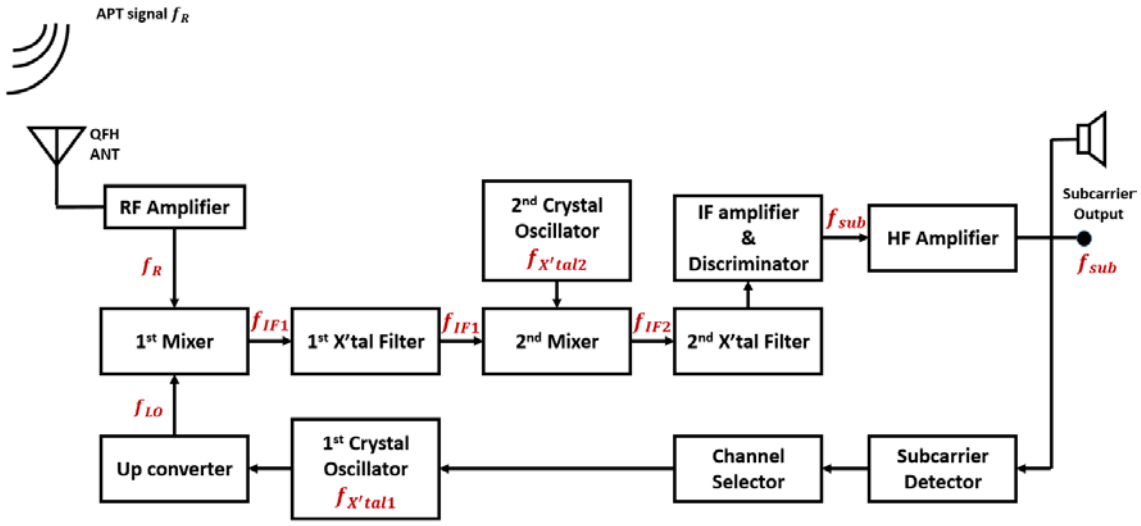

Figure 4.2: System diagram of receiver for NOAA APT

The basic steps, for the most parts, are the same, as any typical FM receiver – received signal with carrier frequency gets amplified through RF amplifier, downconverted into intermediate frequency, demodulated into HF signal and then outputted after amplification.

In this APT receiver two IF are used, f_{IF1} and f_{IF2}, with values

$$f_{IF1} = 10.7Mhz \text{ and } f_{IF2} = 455KHz$$

Those intermediate frequencies are generated through two stages of down-conversion through mixers. The mixers uses superheterodyne principle for down-conversion, where the input frequency f_R, local oscillator frequency f_{LO} and output frequency (IF) in this case is described by the equation: $f_{IF1} = f_R - f_{LO}$.

The local oscillator frequencies are generated from discrete crystal oscillators, where their frequencies are denoted as f_{Xtal} in the design of this receiver. There are two sets of LO corresponding to two mixers that generates two sets of IF, as it is described in paragraph above. In the first local oscillator, 3 sets of crystal oscillator corresponding to 3 APT carrier frequency from 3 satellites (NOAA19, 18, 15) are employed. In APT receivers an up-converter is designed between the 1st crystal oscillators and the 1st mixer, for the frequencies required to down convert carrier frequency f_R into f_{IF1} could not be generated by crystal oscillator with sufficient stability.

Filters used for filtration of IF signals are also consisted of ceramic filters. Detail and their principles are introduced in forthcoming chapter.

The subcarrier signal with frequency $f_{sub} = 2400hz$, which treated as output in APT receiver, is amplified through a HF amplifier (here class C amplifier with BJT is used) and divided into 3 routes. The first one is the speaker, which in application is used for checking the signal receiving. Second output goes through a 3.5mm audio jacket and will get transferred into PC for 256-level AM demodulation and frame construction as described in chapter 1.3.

Another part of subcarrier signal is used for a flag for channel selection. That is, if the receiver successfully receives and demodulates an APT signal of specific satellite, subcarrier will get transferred into channel section part and local oscillation frequency gets fixed into a specific channel. A rather abnormal use of PLL (Phase-locked loop) circuit is applied here. Details are explained in Chapter 2.5

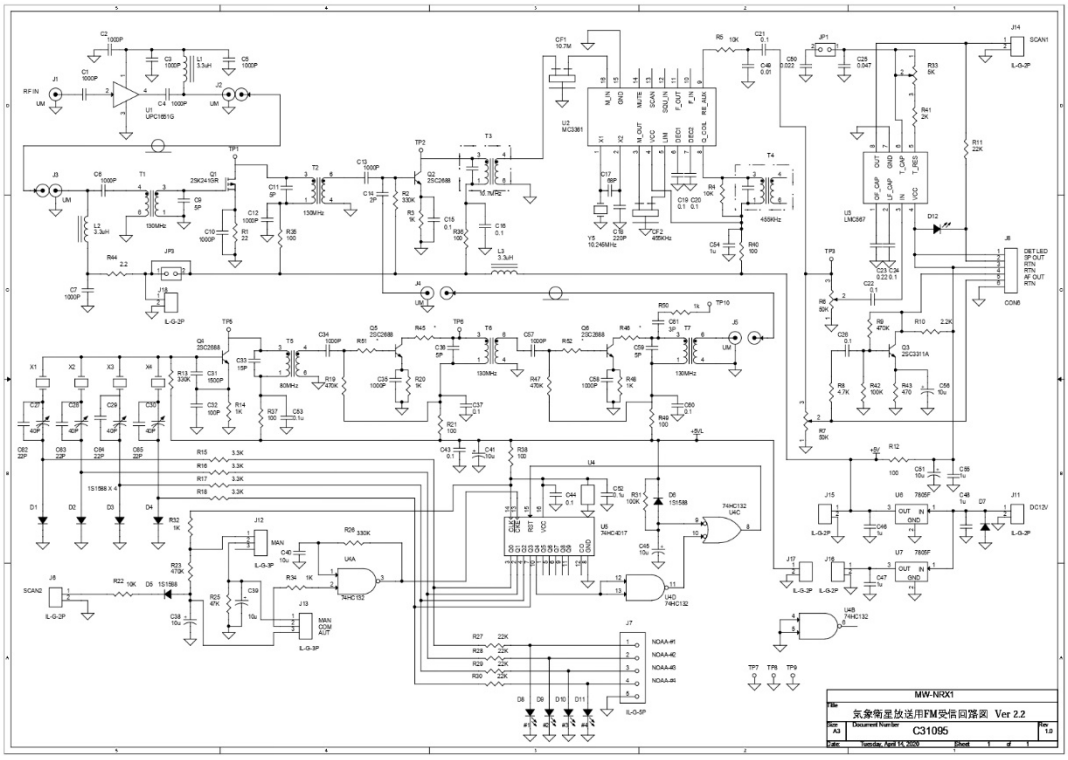

Figure 4.3: Complete design circuit diagram for NOAA-APT receiver

Finally, the complete circuit design diagram for the whole APT receiver is shown in Figure 4.3, corresponding to the simplified diagram in Figure 4.2.

Design of main components consisting the receiver circuit and their working principle are introduced in following chapters in an order of signal path. The next chapter, Chapter 4.3 will be focusing the local oscillator- the crystal oscillators used in signal generation and frequency multiplier. Superheterodyne mixer and its nature as a signal multiplier will be analyzed in Chapter 4.4. Main IF BPF used in this circuit, a ceramic resonant filter is then introduced in 4.5. Finally the FM demodulation chip, heart of this receiver, is elucidated with FM demodulation principle.

4.3 Local Oscillator Circuit

4.3.1 Crystal oscillator

For local oscillation circuit operating under VHF frequency, two common approach are used by means of generating the oscillation.

The first and rather primitive way is the LC circuit oscillator. Just as its name indicates, LC oscillator uses the inductance and capacitance of a circuit, arranged in certain ways, to generate electrical oscillation. Thus providing oscillation signal (or clock) of a specific frequency. There are several proven LC circuit for outputting oscillation signal, but description including principle of LC oscillation circuit is omitted here.

The second major approach is the usage of crystal oscillator. It is a simple device which utilizes quartz's piezoelectric characteristics to generate varying voltage signal with certain frequency. Figure 4.4 shows the appearance of a common crystal oscillator, and Figure 4.5 shows the inside cut of a quartz.

Figure 4.4: Exterior of a typical crystal oscillator with HC49 package. Oscillator with same package is used in LO of APT receiver (ACT, 2020)

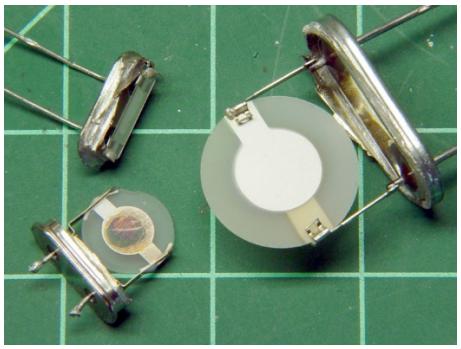

Figure 4.5: Inside of crystal oscillator of common package. (Circuitscrush, 2020)

It could be seen in the Figure 4.5 that two electrodes are attached onto faces of a quarts cut in specific shape. As it is already pointed out previously, the quartz itself is but a mechanical oscillator that oscillates with a frequency dominantly determined by its shape. It is the piezoelectric characteristic of quarts that produces potential difference between electrodes with certain periods, which leads to the alternating voltage at the output with certain frequency noted as $f_{Xıtal}$.

Relationship between mechanical oscillation of crystal and its shape is yet another complicated subject out of context, thus only conclusion and characteristic of oscillation circuit is introduced here.

The crystal oscillator could be drawn as an equivalent electronic circuit, shown in Figure4.6.

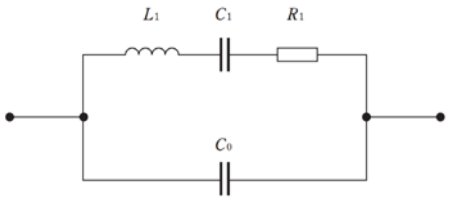

Figure 4.6: Equivalent circuit of a crystal oscillator

Where all the notation is denoted in Table 2.2:

L_1	Equivalent series inductance
C_1	Equivalent series capacitance
R_1	Equivalent series resistance
C_0	Parallel capacitance

Table 3.2: Notation of equivalent circuit parameters of a crystal oscillator

Simple analogy is given for better understanding the equivalent circuit value.

The series inductance L_1 stands for the mass in mechanical oscillator, and series resistance represents internal friction during the mechanical oscillation of crystal. The equivalent series capacitance represents compliance of the crystal, a value to quantify the elasticity and plasticity during deformation of crystal. Parallel capacitance in equivalent circuit represents the capacitance between two electrodes, basically the same to that shown in Figure 4.5. The characteristic oscillation frequency could be explained as:

$$f_{X'tal\,C} = f_{series} = \frac{1}{2\pi\sqrt{L_1 C_1}} \quad (4.1)$$

Which is also the series resonance frequency of the crystal.

In the design of an actual oscillator circuit, equivalent oscillation circuit using crystal oscillator could be drawn as Figure 4.6. The mark on left side stands for crystal oscillator.

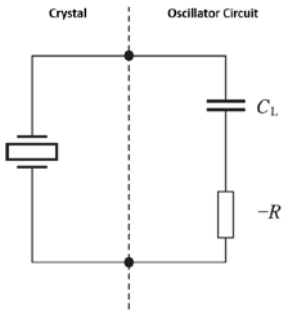

Figure 4.7 Simplified circuit diagram of equivalent oscillation circuit

$\boldsymbol{C_L}$ stands for the equivalent load capacitance from perspective of crystal, and the $\mathbf{-R}$ represents the negative resistance (not discussed here) from perspective of crystal. The actual conditions for oscillation involves impedance matching between circuit side and crystal side, thus heading to the conclusion, the actual oscillation frequency (frequency under load) could be derived as:

$$f_{Xrtal} = f_L = f_s\left(\frac{C_1}{2(C_0 + C_L)} + 1\right) \quad (4.2)$$

From the equation it is clear that the load capacitance C_L has a major influence on the final output frequency excepting the inherent characteristics of quartz crystal itself. In practice, parasitic capacitance always exists in the actual printed circuit board (PCB).Thus the load capacitance is almost certain to be having a value different than designed value. In the actual design shown in Figure 4.7, a trimmer capacitor (capacitor that could alternate its own capacitance in a designated range) is added for compensation of this phenomenon.

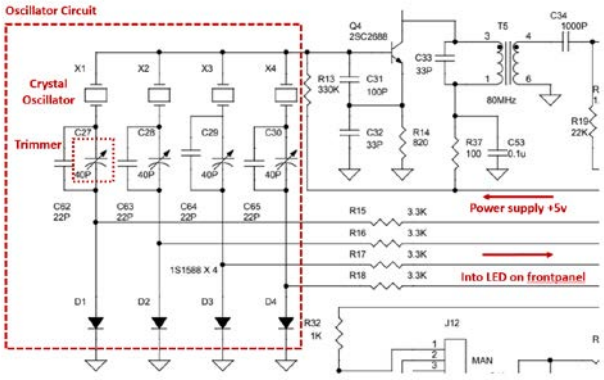

Figure 4.8: Circuit diagram of Crystal oscillator part.

It is obvious that in any design scenario, starting the local oscillator from cutting the quartz crystal is an abysmal idea. In the design of 1st LO in APT receiver, based on the required frequency to mix and down-convert 3 different carrier signals coming from 3 NOAA satellites, 3 sets of crystal oscillators are ordered with frequencies denoted in Table 4.3.

Satellite	Carrier f_R	1st IF f_{IF1}	Crystal frequency f_{Xtal}
NOAA19	137.1MHz	10.7MHz	21.0667MHz
NOAA18	137.9125MHz		21.2000MHz
NOAA15	137.62MHz		21.1533MHz

Table 4.3: Carrier frequencies, IF and corresponding crystal oscillator frequencies of receiver

Obviously for the ordered crystal frequency is too low that, difference between the crystal frequency and any carrier frequency amongst, would not derive the 1st IF frequency of 10.7MHz. This is due to the fact that a crystal's oscillation frequency and its stability (or even the absolute value itself!) has a rather arduous relationship in-between, with instability generally increasing with its frequency. (Crystal with frequency higher than 50MHz usually uses overtone for oscillation, so overtone of crystal could be one of the reason). Thus crystals with relatively low frequencies are selected as an empirical solution.

Also, selection of crystal with a weird frequency lower than the difference $f_R - f_{IF1}$ is the reason of adding up-converter into the local oscillator. The working principle and design of up-converter is introduced in next section.

4.3.2 Frequency multiplication and up-converter circuit

Frequency multiplying circuit, by definition, is a certain type of circuit that outputs a signal with frequency multiplied by certain magnifications compared to input signal. Note that frequency could only be multiplied by a whole number.

As it is explained in 2.2.1, the output frequency of crystal oscillators are derivatively selected at a lower frequency that, directly inputting the crystal's output cannot generate intended intermediate frequency of $f_{IF1} = 10.7MHz$. Thus a frequency upconverter, or a multiplier is required. Relationships between f_R, f_{IF1} and $f_{X'tal1}$ are given in table 2.3.

Satellite	f_R	f_{IF1}	$f_R - f_{IF1}$	$f_{X'tal1}$
NOAA19	137.1MHz	10.7MHz	126.4MHz	21.0667MHz
NOAA18	137.9125MHz		127.2125MHz	21.2000MHz
NOAA15	137.62MHz		126.92MHz	21.1533MHz

Table 4.5: Carrier frequency, IF, Crystal frequency and corresponding 1st LO frequency

It is not hard to see that the difference between f_R and f_{IF1}, namely the value of $f_R - f_{IF1}$ is 6 times the value of $f_{X'tal1}$ in each corresponding carrier frequency, which means the design of APT receiver employ a 6-time multiplier to upconvert crystal oscillator frequency into required local oscillator output. Usually, phase-locked loop circuit is used for multiplying oscillation frequency of a LO, however, due to its complexity and natural need for control chip, a set of nonlinear circuit employed multiplier is used in the design of this receiver. It is essentially a class-C nonlinear amplifier coupled with a band pass filter. A simple system diagram is shown in Figure 4.8.

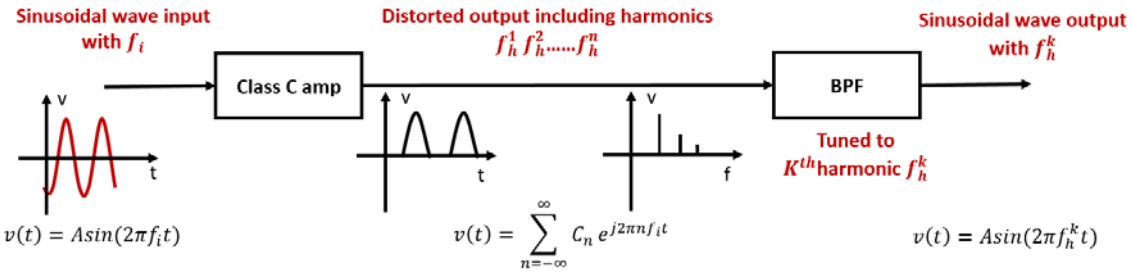

Figure 4.8: Simple system diagram of frequency multiplier consists of class C amp and BPF

When a sinusoidal wave $v(t)$ with frequencyf_i is assumed to be inputted into a class-C amplifier, or any circuit with certain non-linearity, the non-linearity of circuit itself generates a series of harmonics (integer multiply of input frequency) expressed as a Fourier series. By filtering the output with corresponding BPF (band-pass filter) tune to Kth harmonics, particular harmonic of input frequency f_h^k could be extracted.

The non-linearity of class-C amplifier comes from its working condition relative to what is called a linear amplifier, like class-A amp. Putting it simply, by biasing the NPN Bipolar Transistor (used in this case) below the cut-off region to a point that its DC operating Q is below zero v_{CE}, only a "Part" of input waveform gets amplified and outputted, just like the "Half shaped" waveform.

Figure 4.9 shows the relationship between input waveform, collector-emitter potential v_{CE} and collector current I_C which is the output.

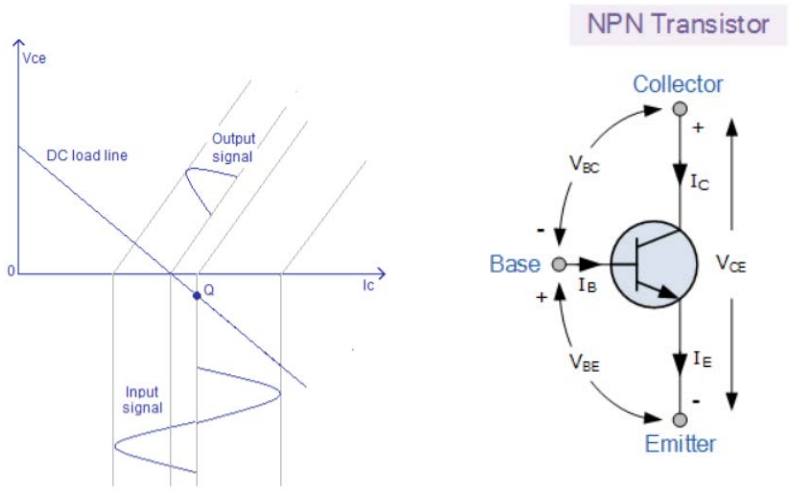

Figure 4.9: Relationships between input/output waveform, Vce and Ic (left) and simple current and voltage relationship in a typical NPN transistor. (CircuitsToday, 2001)

Circuit diagram of a typical class-C amplifier is shown in Figure 4.10.

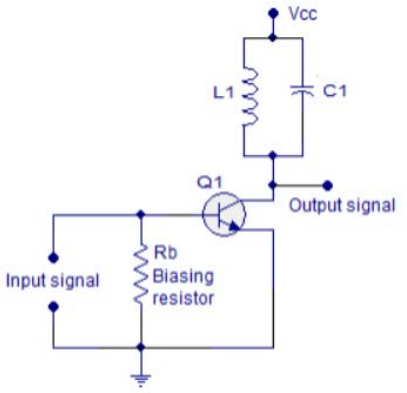

Figure 4.10: simplified circuit diagram of a typical class-C amplifier (Circuitstoday,2001)

It is easy to see that this class-C amplifier is essentially an emitter-grounded amplifier with input on base and output from collector. A sufficient bias resistor is selected order to accomplish a minus bias on v_{BE}.

In the design of frequency multiplier used in APT receiver, two stages of frequency multiplier is used in order to multiply crystal frequency 6 times. Figure 4.11 shows simple system diagram of multiplying circuit and 2.12 shows the actual circuit diagram.

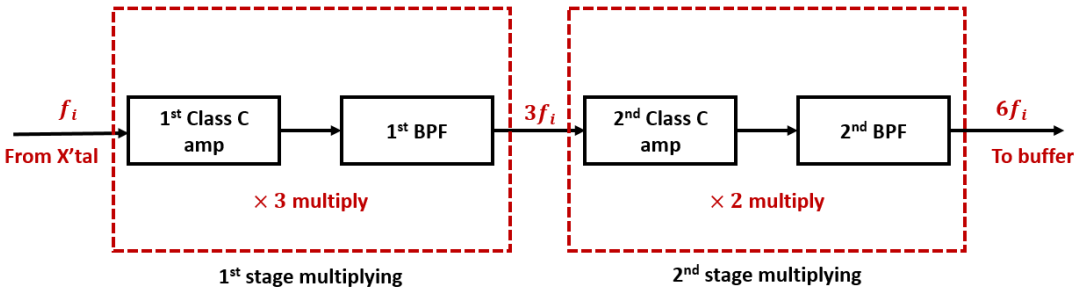

Figure 4.11: system diagram of 6 times frequency multiplier used in APT receiver

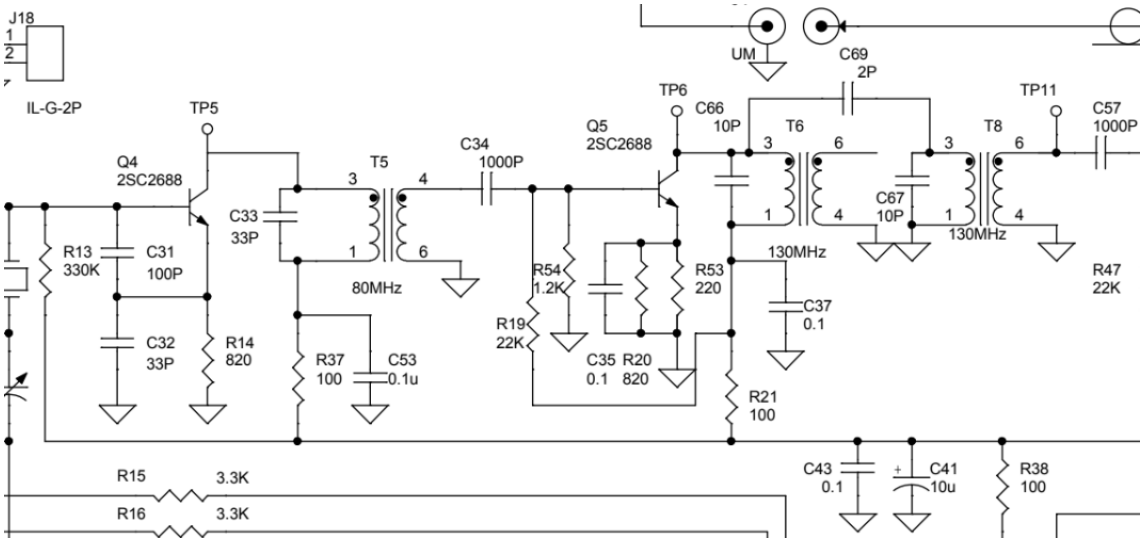

Figure 4.12: Circuit diagram of 2-stage frequency multiplier

In the actual circuit design, two class-C amplifiers with 2SC2668 as transistor are used. The 1st stage of 3x multiplier up-converts the input frequency from crystal oscillator around 21MHz into around 63MHz, then the 2nd stage 2x multiplier up-convert the frequency into 126MHz. From the diagram it is easy to identify the class-C amplifier structure similar to that shown in Figure 4.10. Grounding capacitors and blocking capacitors on inputs and power supply are added for performance. For instance capacitor C34 is placed to block DC power supply voltage from reaching the secondary winding of transformer (or adjustable inductor) T5. Test point TP5 and TP6 are placed for checking the existence of harmonics.

Adjustable inductors T5 and T6 with centre resonance frequency of 80MHz and 130MHz are used as band pass filters. Similar to the "parasitic capacitance" phenomenon described in 2.1.1, adjustable inductors are applied for mainly two reasons. The first one is to compensate for the deviation caused by parasitic inductance and capacitance. The second reason is that no filter/inductor is sold on market for a particular frequency, for instance 63.2001MHz in NOAA19's case. Even if such a filter exist (in fact chebyshev filter could be designed to fit this frequency if being careful), adjustability is still required to compensate parts' error and parasitic facts, which bring the whole debate back to the first reason. Two buffer amplifiers are added after the second stage frequency multiplier for improving the performance of superheterodyne mixing. To put it simply buffer amplifiers are placed to isolate the multiplication circuit and mixer part so that no direct feedback through pattern is transferred back to the previous circuit.

4.4: Super-heterodyne mixer

From figure 4.2, it is easy to notice that two mixers are present in APT receiver's design. Here in Chapter 4.4, the first mixer that downconverts 137MHz carrier signal into 10.7 1st IF signal is focused, for the 2nd mixer is principally the same with the 1st, only working in a different frequency range.

Before explaining the working principle of superheterodyne and mixer used in design of APT receiver, the working principle of the process "heterodyning" is introduced.

Heterodyning, to put it in simplicity, is a process that shifts the frequency range of input signal by combining or mixing two frequencies. This classic method usually utilize nonlinearity of specific circuits to produce two major sets of new signals based on two inputs: The sum of two frequencies and difference of two frequencies. Figure4.12 shows a simple system diagram of a typical heterodyne mixer outputting a differentiated frequency. The central mark of circle with a cross inside stands for the mixer. Note that the word "mixer" here specifically represents "Frequency mixer".

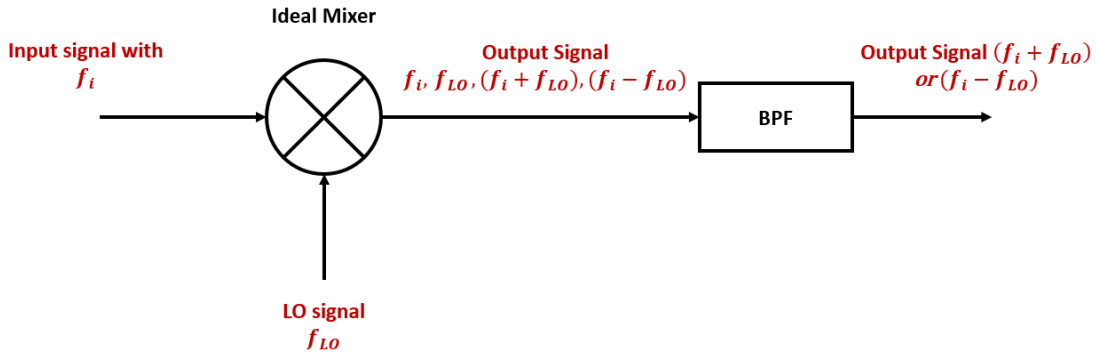

Figure 4.13: system diagram of an arbitral heterodyne mixer using Local Oscillator as one of the input.

The word "Superheterodyne" stands for Heterodyning operation where the lower frequency signal is taken as the desired output. That is, if the BPF (band pass filter) in figure 4.12 is tuned for the frequency $f_i - f_{LO}$, we call the whole operation of mixer and coupled BPF "superheterodyne". The frequency f_i is assumed to be higher than local oscillator f_{LO}, for it is dominantly the case in practical application.

There are a wide varieties of mixer to be used in RF frequency mixing, for instance RF

mixers used in Spectrum Analyzer (for ADC to sample the input within its frequency range) is specifically designed for a certain frequency range.

In the design of APT receiver, a Base-Injection BJT mixer is used for 1st IF superheterodyne circuit. The circuit diagram and simplified diagram is shown in Figure 4.14 and Figure 4.15.

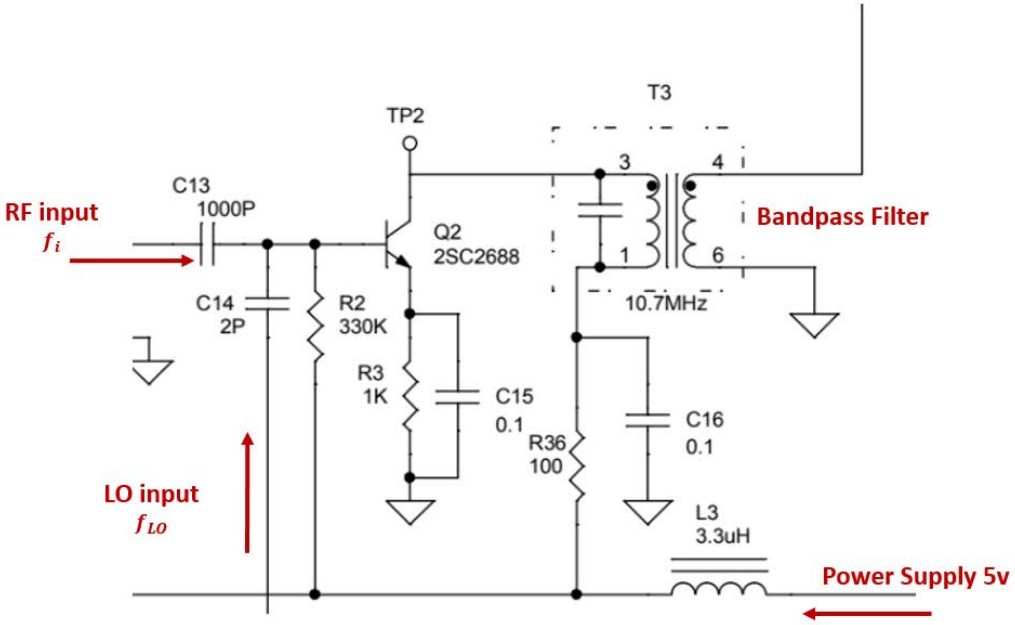

Figure 4.14: Superheterodyne mixer (1st IF part) of APT receiver design

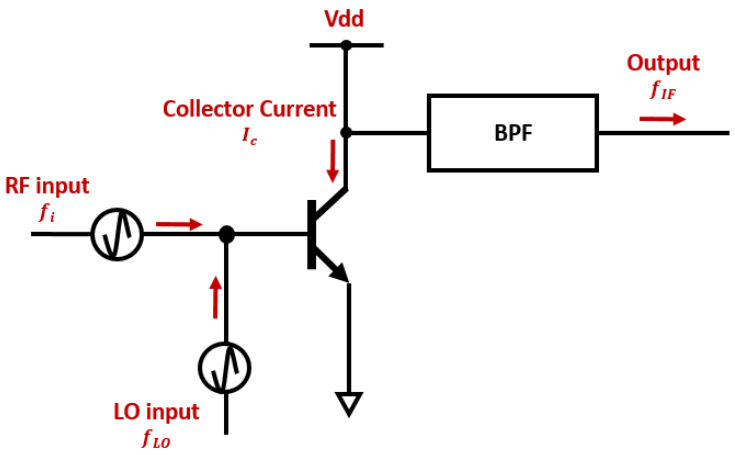

Figure 4.15: system diagram of mixer circuit shown in Figure 4.14

Tank circuit and base-collector biasing element is removed for simplicity in Figure 4.14.

It is easy to figure out that, the mixer component and structure is quite similar to that used for frequency multiplier circuit used in LO. Predominantly, frequency multiplier and BJT mixer is using the same principle where a non-linear circuit would create harmonics with higher frequency when input with certain frequency.
The relationship between the potential applied on base and the collector current I_c under its active region could be expressed as:

$$I_C \cong I_S e^{\frac{v_{be}}{v_T}} \quad (4.3)$$

Where I_S is the saturation current of BJT, v_{be} is the voltage between the base and the emitter of BJT. The value v_T stands for the temperature voltage of a certain BJT, related to working temperature of BJT. In this case the BJT is assumed to be working in static temperature thus v_T is treated as constant value.

Notice the LO input and RF input are combined before BJT's base in figure 4.14, which is essentially adding up the voltage of two different signal v_{LO} and v_i. Note that there is another DC biasing voltage v_b applied on base, which is emitted in the figure above. To sum up, base-emitter voltage v_{be} could be described as:

$$v_{be} = v_b + v_{LO} + v_i \quad (4.4)$$

Taking it into equation 4.3 we have:

$$I_C \cong I_S e^{\frac{v_b+v_{lo}+v_i}{v_T}} = I_s\, e^{\frac{v_b}{v_T}}\ e^{\frac{v_{LO}}{v_T}}\ e^{\frac{v_i}{v_T}} = I_{CQ}\, e^{\frac{v_{LO}}{v_T}}\ e^{\frac{v_i}{v_T}} \quad (4.5)$$

I_{CQ} stands for the collector current at the bias point applied on a specific transistor. For the same reason we treat this parameter as a constant. Expanding both v_{LO} term and v_i term based on assumptions respectively, we have the following equations.

$$e^{\frac{v_i}{v_T}} = 1 + \frac{v_i}{v_T} + \frac{1}{2}\left(\frac{v_i}{v_T}\right)^2 + \cdots \frac{1}{n}\left(\frac{v_i}{v_T}\right)^n \quad (4.6)$$

$$e^{\frac{v_{LO}}{v_T}} = 1 + \frac{v_{LO}}{v_T} + \frac{1}{2}\left(\frac{v_{LO}}{v_T}\right)^2 + \cdots \frac{1}{n}\left(\frac{v_{LO}}{v_T}\right)^n \quad (4.7)$$

For the RF input v_i, an assumption is made that $\frac{v_i}{v_T} \ll 1$, which means the input RF signal is much smaller than BJT's temperature voltage. Thus equation 4.7 could be simplified as:

$$e^{\frac{v_i}{v_T}} = 1 + \frac{v_i}{v_T} \quad (4.8)$$

Taking equation 4.8 and 4.7 into equation 4.5, we have the expression for collector current I_C which is also transistor's output current before BPF.

$$I_C \cong I_{CQ}\left(1 + \frac{v_i}{v_T}\right)\left(1 + \frac{v_{LO}}{v_T} + \frac{1}{2}\left(\frac{v_{LO}}{v_T}\right)^2 + \cdots \frac{1}{n}\left(\frac{v_{LO}}{v_T}\right)^n\right)$$

$$= I_{CQ}\left(1 + \frac{v_{LO}}{v_T} + \frac{1}{2}\left(\frac{v_{LO}}{v_T}\right)^2 + \cdots \frac{1}{n}\left(\frac{v_{LO}}{v_T}\right)^n\right) + \frac{I_{CQ}}{v_T}\left(\frac{v_i}{1} + \frac{v_i v_{LO}}{v_T} + \frac{v_i}{2}\left(\frac{v_{LO}}{v_T}\right)^2 + \cdots \frac{v_i}{n}\left(\frac{v_{LO}}{v_T}\right)^n\right) \quad (4.9)$$

In APT receiver design, we already know that LO input is in sinusoidal waveform, and the RF input v_i is a frequency-modulated carrier signal (or in another term, pass band signal). Thus both signals are time-dependent and could be noted as $v_{LO}(t)$ and $v_i(t)$.

For convenience the LO signal is assumed to be in cosine form, where

$$v_{LO}(t) = cos2\pi f_{LO} t \quad (4.10)$$

In equation 2.7 expression in the first parentheses stands for the passing-through LO input v_{LO} and its higher order harmonics. This is obvious for squaring a cosine always ends up leaving a higher order term. Where in the second parentheses, the second term indicates a signal multiplication existing in the output current signal $v_{LO}(t)v_i(t)$, which is the reason why the circuit shown in Figure 4.15 is called "signal multiplier".

Now if we recall Euler's' equation, the cosine waveform of local oscillator signal could be written as:

$$v_{LO}(t) = \frac{1}{2}\left(e^{j2\pi f_{LO} t} + e^{-j2\pi f_{LO} t}\right) \quad (4.11)$$

Substituting equation 4.11 into the multiplication term in equation 4.9, we have:

$$v_{LO}(t)v_i(t) = \frac{1}{2}\left(v_i(t)e^{j2\pi f_{LO}t} + v_i(t)e^{-j2\pi f_{LO}t}\right) \quad (4.12)$$

For ease of understanding and calculation, the time domain explanation of equation 2.10 would be taken into frequency domain. Here we assume the frequency term of FM signal $v_i(t)$ as f_i. Here we're taking the carrier signal as the input, the actual explanation of FM signal is having infinite frequency but the result would be the same. If Fourier transformation is applied onto the equation 4.12, from frequency translation property of the transformation shown in equation 4.13, there exists a set of frequencies that includes $f_i - f_{LO}$ and $f_i + f_{LO}$.

If $\mathrm{F}(\omega) = \mathcal{F}\{v(t)\}$ where $\omega = 2\pi f$

$$\mathcal{F}\left\{v(t)e^{j\omega_0 t}\right\} = \mathrm{F}(\omega - \omega_0) \quad (4.13)$$

Detailed derivation of this conclusion is omitted here, for translation property of Fourier transform is one of several basic characteristics. Simple notation however, is given in equation 4.14.

$$\begin{aligned}\mathcal{F}\{\, v_{LO}(t)v_i(t)\} &= \mathcal{F}\left\{\frac{1}{2}\left(v_i(t)e^{j2\pi f_{LO}t} + v_i(t)e^{-j2\pi f_{LO}t}\right)\right\} \\ &= \frac{1}{2}\left\{\mathcal{F}\left[v_i(t)e^{j2\pi f_{LO}t}\right] + \mathcal{F}\left[v_i(t)e^{-j2\pi f_{LO}t}\right]\right\} \\ &= \frac{1}{2}\mathrm{F}(2\pi f_i + 2\pi f_{LO}) + \frac{1}{2}\mathrm{F}(2\pi f_i - 2\pi f_{LO}) \qquad (4.14)\end{aligned}$$

In the case of APT receiver, where the intended IF frequency, which is $f_i - f_{LO}$ inside the context here, is much lower than both f_i and f_{LO}. If we look at the expression in equation 2.7, it is easy to find that every single term but themselves are higher order terms of $v_{LO}(t)$ $v_i(t)$. Corresponding it to frequency domain it indicates that basically all of the frequency component of output signal is higher than two inputs themselves, let alone $f_i - f_{LO}$.

This means that by using band-pass filters (or, low pass filter in this case) tuned to certain frequency range, all other frequency component could be filtered out without meddling IF signal itself. Which, is the main purpose of adding a ceramic filter after the superheterodyne mixer. It should be noted that discussion of throughput gain and other properties of signal strength are omitted here for several ways of compensation could be

applied (such as adding extra buffer amplifier on output or RF amplifier at the antenna side).

4.5: Ceramic filter and IF filtration

As it is already noted in chapter 4.4, the output of superheterodyne contain numbers of frequency components other than desired 10.7 MHz IF signal, which poses a contamination to output signal. This phenomenon is happening under the ideal assumption that only clean LO signal and desired RF signal are inputted into mixer, and the output is already complicated as such. Those contamination signals are mainly made up of higher-frequency harmony of LO signal and their modulation between input RF signals. In the manner of signal strength, the harmonics of LO are dominant, because LO signal is usually much stronger than that of RF input.

Figure 4.16 shows the actual output of 1st superheterodyne mixer, measured from the prototype of APT-mixer, with LO, 137MHz RF penetrations and 10.7MHz IF being circled out. Other significant peaks marked out in blue are the harmonics of LO signals. From this figure it is obvious that most of contaminations are composed of higher frequency LO harmonics, while cross modulations are insignificant. In fact the RF signal inputted when obtaining Figure 4.16 is 50dbm stronger than calculated signal strength on receiving side, thus the cross modulations are expected to be weaker in actual usage.

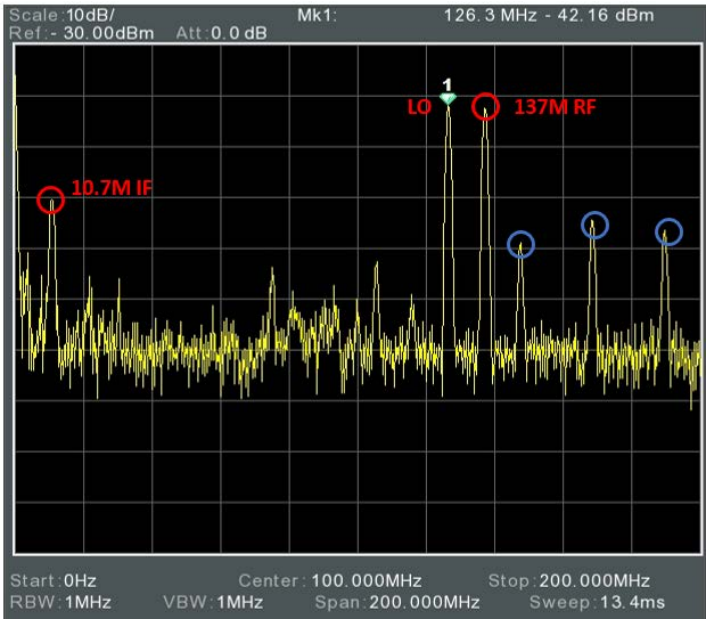

Figure 4.16: Output of first mixer measured in spectrum analyzer. The table below frequency spectrum shows the frequency and measured power of each marked peak

It is already explained in previous chapter that, all other frequency components in output signal except IF frequency, in the case of APT receiver (or typical FM receiver), is much higher than IF itself. Thus adding a Low-pass filter (LPF) after the mixer output could in theory filter out all the excessive distortions and create a relatively clean IF signal.

This is where the ceramic filter comes into the context. In major FM receiver that relies on superheterodyne mixing, a ceramic filer is almost always added to filter out high frequency harmonics of input signals and cross-modulation.

In the case of APT receiver, the IF signal is set to be 10.7 MHz just as any typical FM receiver, thus a widely adopted ceramic filter is applied for filtration. Figure 4.17 shows the circuit diagram of this part.

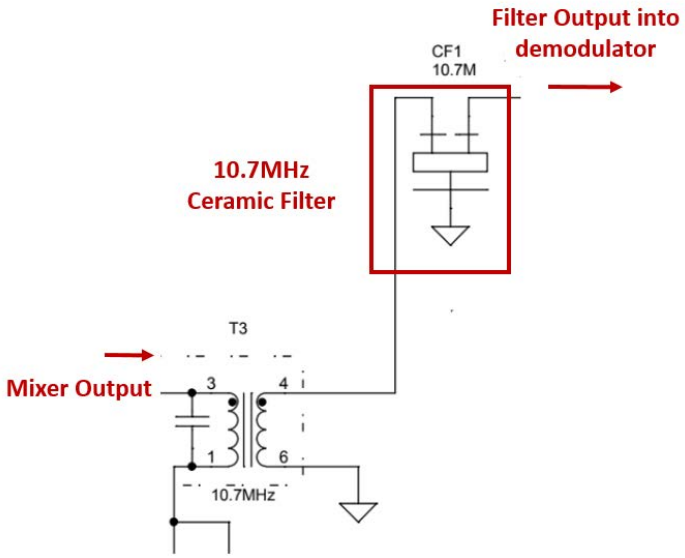

Figure 4.17: Circuit diagram of ceramic filter part

The output signal of superheterodyne mixer is first filtered at a certain degree though the adjustable inductor (also called IF transformer), then inputted into the ceramic filter.

The ceramic filter used here is a 3-pin transducer 10.7MHz ceramic filter produced by Murata Manufacturing.inc. The basic working principle and band-pass data is provided in following parts.

4.5.1: Working principle of Ceramic filter

In short, electronic ceramic filters share the same basic working principle with a crystal oscillator or crystal filter. Namely, ceramic filter is mostly a crystal oscillator, but the vibrating piezoelectric matter is changed into a certain type of ceramic.

Although the vibration mechanic is slightly difference between a typical crystal oscillator and a ceramic filter (Wang et.al, 207), ceramic filter still share the same equivalent circuit that of a crystal with same parameters. Equivalent circuit and parameters are shown in Figure 4.18 and Table 4.6

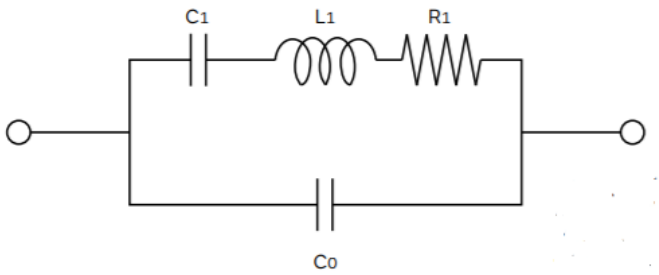

Figure 4.18: equivalent circuit of a typical ceramic filter

L_1	Equivalent series inductance
C_1	Equivalent series capacitance
R_1	Equivalent series resistance
C_0	Parallel capacitance

Table 4.6: parameters of ceramic filter equivalent circuit

Basically the same to those of a crystal oscillator, equivalent parameter of a ceramic oscillator is explained as:

The series inductance L_1 stands for the mass in mechanical oscillator, or the inertia of oscillating part itself. Series resistance represents internal friction during the mechanical oscillation of crystal. The equivalent series capacitance represents compliance of the crystal, a value to quantify the elasticity and plasticity during deformation of crystal. The capacitance between two electrodes in ceramic oscillator (not between two electrodes off the package, for parasitic capacitance is not accounted in this model) is represented by the parallel capacitance.

The image of 10.7MHz ceramic filter used in the prototype of APT receiver is shown in Figure 4.19, along with the corresponding symbol/pin assignment of the symbol used in circuit diagram. For additive information.

Figure 4.19 Image of 10.7MHz ceramic filter used in APT receiver, its syumbol in circuit diagram and corresponding pin allocation

4.5.2 Characteristic and performance of Ceramic Filters

While embedding a ceramic filter into the design of a receiver, several important characteristics have to be considered. We take the performance parameters of the ceramic filter used in APT receiver, shown in Table 4.7, as an example

Parts designation	SFE10.7
Center Frequency	10.7MHz
3db Pass Bandwidth	280±50KHz
20db Attenuation Bandwidth	590KHz max
Insertion Loss	3.5dB
Input/ Output matching impedance	330Ω

Table 4.7: Basic parameters of SFE10.7 ceramic filter used in APT receiver

Here, the center frequency, 3dB bandwidth and input/output matching impedance is the first to consider when evaluating ampleness.

The center frequency, without much debates, decides which frequency is intended to be passed in a BPF. Most of the design (on this part) start with selecting a BPF with corresponding center frequency. The 3dB pass bandwidth basically defines the band-pass of a BPF. 3dB means that the signal strength (in measure of dbm in this case) is attenuated into the half of input level. Namely, a BPF's pass-band is defined to be the frequency where the output strength of that particular frequency is the half of input. It is usually symmetrically located on both sides of center frequency. Thus in the case of SFE10.7, the 3db bandwidth could be calculated as: 10.56MHz~10.84MHz.

The input/out matching impedance defines the circuit design around the BPF. From the principle of impedance matching, only by matching the output/input side impedance of a node, could a sufficient signal strength be transferred. In this case the matching impedance is 330Ω in SFE10.7, which is a typical value for IF filter. This means that both the output impedance on mixer side and input impedance on demodulation IC side should be set as 330Ω. The IC is designed to be used with 330Ω impedance thus nothing special has to be done there. On the mixer side, by the tuning of adjustable transformer the impedance is corrected to be 330Ω. One thing to note here, there will always be an error existing in the impedance matching, thus some reflection on input/output of BPF will certainly occur. The idea there is that by matching the impedance to a certain level, reflection could be attenuated into an acceptable value. Band pass graph provided by manufacturer and actually measured band pass curve of a 10.7MHz ceramic filter is provided for intuitive understanding.

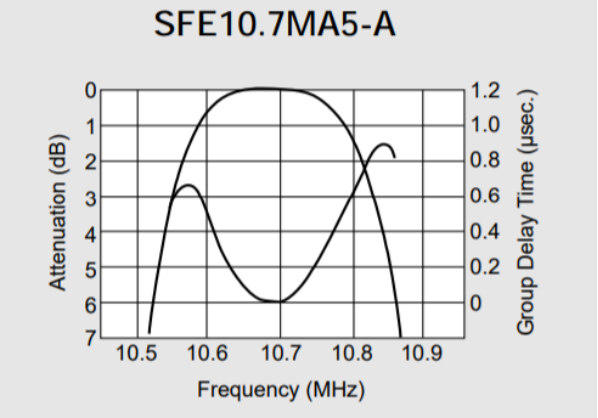

Figure 4.20: Provided attenuation-frequency curve and measured curve of SFE 10.7 ceramic filter (Murata, 1998)

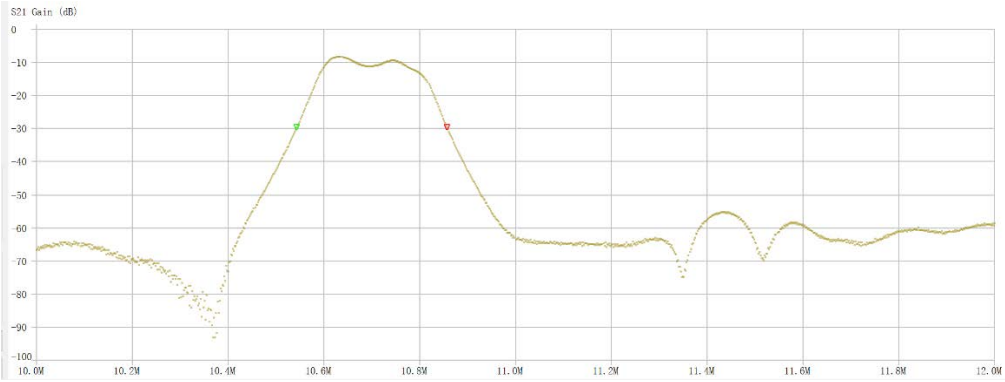

Figure 4.21: Measured throughput frequency-gain diagram of SFE 10.7.

The green and read marker on the -30dB gain indicates the frequency of 10.54MHz and 10.85MHz respectively. Compared to the -3dB passband frequency discussed above, it is clear that the bandpass-characteristic of this measurement is severely broadened.

It is mainly caused by the parasitic capacitance on the circuit etched to make this measurement, and the capacitance along the feed cable connecting the filter and the measurement equipment.

Additional information about the measurement of SFE10.7:
Because the filter itself is having input/output impedance of 330Ω while both port of Vector Network Analyzer (VNA) have the impedance of 50Ω, connecting two pins directly into the analyzer was just insufficient. A modification, or specifically designed matching circuit has to be made for measuring with sufficient result.

In fact measuring the signal in other parts of this circuit faces the exact same problem. But for those measurement are just for sake of validating the signal existence, thus a low-impedance probe could be used without much problem. Problems in signal strength is still resolved by tweaking adjustable components thus designing a specific circuit just for measurement is simply not worth the time and effort.

4.6: MC3361 Chip and FM demodulation

4.6.1: FM modulation

In order to introduce and discuss about the FM demodulator used in APT receiver design, the FM modulation itself should be clarified to some extent.

In chapter 2.5, while discussing the superheterodyne mixer and its frequency translation characteristics, the FM modulated RF wave is simply taken as:

$$v_i = v_i(t) \quad (4.15)$$

This was fine, to the most part, while discussing the mixer. Because the sideband in actual FM pre-envelope would get mixed with LO signal respectively, resulting in the complete shift of both sidebands in frequency. But while trying to explain the FM demodulation principle, several nature aspect of FM modulation and its expression has to be taken as a preliminary information.

For any angle modulation, where the phase angle varies based on the baseband signal amplitude, the modulated waveform could be given as:

$$\mathrm{F(t)} = \mathrm{A(t)}\cos\varphi(t) = \mathrm{A(t)}\cos[\omega_c t + \theta(t)] \quad (4.16)$$

Where the waveform itself is fully described by the amplitude A(t), carrier frequency ω_c and the phase angle $\Theta(t)$. In angle modulation, the amplitude of waveform (or pre-envelope) is fixed while the phase angle $\Theta(t)$ is controlled by the baseband modulating signal.

Frequency Modulation, a "branch" of angle modulation before anything else, is the result when the frequency derivation $\delta\omega$ of the instantaneous frequency $\omega(t)$, from the carrier frequency ω_c is directly related proportionally to the instantaneous voltage of baseband modulating signal.

Since the instantaneous frequency is the time differential of phase, substituting the previous equation, we have:

$$\omega(t) = \frac{d\varphi(t)}{dt} = \omega_c + \frac{d\Theta(t)}{dt} \quad (4.17)$$

For the derivation of instantaneous frequency $\delta\omega$, its relationship between carrier frequency and instantaneous frequency is given as:

$$\delta\omega = \omega(t) - \omega_c \quad (4.18)$$

Substituting the previous equation, the deviation of frequency $\delta\omega$ is given by:

$$\delta\omega = \frac{d\Theta(t)}{dt} \quad (4.19)$$

In frequency modulation, as it is noted in previous paragraph, the frequency deviation $\delta\omega$ is directly proportional to the instantaneous voltage of baseband-modulating signal $v_m(t)$, that is,

$$\delta\omega = k_m v_m(t) \quad (4.20)$$

k_m stands for the modulator sensitivity. Usually in telecommunication the modulator is thought to be a stable "thing" thus the sensitivity is taken as a constant. Namely for a specific FM transmission the instantaneous frequency deviation is dominated by the time varying modulating voltage $v_m(t)$

Thus, the phase of modulated signal and the voltage of modulating signal have the relationship while assuming initial condition to be zero:

$$\Theta(\mathrm{t}) = \int_0^t k_m v_m(t)dt \quad (4.21)$$

From the relationship of angle modulated waveform, we have the expression of FM modulated wave as:

$$F_{FM}(\mathrm{t}) = \mathrm{A(t)}\cos\left[\omega_c t + \int_0^t k_m v_m(t)dt\right] \quad (4.22)$$

There the modulating wave form is taken as a simple time varying signal. In the case of APT signal we already know the modulating waveform is a sinusoid signal with varying amplitude (which is amplitude modulated). Thus, if the modulating waveform is assumed to be a sine wave with varying amplitude expressed as:

$$v_m(t) = V_m(t)\cos\omega_m t \quad (4.23)$$

Substituting the relationship into eq. we get another expression of FM modulated wave:

$$F_{FM}(t) = \mathrm{A}\cos\left(\omega_c t + \frac{k_\omega V_m(t)}{\omega_m}\sin\omega_m t\right) \quad (4.24)$$

From previous analysis, it is not hard to figure out that the term $k_\omega V_m(t)$ is corresponding to the instantaneous frequency deviation δω. It the maximum deviation is defined as Δω, peak voltage of modulating signal is V_m, then we have the relationship:

$$\Delta\omega = k_\omega V_m \quad (4.25)$$

The ratio between maximum frequency deviation and carrier frequency is called modulation index. m_f

Any attempt of demodulating FM signal into baseband could be considered as a process of detecting the instantaneous frequency deviation and outputting signal proportion to that.

Note that the "carrier" frequency there does not only refers to the RF frequency of FM being transmitted from antenna. In the case of demodulator used in APT receiver the second IF frequency of 455 KHz is considered as the carrier.

4.6.2 MC3361 Chip and FM demodulation

4.6.1.1: MC3361 basic architecture and connection

In APT receiver, a compact FM demodulating IC with built in second IF amplifier, MC3361 from Motorola Semiconductor is selected. As it is already slightly touched in Chapter 2.5, the filtered 10.7MHz IF is taken as the input of demodulator, and the output here is the 2400Hz subcarrier signal. Placement and pin connection of MC3361 in the circuit diagram is shown in Figure4.22.Representative block diagram of MC3361 with inner connection is also shown in Figure 4.23

Note that the pin 10~14 is not used in this design, for those connections are deemed obsolete in APT receiver. In particular, squelch trigger, a method to turn off the demodulator (in order to shut the white noise) is omitted, for the receiver itself is not expected to be operated outside AOS and LOS of NOAA satellite.

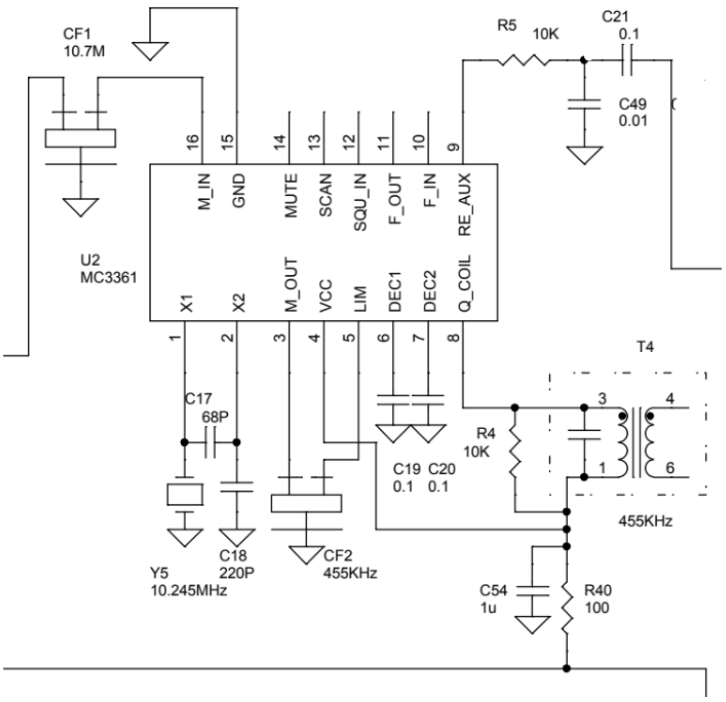

Figure 4.22: Circuit diagram showing pin connection of MC3361

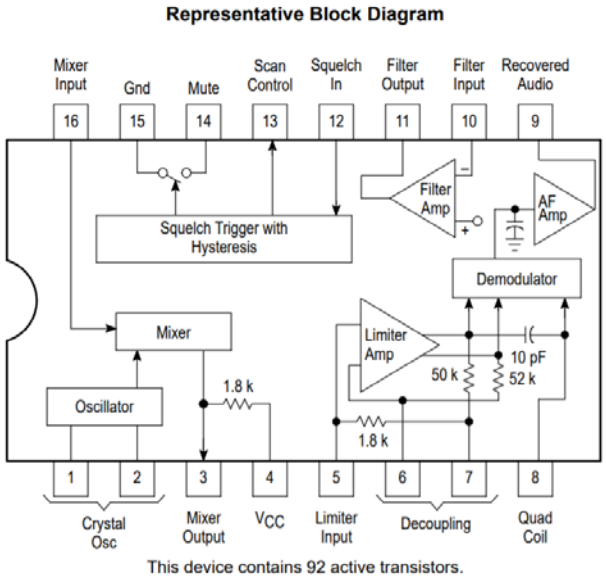

Figure 4.23: Representative block diagram of MC3361 with inner connection (Motorola.inc 1996)

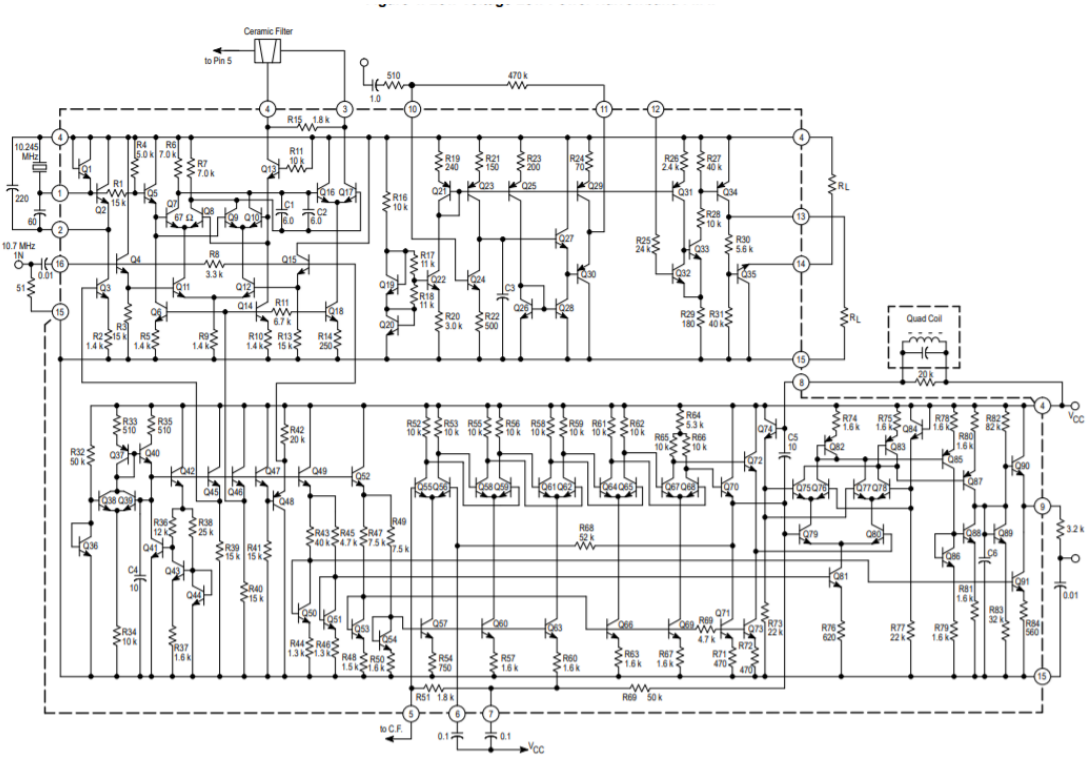

Figure 4.24: Transistor circuit diagram of MC3361. (Motorola.inc 1996)

It could be seen from Figure 4.23 and 4.22 that 1st IF signal with 10.7MHz frequency inputted through pin 16 reaches the mixer inside MC3661. This is the second

superheterodyne mixer designed to donconvert 1st IF into 2nd IF with lower frequency.

In the case of APT receiver, a common value of 455 KHz is designed to be the second IF, thus according to the discussion in 2.5, the second LO with 10.245MHz frequency is placed. Crystal oscillator for this purpose, marked as Y5 could be seen in figure 4.22. The superheterodyne is designed to deal with only one single center frequency thus only a single crystal oscillator is placed.

The mixer used here is different than Base-injecting BJT mixer used in 1st mixer, from the inner transistor diagram provided with the data sheet, Figure 4.25, it could be seen that a double balanced BJT mixer architecture is used here. In particular, BJT Q7~12 forms the double balanced BJT mixer which is usually called Guilbert cell. Other transistors in the region are for switching purpose.

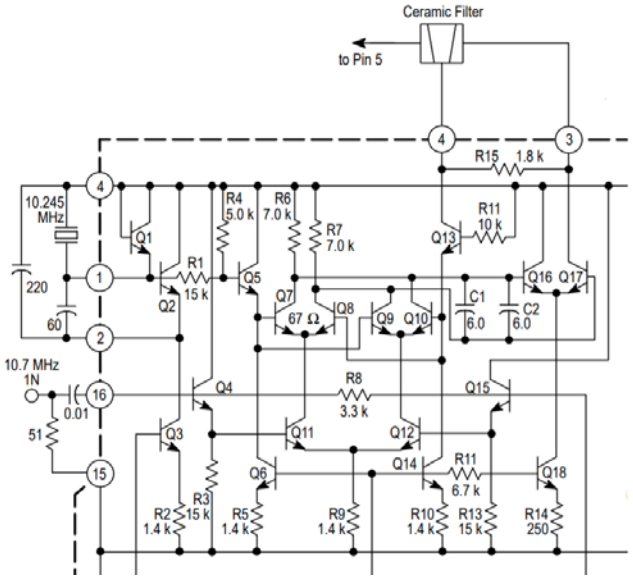

Figure 4.25 Magnified transistor diagram of 2nd IF micer part in MC3361

The mixer output is then outputted through pin 3 into the 2nd ceramic filter, as shown. There the ceramic filter with 455 KHz center frequency and 45 KHz bandwidth is chosen for better quality. The working principle is the same with SFE10.7 discussed in Chapter 2.5

After the filtration through CFULA45, the signal comes back into the IC through pin 5 as the limiter amplifier input. The signal itself is split into two section here, one going

into the limiter amp. The other gets outputted from the IC and goes through a transformer that is a Hilbert phase shifter. The architecture here is in fact forming a quadrature demodulator of FM signal, detailed operation and quadrature demodulation will be discussed in a separate section.

Limiter amplifier is used for normalizing the instantaneous amplitude, or voltage of the inputted 2nd IF signal. As it is noted in the FM modulation part, the amplitude or instantaneous amplitude of FM modulated signals does not change. However due to on-linearity of mixers and noise there are fluctuations in FM modulated IF signal.

After the IF signal gets demodulated into acoustic frequency baseband, it is amplified by the inner AF amplifier of MC3351 for output. The voltage after amplification is still not sufficient to drive any speaker or bear the transmission loss into soundcard thus another AF amplifying stage is set outside MC3361.

4.6.1.2 Quadrature FM demodulation used in MC3361

In MC3361 a FM demodulation method name Quadrature demodulation is applied. It is essentially a mixer and low-pass filter with two inputs: raw FM IF input and 90deg phase shifted IF input with same frequency. Mixing two signal with same frequency and 90deg center frequency phase shift produce series of outputs including a low-frequency term proportional to the instantaneous frequency deviation. By filtering out the low-frequency component of mixer output, the acoustic frequency is outputted. Mathematical explanation of quadrature demodulation and working principle follows.

It should be noted that the "Quadrature Demodulation" discussed there should not be garbled with I/Q demodulation method applied in digital modulation/demodulation (used in QAM mainly). There the RF input is directly put through a hilbert phase shifter and split into two I/Q signals. A system diagram of quadrature demodulator/detector is shown in Figure 4.26.

The quadrature demodulator, as shown in Figure 4.26 is a circuit operates in following sequences: (1) splits the IF signal into two parts (2) Passes one part through a network with 90deg plus certain constant times the IF deviation off center frequency (3)Mix the shifted and un-shifted components together (4) Select the audio spectrum parts of output components.

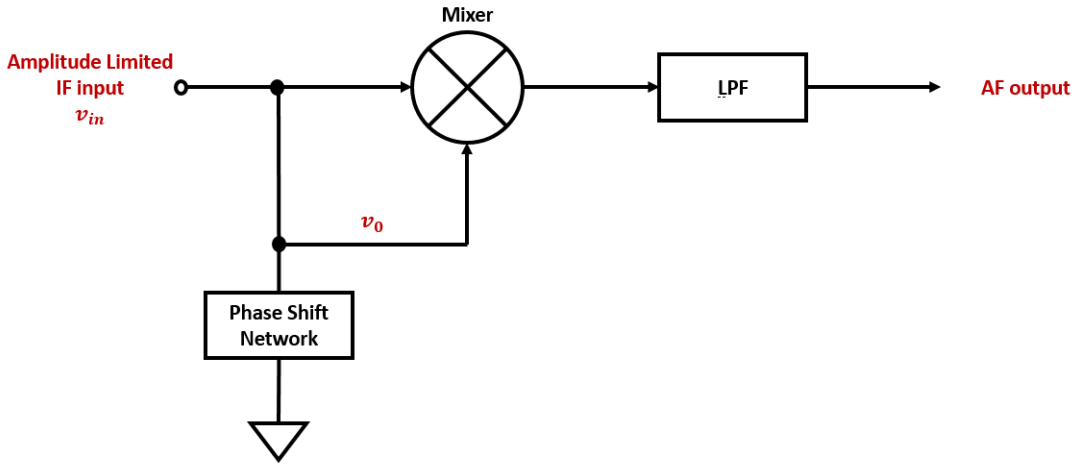

Figure 4.26: simple system diagram of a quadrature demodulator

Here we recall the FM modulated waveform in equation 4.26

$$F_{FM}(t) = \mathrm{A}\cos\left(\omega_c t + \frac{k_\omega V_m(t)}{\omega_m}\sin\omega_m t\right) \quad (4.26)$$

While the modulation index is defined as

$$m_f = \frac{\Delta\omega}{\omega_m} = \frac{\Delta f}{f_m} \quad (4.27)$$

Substituting the relationship into the $F_{FM}(t)$, we have

$$F_{FM}(t) = \mathrm{A}\cos\left(\omega_c t + m_f \sin\omega_m t\right) \quad (4.28)$$

Assume the IF central frequency ω_c (Krauss, 1980) and the instantaneous frequency ω, after the 90deg phase shift of center frequency, the phase difference $\Delta\theta$ could be expressed as:

$$\Delta\theta = \frac{\pi}{2} - \mathrm{C}(\omega_c - \omega) = \frac{\pi}{2} - C\Delta\omega \quad (4.29)$$

The term C stands for the constant ratio of phase shift relative to 90deg, based on the instantaneous frequency difference. It is fully dominated by the phase-change network hardware thus for a particular receiver it is set to be constant. The actual value of this parameter does not influence the working principle.

The FM modulated 90-deg shifted input could be expressed as:

$$F_{FM}(t) = \mathrm{A}\cos\left(\omega_c t + m_f \sin\omega_m t + \frac{\pi}{2} - C\Delta\omega\right) \quad (4.30)$$

Note that the amplitude A is thought to be a constant, due to the limiter amplifier designed in the previous stage.

The inputs into the mixer are then specified as:

$$v_0(t) = \mathrm{A}\cos\left(\omega_c t + m_f \sin\omega_m t + \frac{\pi}{2} - C\Delta\omega\right) \quad (4.31)$$

$$v_{in}(t) = \mathrm{A}\cos\left(\omega_c t + m_f \sin\omega_m t\right) \quad (4.32)$$

As it is already noted in 2.5, the mixer would output a term which is essentially the multiplication of two input signal (in time domain), expressed as:

$$v_{out,m}(t) = A^2 \sin\left(\omega_c t + m_f \sin\omega_m t + \frac{\pi}{2} - C\Delta\omega\right)\cos\left(\omega_c t + m_f \sin\omega_m t\right) \quad (4.33)$$

From the multiplication of trigonometric functions, there exists a term:

$$v_{out,AF}(t) = -\frac{A^2}{2}\sin C\Delta\omega \quad (4.34)$$

For FM modulation the frequency difference $\mathrm{C}\Delta\omega$ is sufficiently small that a very convenient approximation could be applied in sinusoidal function, which is:

$$\sin C\Delta\omega \approx \mathrm{C}\Delta\omega \quad (4.35)$$

Recall the definition of FM as an angle modulation, which define the instantaneous frequency deviation as a direct correspondent of voltage in modulating waveform.
We already know the term $\Delta\omega$ is directly proportional to the amplitude variance of baseband modulating signal. Thus, by filtering out the lower-frequency $\mathrm{C}\Delta\omega$ signal out of the mixer output could theoretically extract the baseband signal.

In MC3361, this demodulation is realized through connecting an outer phase shifting circuit (which is called balun) and mixing the signal through a gilbert's cell 4-dimentional

multiplier. The phase-shifting circuit is exerted from the IC design itself for a phase-shifting circuit tuned into a certain frequency only work with “that” frequency, while MC3361 itself does not restrict the IF input frequency, though loosely expected to be used in the frequency employed in APT receiver.

From Figure 4.27, it could be seen that the quadrature coil (another term of phase-shifting circuit) output is connected to pin 8, marked as Q_coil in Figure2.26. The inner connection is shown in Figure 24.27, a magnified image of transistor diagram is provided in Figure 4.25. The input from pin 8 is then inputted into another gilbert cell composed by transistor Q70~80. The direct input from pin5 goes through a set of limiter amplifier (identifiable from transistor connection) then taken as the input into gilbert cell mixer. The output is then amplified through several other transistors.

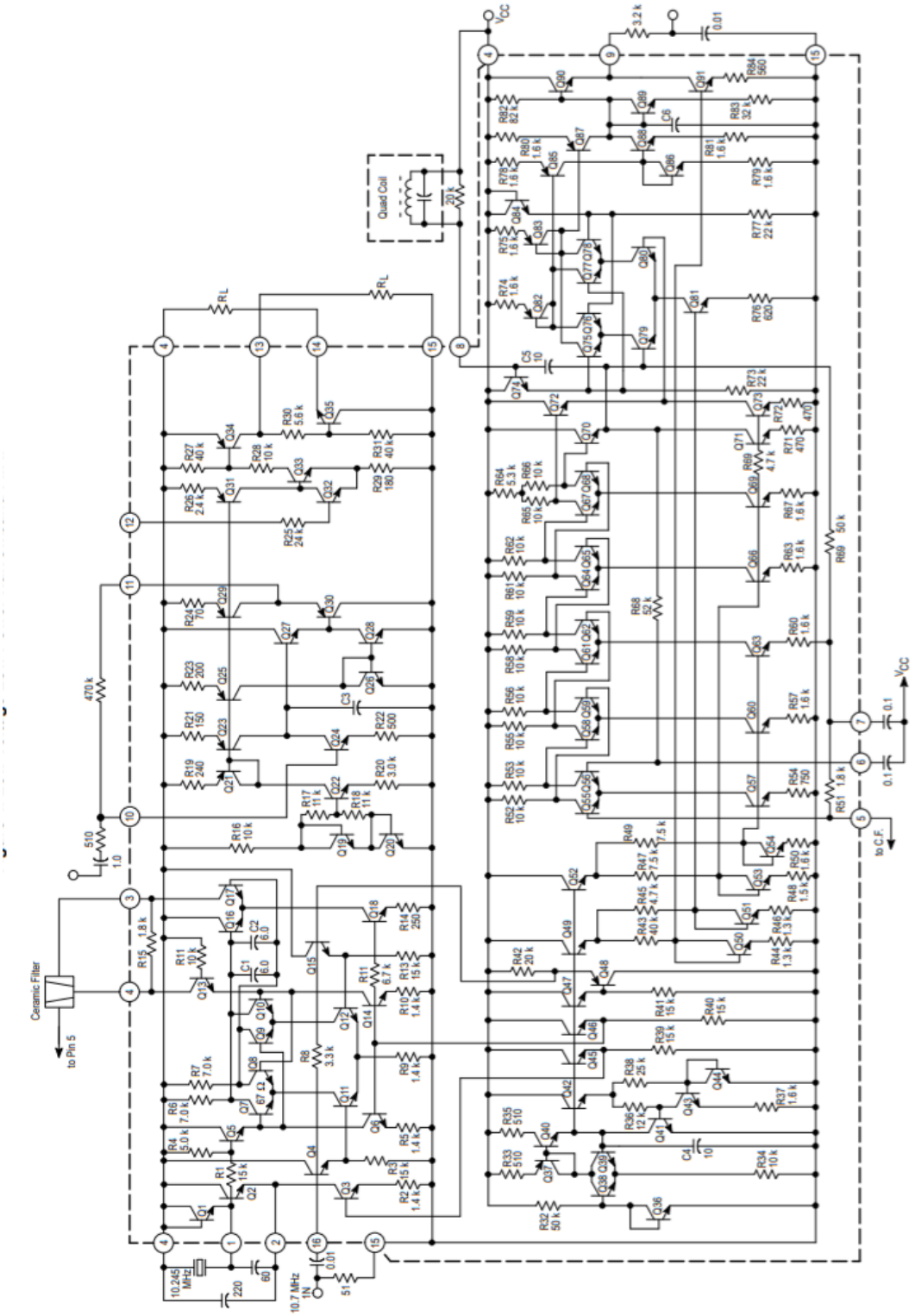

Figure 4.27: Magnified image of MC3361 transistor connection

Chapter 5: Evaluation of APT receiver performance

5.1 Local oscillator and up converter

The local oscillator of APT receiver design consists of 3 crystal oscillator tuned into different frequency and a set of up-converter/buffer, as it is already explained in Chapter 4.2.

Temperature compensated crystal oscillator (TCXO) commonly used in radio receiver design is not used in the design, for the receiver itself is not expected to be powered-on for any span of time that is longer than NOAA satellite pass duration. This implies that there is no closed-loop feedback system as a manner of keeping oscillation frequency stable. On the other hand as a narrow-FM receiver, frequency stability of local oscillator is an important aspect in good receiving quality. Thus the oscillation precision and steadiness of crystal itself, and upconverter/buffer quality need to be evaluated.

Before implementing, or soldering the crystal oscillator into the radio itself, ever single crystal oscillator ordered in the batch has been tested for its frequency. As it is already introduced in local oscillator chapter, an ideal crystal oscillator has two resonant frequencies: series frequency and parallel frequency. In most of the application, series resonant frequency is used thus in the measurement of crystal itself we're mainly discussing about it.

The measurement of a crystal's characteristic frequency is conducted by a vector network analyzer. A simple diagram showing the measurement setup is shown in Figure 5.1

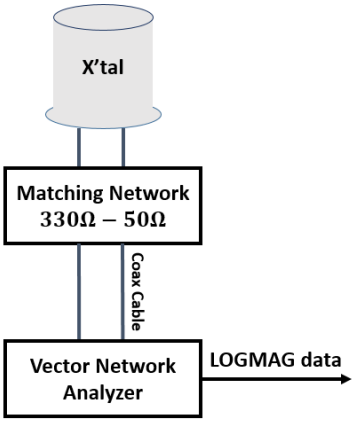

Figure 5.1 Simple system diagram of crystal measurement

The crystal oscillator itself has a characteristic impedance of 330Ω while the vector network analyzer has 50Ω, thus a matching network has to be designed for accurate measurement. Although the impedance matching itself does not impress a huge effect on the frequency accuracy.

The design of matching network is a rather tedious process of fighting with weird calculation result and parasitic capacitance while soldering the parts.

The "logmag" data shown in Figure 5.2 stands for the passing characteristic of crystal oscillator. As it is explained in IF ceramic filter part the impedance at the serial resonance frequency would be the smallest (i.e. an extremely narrowband BPF) thus by measuring the frequency response would provide the exact resonance frequency.

Typical log-mag result is shown in Figure 5.2 with horizontal axis as frequency from 10.2MHz to 10.3MHz, and vertical axis as gain (dB) The figure itself is a result while measuring the 10.245MHz crystal for 2nd IF generation.

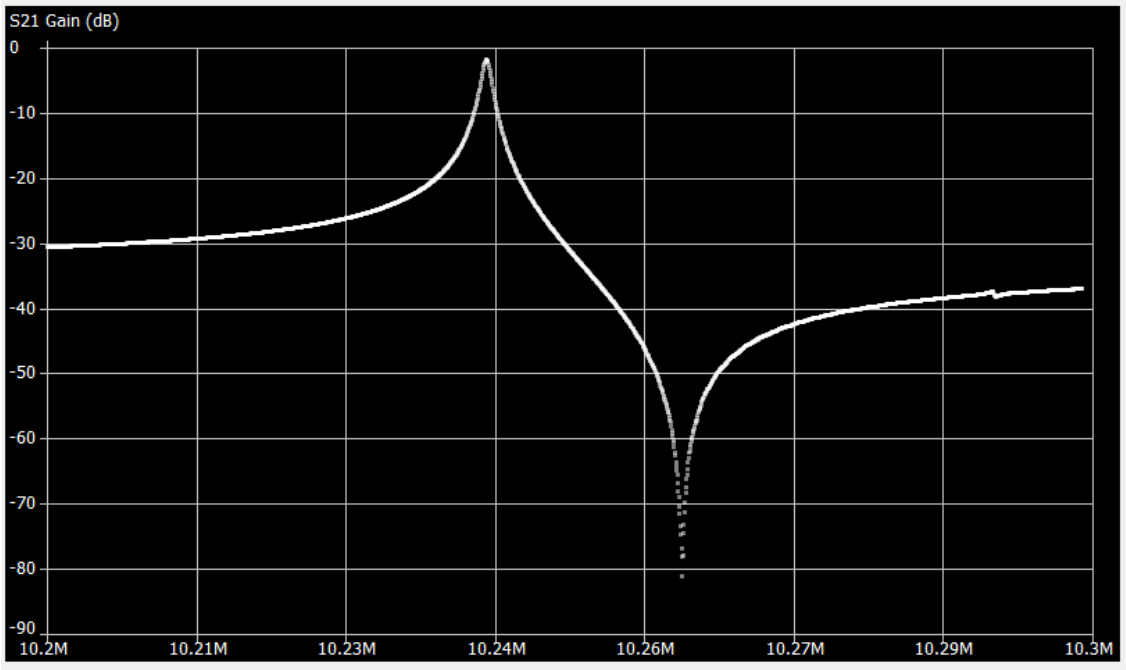

Figure 5.2: S21 Gain (Log-mag) plot of transfer characteristics generated from VNA (measured on 10.245MHz crystal)

It is obvious that the return loss is the smallest at the series resonant frequency. Showing all the result from measured crystal would be too obsolete thus a table is provided with labeled crystal frequency and measured result.

satellite	Marked	Batch number	measured frequency

channel	Frequency		
NOAA19	21.0665MHz	1	21.0568MHz
		2	21.0567MHz
		3	21.0565MHz
NOAA18	21.2000MHz	1	21.1905MHz
		2	21.2908MHz
		3	21.1906MHz
NOAA15	21.1533	1	21.1437MHz
		2	21.1437MHz
		3	21.1436MHz

Table 5.1: Measured frequency of ordered crystal oscillator

It could be seen from the table that the measured frequency of ordered crystals are all very close to the marked frequency to a point that no effect on mixing RF signal will occur in the current bandwidth.

Certainly all these crystals are ordered and specially cut for this frequency, which means that the frequency would be checked in-site. However, another batch of crystal ordered from a different place had a huge frequency deviation to a point that nothing would get demodulated from APT signal, deeming the necessity of frequency checking procedure. The next important aspect in this LO design is the performance of up-converter and the quality of output LO signal into the mixer.

Different to the frequency of a crystal oscillator, upconverter's performance and LO signal could only be sampled after soldering everything into the designed PCB, thus there will not be any "convenient" matched connector plug to insert the measuring device (in this case, a spectrum analyzer). Thus a probe is required to sample the electronic signal directly from the pin of a transistor or inductor. Similar to the crystal oscillator's case a simple system diagram of the sampling process is shown in Figure 5.3 and Figure 5.4

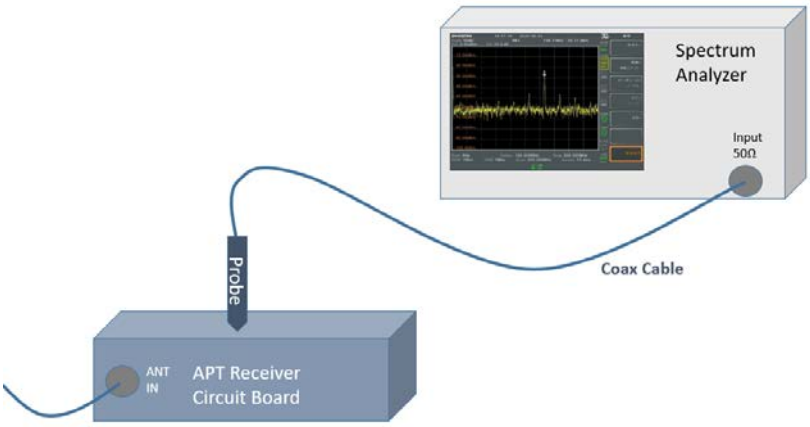

Figure 5.3: Simple image showing the measurement of APT receiver using spectrum analyzer

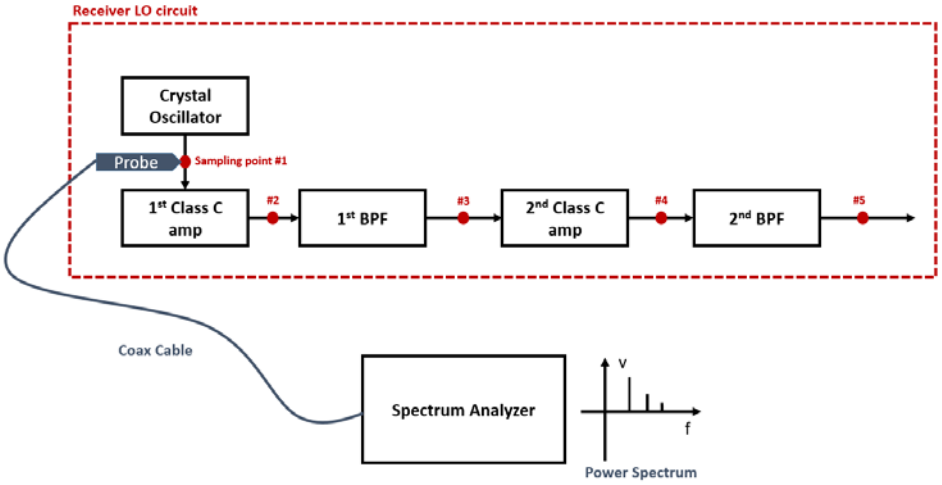

Figure 5.4: Sampling point relative to different module in LO

Several sampling points are chosen:

#1 the output of crystal oscillator/input of first stage up-converter

As it is already discussed in LO section the crystal oscillator's oscillation itself is slightly controlled by trimmer capacitor, in order to compensate for parasitic properties. Measuring the oscillation at this output is in fact necessary for modifying the oscillation in to desired value.

Another aim of this sampling point is to measure the time variance and temperature related variance of crystal oscillator. For the receiver is not expected and deigned to operate for extensive time period both of the measurement is qualitative.

#2 Output of first class-C amplifier

Based on the non-linearity of class-C amplifier the harmonics of input frequency are generated. Measuring the frequency component at this point mainly focuses on the existence of 3rd pitch harmonic.

Based on the architecture of class-C amplifier the measurement the probe is connected to the collector pin of transistor.

#3 Output of First BPF (up converter)

During the initial set-up of receiver, measuring signal's frequency at this point is necessary for adjusting BPF which is an adjustable transformer. Because the whole up-conversion circuit include 2 stage of class-C amplifiers, passing through unwanted frequency could lead so several problems. By comparing this measurement from that of #2 could also indicate how much attenuation the transformer is adding on the signal.

#4 Output of second class-C amplifier

Similar to that of the first class-C amplifier, this measurement is mainly for the existence of "wanted" frequency to be passed through BPF. Ideally the frequency component should only be consisted by the 6th harmonic of crystal frequency and leakage of input frequency.

#5 Output of second BPF (output of the LO before buffer)

Due to the fact that Buffer circuit is designed to be balanced and thus not meditating frequency, the output of second BPF could be considered as the final LO output (frequency-wise). Ideally only the LO frequency around 127MHz is observed.

Another important aspect there is the probe used in measurement. In the measurement LO and following mixers, an oscilloscope passive probe shown in Figure 5.5 is used. The probe itself is set to be high impedance so that the measurement itself would not bring excessive effect on the measured circuit.

In fact the passive probe is not recommended for being used in spectrum analyzer, for its throughput frequency response varies on different frequency range. Namely, the attenuation of probe itself could be drastically different while measuring 100MHz and 1500GHz. However, we're only measuring frequencies within the range of 0.0024~100MHz thus the deviation of attenuation characteristic is assumed to be a constant.

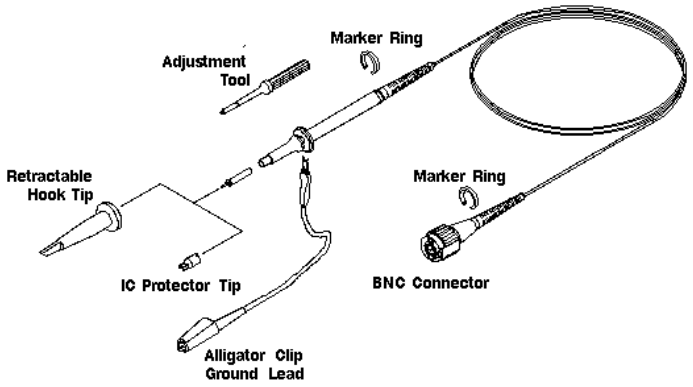

Figure 5.5: Image of a typical high impedance passive-probe (David Heeres, 206)

The attenuation characteristic of this passive probe is obtained by connecting the probe itself into a calibrated signal generator then observe the power obtained and displayed by the spectrum analyzer. Table 3.2 provides the measurement data on several frequency and power.

Signal Source	Power/Amplitude	Frequency	Measured Power
Tektroniks AGF1001	-35dBm	1MHz	-47.35dBm
	-35dBm	5MHz	-47.50dBm
	-35dBm	7MHz	-48.50dBm
	-35dBm	10.7MHz	-48.58dBm
	-35dBm	15MHz	-48.44dBm
	-35dBm	20MHz	-49.73dBm
	-35dBm	21.15MHz	-49.39dBm
	-35dBm	25MHz	-49.20dBm

Table3 .2: Measurement of Probe attenuation prperty

In practice, active probe with compensated attenuation property is preferred for constant frequency response over designated frequency range. An attempt of designing an active probe has been done and if there's any outcome the report will be included in Appendix section. Frequency diagrams measured from passive probe are listed in sections below. Note that in all of the frequency plot shown in this part, frequency (horizontal axis) increase from left to right, and the vertical axis stands for the power with dBm unit.

Also, the zero-point of vertical axis also changes with preset reference level. All the figure shown in this thesis omits the scale display to avoid interference with actual signal peak. For description of reference level and scale, refer Appendix 02.

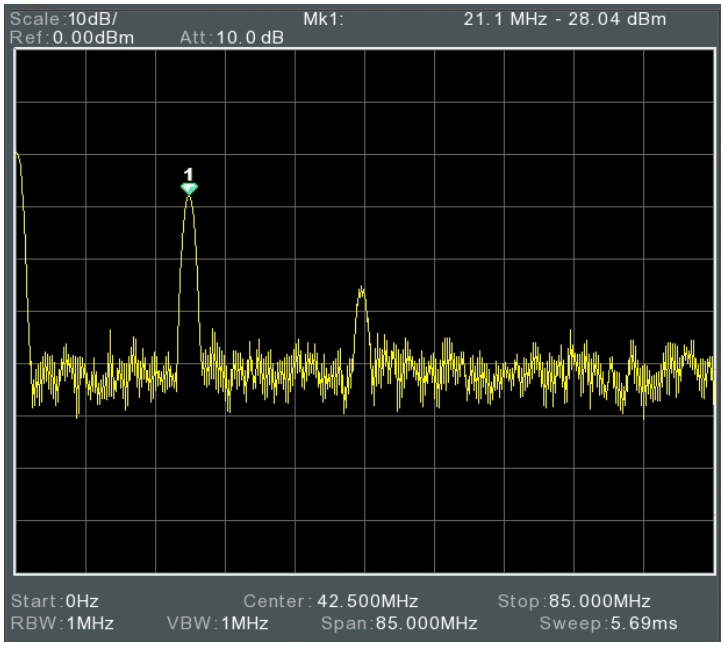

Figure 5.6: Spectrum analyzer plot of signal captured on sampling point 1 (21.1MHz crystal used)

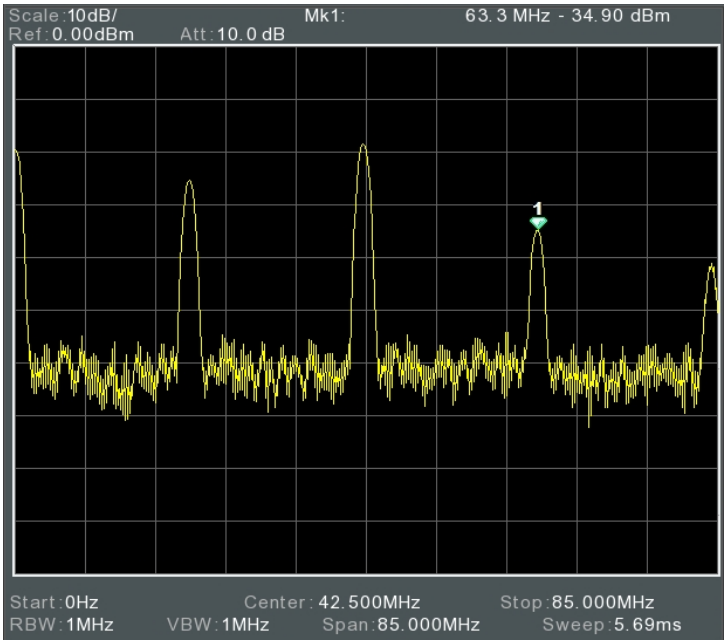

Figure 5.7: Spectrum analyzer plot of signal captured on sampling point 2

Figure 5.6 and 5.7 shows the frequency profile captured at the 1st stage of up-converter, (with 42.5MHz center frequency and 85MHz span) where the crystal oscillator frequency of 22MHz is brought up to its triple harmonic of 66MHz. Details were discussed in LO section of chapter 2.

The sampled signal in Figure 5.6 comes from the base of 1st upconverter transistor (No TP is designed in the actual board thus only available signal source closest to crystal was there). Two frequency peak could be observed in the figure, which is the basic oscillation frequency and its second harmony. Usually there should only be base frequency with 22MHz for all parts before sampling point #1 is supposed to be having a linear response. This harmonic is acceptable though, for the exact frequency appears after the class-c amplifier.

Figure 5.7 shows the signal sampled from point #2, right at the collector of 2sc2668, the transistor used in upconveter. Centre frequency and range are the same with Figure 5.6. 2nd and 3rd harmonics of 22MHz signal, with 3rd harmonic 66MHz being the desired frequency, could be observed. From the circuit design of Figure 2.3, mixed-frequency output is then filtered through a single transformer (as a BPF), which is then sampled from point #3. Result taken from spectrum analyzer is shown in Figure 5.8.

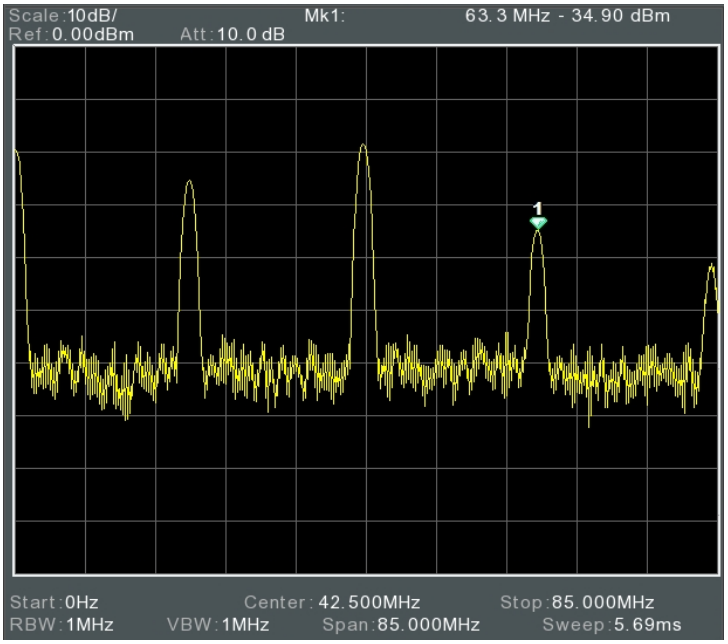

Figure 5.8: Spectrum analyzer plot of signal captured on sampling point 3

It is obvious that the adjustable transformer is suppressing all but 66MHz harmonic quite efficiently, attenuating the (previously) largest 44MHz frequency component by approximately 30dBm. Although the unwanted signal could barely be seen in the figure, those signals still exist with much lower intensity. For some extent this is due to the reference level of spectrum analyzer itself, thus the "filtered" out signal could still be

observed clearly if reference level is lowered into certain value. Signal sampled from the second stage of LO upconverter is shown in Figure 5.9 and 5.10.

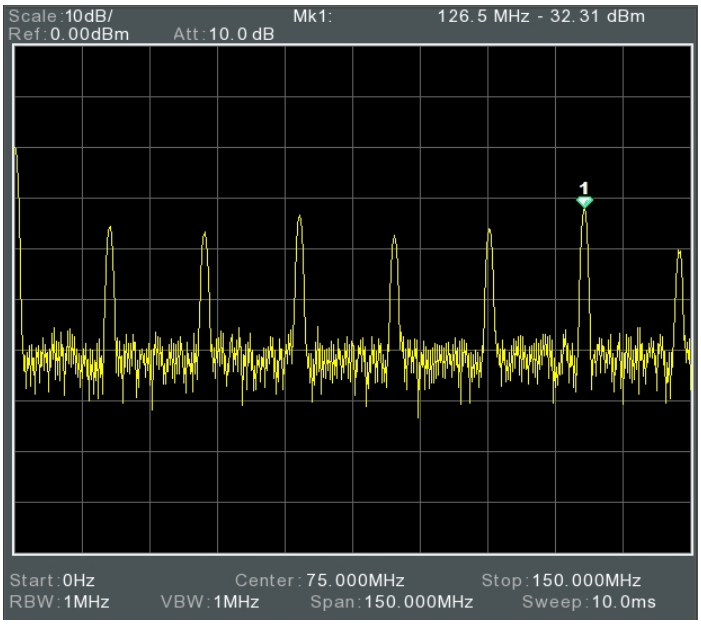

Figure 5.9: Spectrum analyzer plot of signal captured on sampling point 4

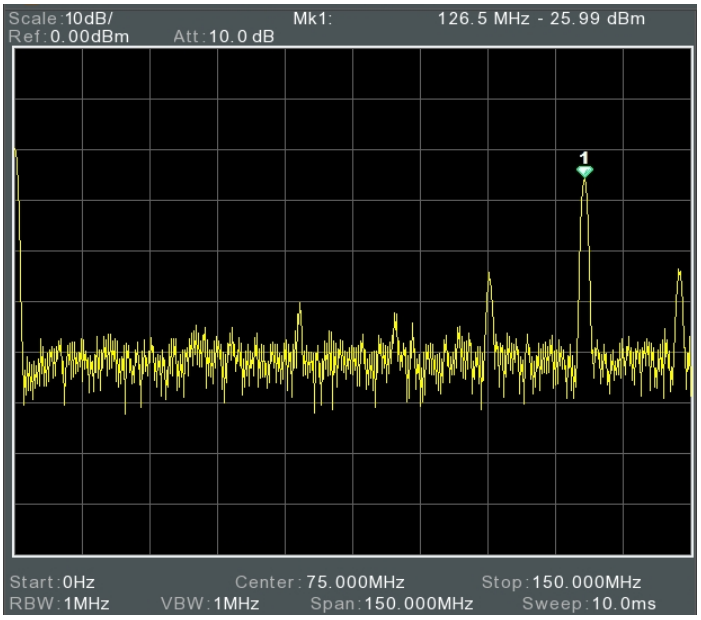

Figure 5.10: Spectrum analyzer plot of signal captured on sampling point 5

Figure 5.9 shows the frequency plot of signal sampled from point #4, with a wider span of 150MHz (in order to display all the frequency up to 6th harmonic of crystal) and centre frequency of 75MHz. It could be seen in the figure that all the harmonics from 2nd to 7th is present in the signal, but with lower intensity than that observed in point #3. This is caused by the signal presence after filtration (as described in previous paragraph) getting amplified in the transistor. After passing the transformer tuned into 120MHz, it

could be seen from the Figure 5.10 that the lower-frequency part of the signal is basically attenuated into the noise floor. In typical band-pass filters constructed by tuning transformers the attenuation characteristic in low-frequency side is usually better than the higher-frequency side(when reaching UHF band the attenuation will deplete quickly due to the coupling effect between parts), and the pass-band is always quite wide (corresponding to a low Q number) thus the component around 150MHz still exists.

The 150MHz "leak-through" from BPF into the superheterodyne mixer will produce a frequency component around 20MHz after mixing with incoming APT signal. However the frequency component is filtered out by the tandem ceramic filter thus won't affect input into MC3361.

5.2 Superheterodyne mixer

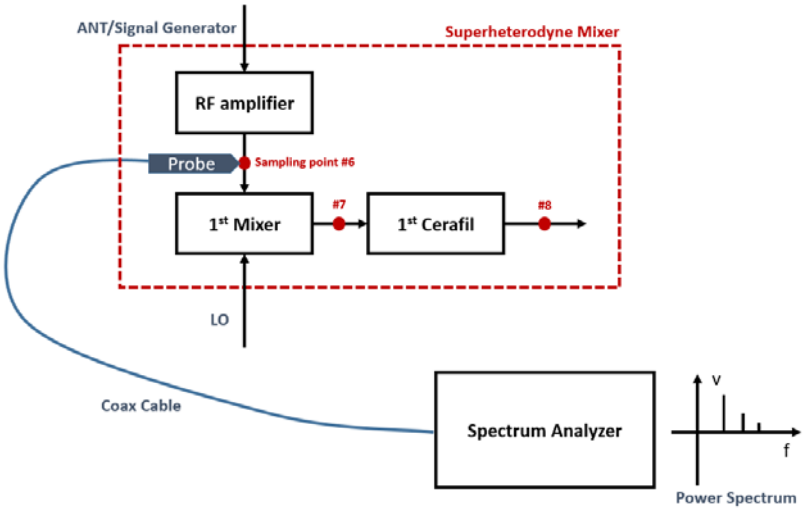

Figure 5.11: Sampling point on superheterodyne mixer

For the superheterodyne mixer part the measurement is basically the same with LO, where passible probe is connected into several sampling points to measure frequency component of a signal. Similar to Figure 5.4 the sampling point is shown in Figure 5.11 Because the receiver itself is designed for receiving satellite signal which is not always available and weak, a signal generator is used for generating RF input signal side of superheterodyne mixer. There a simple RF generator using ADF4351 PLL chip, and coupled band-pass filter is used to generate required signal of 137MHz. The ADF4351 PLL chip could only output square-wave under 2.2GHz and clear sine wave over 2.2 GHz thus a band-pass filer is used for filtering out harmonics of 137MHz. The S11 characteristic of band-pass filter used here is noted in Appendix A.01. Here the harmonic

analysis of signal generator before and after inserting BPF is shown in Figure 5.12a and 5.12b.

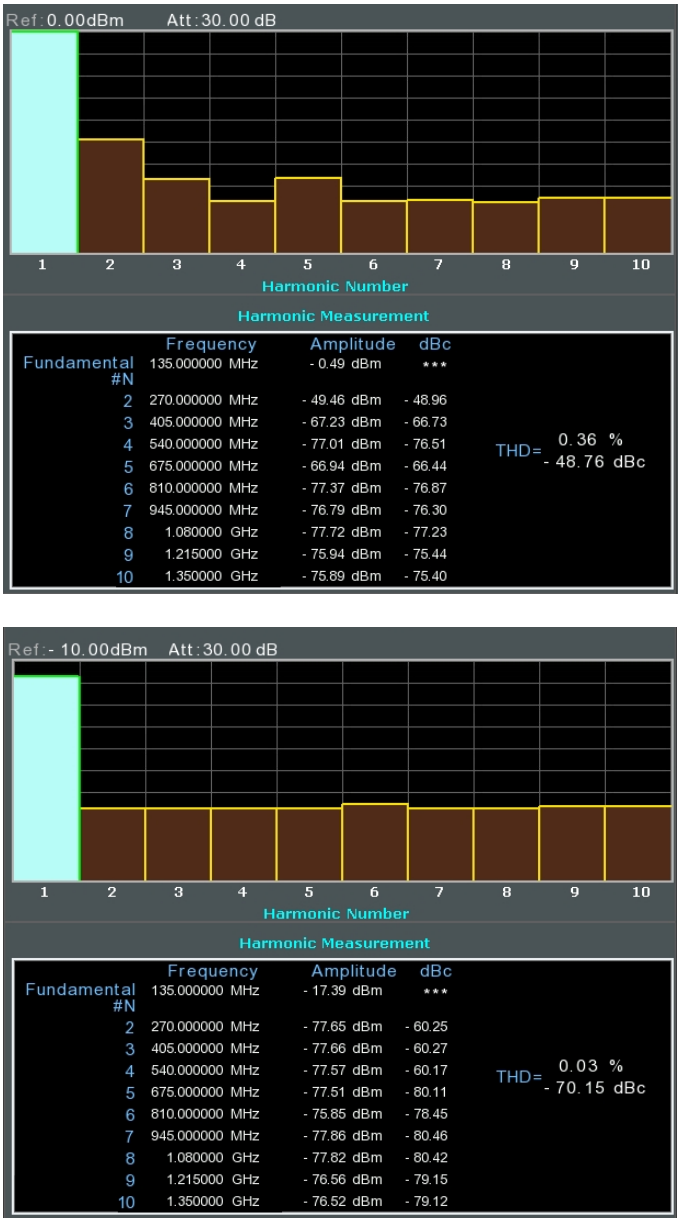

Figure 5.12(a): Measured harmonic profile of 135MHz square wave without BPF

5.12(b): After inserting BPF

For figure 5.12, every square in upper section stands for detected harmonics of input signal with corresponding frequency, the list below shows the frequency of every detected peak and their intensity in dBm. Harmonics of 135MHz is getting attenuated quite substantially into around -70dBm by this BPF with a price of 16db attenuation in desired frequency.

137MHz signal is then inputted into superheterodyne mixer with LO output signal. Result retrieved from sample point #7 after the RF amplifier is shown in Figure 5.13.

Note that the RF signal input is unmodulated clean wave, thus the signal shape itself (in frequency diagram) is different to FM modulated, and thus demodulation could not be tested.

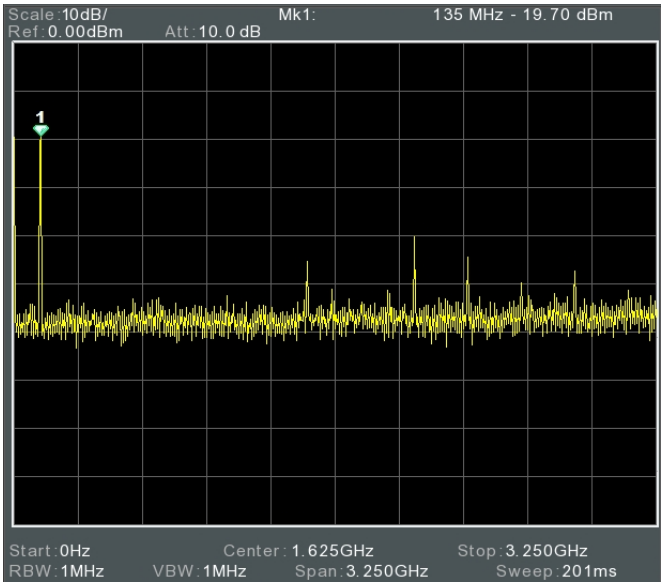

Figure5.13: Sampled signal from point #6 Full Span.

It could be seen that the 137MHz signal (clean wave) is relatively clean, for several stage of filter including T3 in circuit diagram has filtered out substantial amount of noise or harmonics generated by the RF signal generator. After the mixing in superheterodyne mixer the signal is sampled in point #7 in order to observe the direct output of mixer in Figure 5.14. It could be seen that both LO and RF signals have leaked with considerable amplitudes. Desired signal in 10.7MHz could also be observed from the plot.

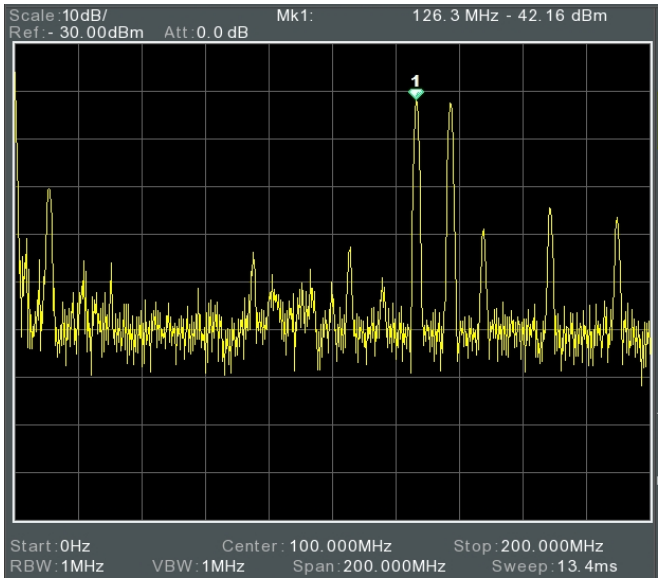

Figure 5.14: Signal sampled from point #7

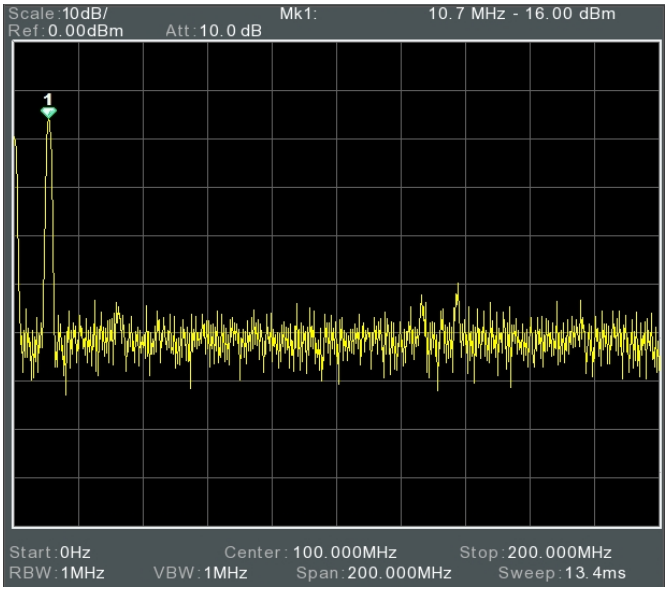

Figure5.15: Signal sampled from point #8 and their peak list

Signal sampled from point #8, after filtration from 10.7MHz ceramic filter is shown in Figure .15 with 0dbm reference compared to -30dbm in previous measurement. The amplitude of 10.7MHz peak5 is increased in the The S11 passing characteristic of this filter is already shown in Figure 4.20 of Chapter 4. A clear peak of 10.7MHz could be seen in the figure with attenuated cross modulation frequency and LO/RF pass-through. This is fully expected from the steep band-pass characteristic of 1st ceramic IF filter.

5.3: 2nd IF and demodulator sensitivity

The signal after SFE10.7 (10.7MHz 1st IF filter) is processed in the MC3361 FM demodulator chip, thus the measurement could only be done on specific external pins.

As it is already discussed in Chapter4, the filtered 10.7MHz output of 1st IF filter is inputted into the 16th pin of MC3361. The signal then goes through another superheterodyne mixer inside MC3361, downconverted with 10.245MHz 2nd LO signal into the 2nd IF signal with 455 KHz. Figure 5.16 shows a simple diagram of MC3361, highlighting the sampled pin and several sampling points.

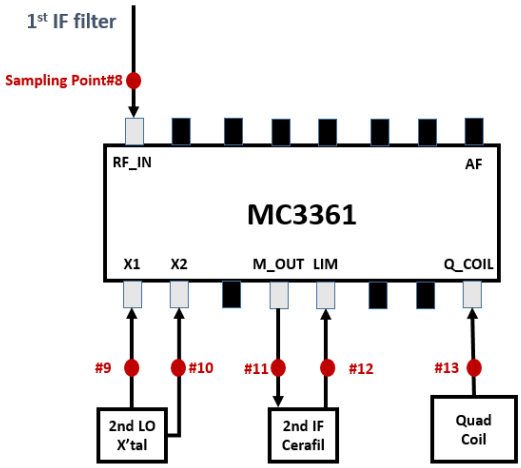

Figure 5.15: Sampling points and sampled pin (highlighted in light grey) of MC3361

The sampling point #9 and #10 are selected to monitor the oscillation of the 2nd local oscillator, which is designed to downconvert the 10.7MHz 1st IF into the 2nd IF with 455 KHz. From the relationship within the superheterodyne mixer the oscillation frequency of 2nd LO is determined as 10.245MHz.

Sampling point #11 and #12 are selected for monitoring the output of 2nd superheterodyne mixer and connecting ceramic filter. The discussion of this 455 KHz filter is negated in Chapter 4, because its only difference to the 10.7MHz filter is the filtering frequency. In particular, the output from 2nd mixer is sampled from #11 and filtered signal from #12.

In order to verify the operation of quadrature coil the sampling point 13 is selected. From discussion in 4.6.2 the quadrature coil is equivalent to the phase shift network. The 455 KHz signal measured there should have a 90 degree phase difference with the one taken from point 12.

No sampling points are placed in AF signal output pin, because non-modulated signal is used in this test process thus no AF baseband is contained in the RF signal input to the receiver. Measured signals are shown in following discussions.

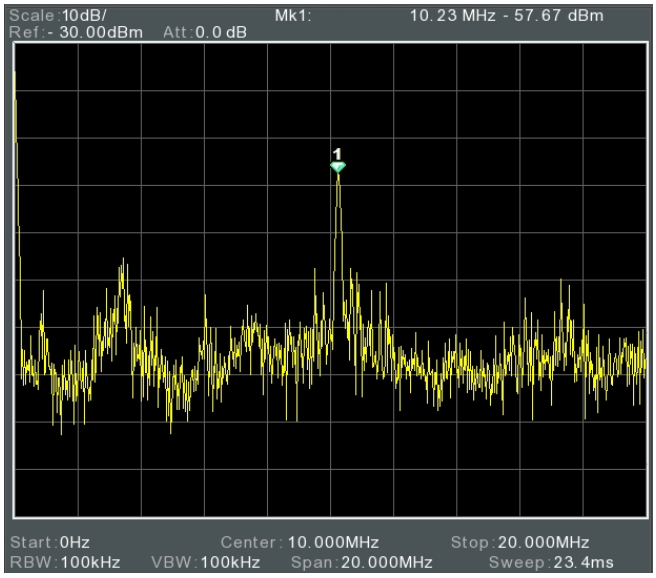

Figure 5.16: Signal sampled from #10

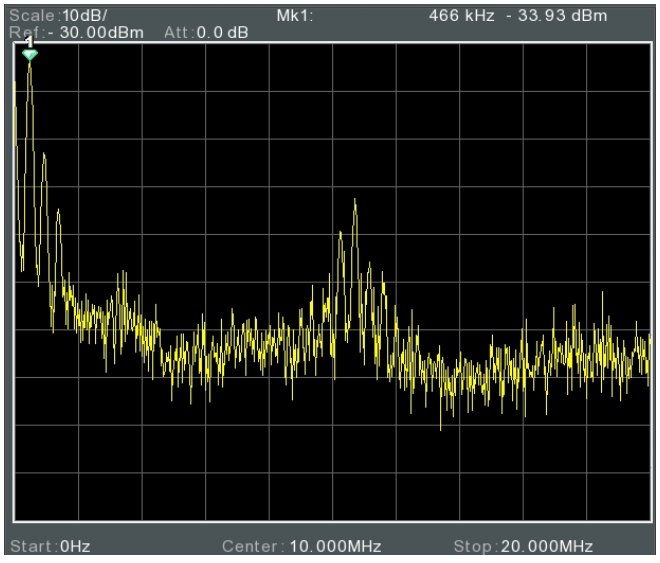

Figure 5.17: Signal sampled from #11

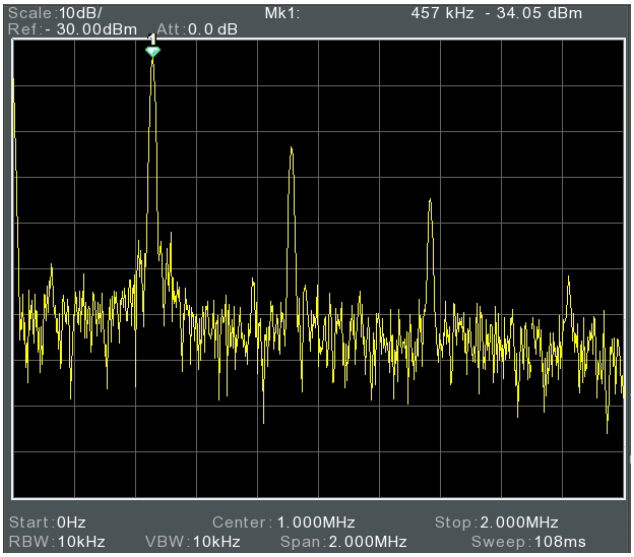

Figure 5.17: Signal sampled from #11 magnified

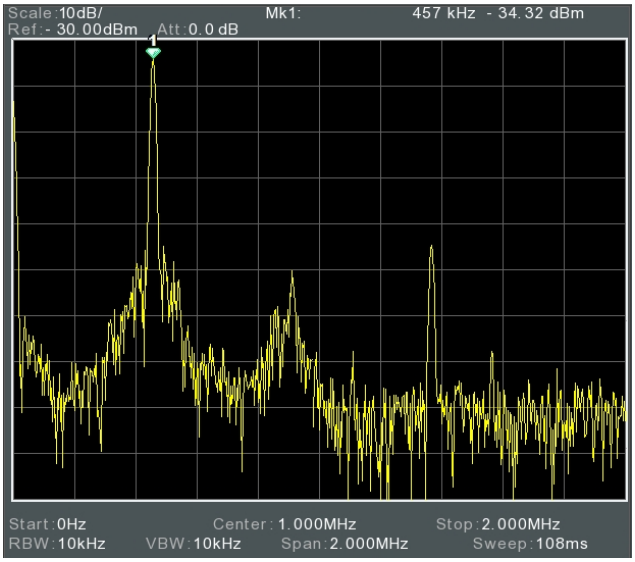

Figure 5.18: Signal sampled from #12 same span with figure 5.17

From Figure 5.16, a clear peak at 10.245MHz could be observed in the frequency plot. The signal is directly sampled from the pin of crystal oscillator thus the power is relatively small at -57dbm. Figure 5.17 shows the signal sampled at the output of 2nd superheterordyne mixer, where LO signal and 1st IF signal could be seen around 10MHz and several peaks at lower frequency side could be spotted. The same measurement result magnified around 1MHz (center frequency set to be 1MHz and Span 2MHz) is shown in Figure 5.17. Note that the 457MHz marker display comes from the sampling rate, the actual frequency is still 455 KHz if the span is set to be smaller.

Three extra peeks could be seen around the 455 KHz, supposedly 2nd, 3rd and 4th harmonics of 2nd IF output caused by transistors before the pin out.

The signal after the filtration of ceramic filter is plotted in Figure 5.18. Compared to unfiltered signal, the second harmonic of 455 KHz IF is obviously suppressed significantly. Attenuation of previous noise floor could also be seen around 455KHz peak, as the concaved shape. The 3rd harmonic of IF signal does not see much attenuation, but the frequency component itself has a power 40dB lower than the IF signal so this is acceptable. In fact all other unwanted components including the carry-over of LO and 1st IF gets attenuated significantly by this filter, but the figure is negated here because 455 KHz signal would emerge with DC component under that span settings.

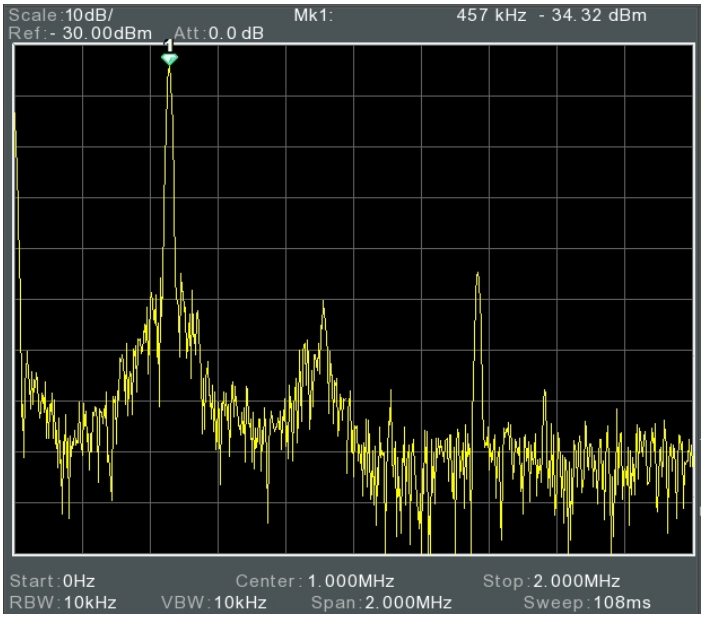

Figure 5.19: Measured time domain signal from sample point #13

The time domain signal of sample point 13 obtained from oscilloscope is shown in Figure 5.19. Obviously the signal itself is distorted by the higher frequency components observed in previous measurements. The comparison between the previous IF signal indicates a phase change around 90 degrees (0.5 pi) and a working quad coil.

5.4: Receiving APT

With liability of analog front-end including local oscillator, all superheterodyne mixer and connected filter been examined in previous chapter, actual receiving of APT signal is then tested. As it is noted in 5.3, only unmodulated 137MHz signal generated by the ADF4351 is used in testing front-ends. In this section actual APT signal broadcasted from NOAA satellite is used. In receiving the APT signal, QFH antenna is set on a place with wide field of view, in order to reduce hindrance blocking signal as much as possible. The Rx input of APT receiver is then directly connected into the antenna, while its AF output is connected into the microphone input of a PC to sample demodulated 2.4 KHz subcarrier signal. The demodulation of subcarrier AM signal and frame reconstruction is either processed in an open source package or demodulated in GNU radio. Detail will not be discussed here. The system diagram of receiver and antenna connection, and photo taken while the author was receiving the signal in Kashiwa Campus shown in Figure 5.20a and 5.20b respectively.

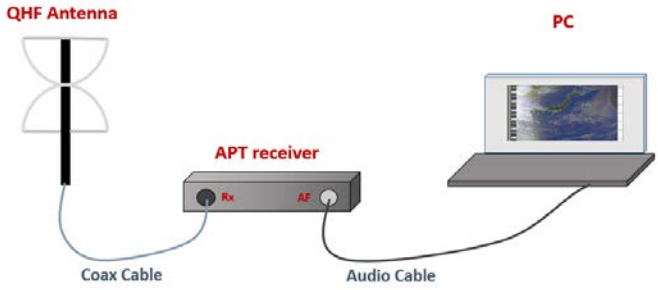

Figure 5.20a: Connection diagram of QFH antenna, APT receiver and PC

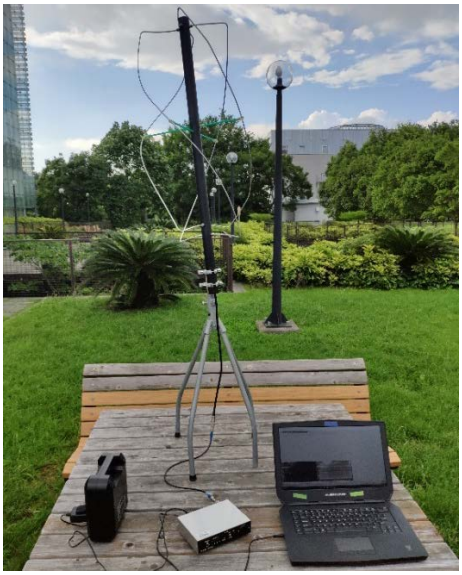

Figure 5.20b: Receiving APT signal with QFH antenna and designed receiver

For the NOAA series are polar orbiting satellites that make approximately 6 pass throughout a day, determination of AOS/LOS time is required to receive the APT signal on time. In addition, the elevation angle for four of those six passes are often too low to stably receiver the signal with sufficient strength. Thus only two of six passes are liable for receiving during a day, for a given satellite.

Determination of satellite passage and AOS/LOS time is done by calculation based on TLE (two-line element set) which is provided by NORAD/NASA for localized calculation/prediction of real time satellite orbit. Details involving TLE format will not be discussed in this thesis, but an example of NOAA 19's TLE is given in Figure 5.21

```
NOAA 19 [+]
1 33591U 09005A   20192.96899716  .00000046  00000-0  50106-4 0  9990
2 33591  99.1948 198.9282 0014201  14.3977 345.7595 14.12420496588452
```

Figure 5.21: Current TLE (two line element set) of NOAA-19

The calculation of based on TLE is done by an open software Gpredict which takes in the TLE from designated domain, calculate the corresponding orbit/passage using SGP4 model and plot the results on world map. The plot of current location of satellites on world map and their coverage is shown in Figure 5.22

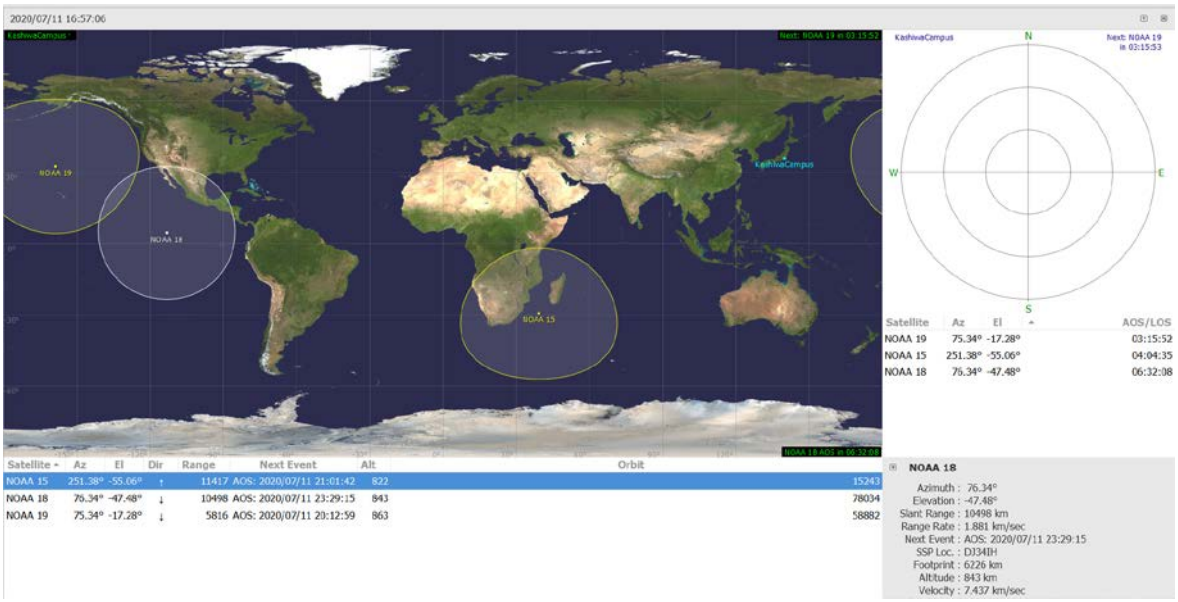

Figure 5.22: G-predict Interface showing current coverage of NOAA15~19 and their passage time on Kashiwa campus ground station

In practice, several relatively ideal pass with more than 60 degree of maximum elevation angle are received by APT receiver. For reference, the retrieved APT frame are shown in following images.

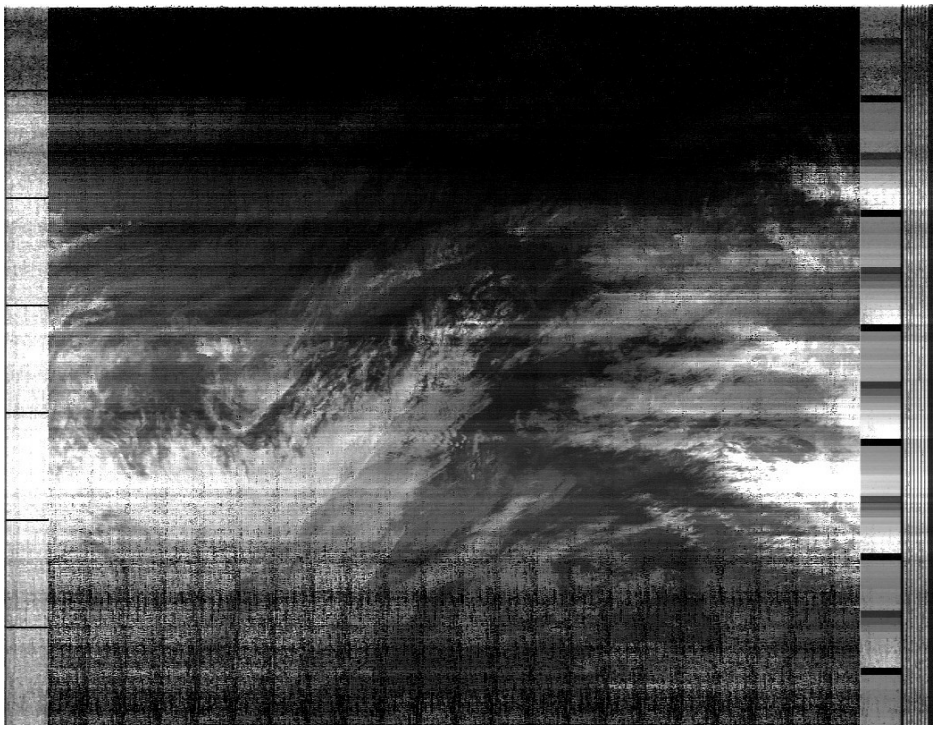

Figure 5.23: A NOAA-15 pass with 80 degree of maximum elevation angle captured by APT receiver (Channel A only)

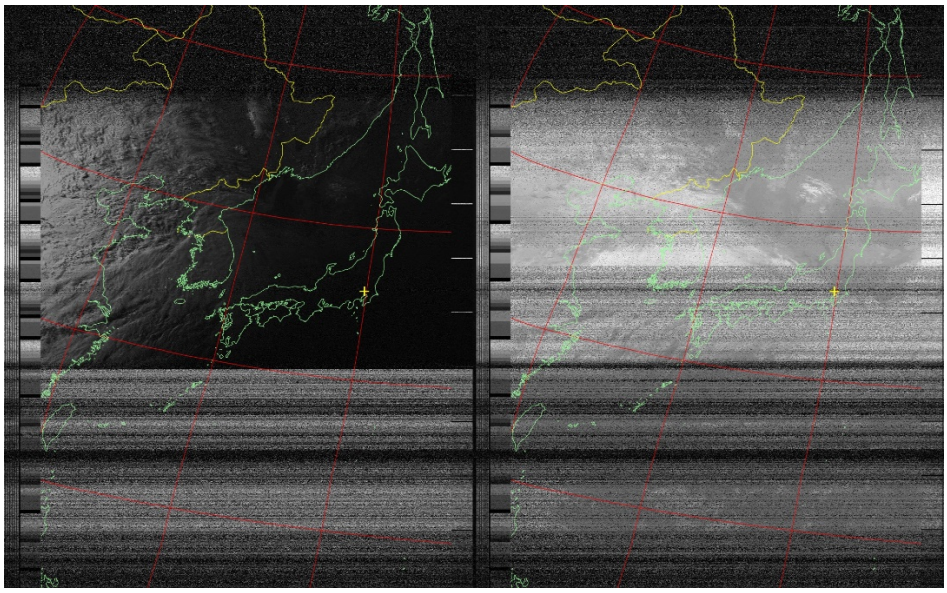

Figure 5.24: NOAA-15 evening pass with 40 degree maximum elevation. NIR channel (Channel 2) left side and IR channel (Channel 4) right side

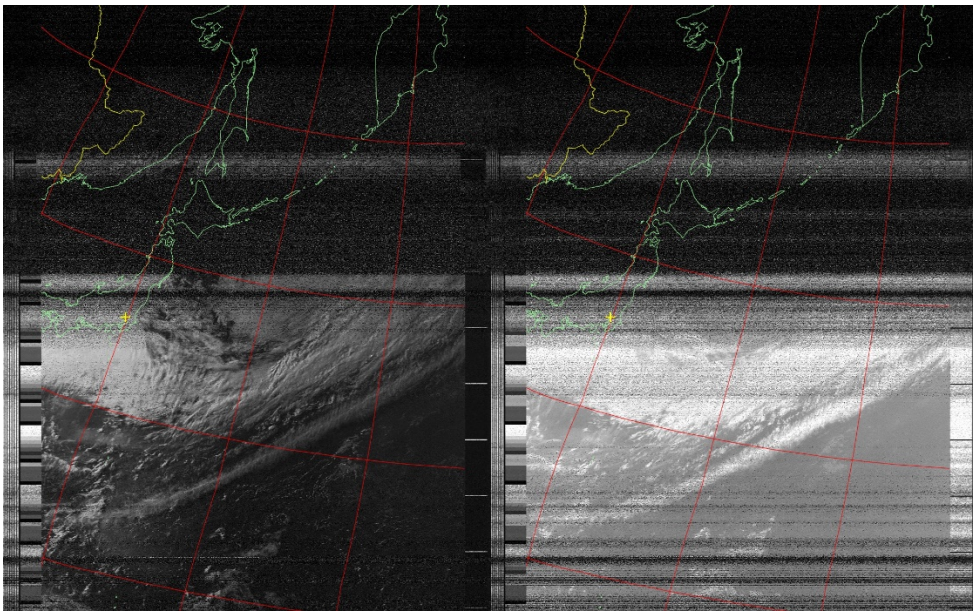

Figure 1.25: NOAA-19 afternoon pass with 40 degree maximum elevation. NIR channel (Channel 2) left side and IR channel (Channel 4) right side

Three images retrieved from APT signal are shown here. Figure 5.23 was retrieved from recorded PCM file thus only a single channel was shown. From its image it could be see that sync, back-scan (space/time marker) and telemetry blocks are rather clear. Depletion of image quality observed on upper and lower edge of image comes from the decreased receiving signal strength due to low elevation angle and obstacles.

Several seemingly periodic vertical noise line could also be observed in Figure 5.25. By counting the line with known period of a scan line we know that this noise appear with frequency around 100Hz. Note that this figure itself is scanned through 10 minutes indicating that this noise is basically static. Usually depletion of receiver sensitivity or sudden change in antenna SWR (by bird, gust or rain) will not result in such a periodic yet stably existing noise like this. From its frequency it is speculated to be caused by power supply problems but specific reasons are still unknown. However, by changing the power supply unit this problem dissipated thus the problem itself is solved.

Figure 5.24 shows a rather representative image retrieved while using a directional antenna, not omnidirectional antenna. Two-element Yagi antenna placed at the roof of Trans disciplinary Sciences Building which in short has a directivity toward the zenith. Thus the image quality (in this case related to the received signal strength and demodulation quality) is substantially lower in low-elevation side. Note that this image

is retrieved from real time decoding using freeware thus a map overlay is generated for reference.

Figure 5.25 is captured outside with omnidirectional QFH antenna when NOAA-19 had a decent high-elevation pass. Photo shown in Figure 5.25 is taken during the signal receiving process of this pass. Several horizontal noise on the bottom side are caused by trees southbound of antenna placement and possibly the author standing near it. The upper half of this retrieved image is completely covered with noises, which means that no (or extremely subtle) signal is picked by the antenna. It is a result of the completely blocked line of sight by buildings/trees. In this case the Trans disciplinary Sciences Building and the laboratory building blocked the signal.

Overall, though the images retrieved from APT receiver demodulated subcarriers suffered from quality depletion in some parts, the image clarity and general quality under proper receiving environment and signal strength could be compared to those received by proper SDRs. Thus as a conclusion the performance of APT receiver is basically acceptable.

6: Conclusion

My work involved in this thesis is dedicated to designing and evaluating a satellite broadcasted FM receiver. In particular, Automatic Picture Transfer (APT) broadcasted by the NOAA-POES satellites is selected due to its relatively simple modulation and frame retrieving process. Based on the signal characteristic of APT a VHF narrowband-FM (NFM) receiver is proposed, designed and evaluated on manufactured prototype.

Signal characteristics including the frequency, polarization, Intermediate frequency and APT's subcarrier, that I deemed critical for documenting APT signal were discussed. The frame structure of APT signal after demodulating AM subcarrier is also provided with detailed explanation. The satellite link budget calculation is carried out, in order to evaluate the liability of receiving the broadcast with given transmitter (specifying power, polarization and modulation) on a particular satellite. Based on the calculated result of transmitted power at the receiving end, and an assumed margin of 30dB, the required sensitivity of minus 120dBm is derived for sufficient receiving of APT signal.

Then, overall design diagram is given, and several major design features of the receiver were discussed. Principle of local oscillator using discrete crystal oscillator is discussed, along with the up-converting circuit designed to multiply X'tal frequency by 6 times. Design principle of active mixer using bipolar junction transistor, involving the non-linearity and signal multiplication caused frequency shift is explained in detail. A set of ceramic filters embedded to filter out desired frequency component out of noisy output from analog mixer, and the working principle of 10.7MHz ones are interpreted. The APT receiver design utilizes MC3361 FM IC for demodulating down-converted signal with quadrature demodulation techniques. Principle of quadrature demodulation, phase-shifting network, mixing and low-pass filtering are explained with inner structure of the IC chip.

As the performance evaluation part conducted on manufactured prototype, several evaluation on previously mentioned parts of APT receiver are conducted by me, using measurement devices including passive probes and a spectrum analyzer.

First, oscillation frequency of each crystal oscillator and corresponding LO outputs are measured on several selected sampling points to evaluate the "cleanness" of generated signals. As shown in the corresponding result the LO signal quality is acceptable after

2nd stage BPF. Stability of ordered crystal oscillators are also acceptable with relative dispersion lower than 3 KHz.
Measurement of temperature variance of each crystal oscillator were attempted but not discussed in this thesis for no liable heat source and measurement were established.

For the evaluation of superheterodyne mixer (downconverter) and connecting band-pass filter, unmodulated 137MHz signal (value shifted to match corresponding channel) generated by ADF4351 was used. The LO and RF carry-over (penetration) in the active mixer is higher than expected, partially due to the synthesized RF power significantly higher than actually receiving one from satellite, but the signal profile after the 1st ceramic filter was basically acceptable. The performance of 2nd LO, and 2nd mixer embedded inside MC3361, and 2nd 455KHz ceramic IF filter are also evaluated by sampling signals on the pins. The intensity of 455KHz component after filtration is significantly higher than its harmonics thus overall performance of front-end parts are deemed acceptable.

Receiving of the actual APT signal is conducted to verity the liability of this receiver prototype. Because of the intrinsic property of polar orbiting satellites, and the fact that no fixed omnidirectional RHCP antenna was available, I had to carry the antenna around to find sufficient places for each particular pass. As a result, only a handful of passes were able to be received with acceptable signal qualities. From those retrieved frame/image it is obvious that a certain pattern of noise is present in the output, however, the details of clouds and (for several ideal occasions) coastal line of Japan could clearly be seen. Appearance of noise in this stage of frame retrieval could be caused by variable things even including the SWR (Standing Wave Ratio) shift originating from wind and cross polarization loss, which means that deriving the reasons of certain “degradations” image quality are quite hard.

As a conclusion to the performance of APT receiver designed throughout my work in this thesis: Beside problems in active mixers’ LO&RF penetration and relatively noisy LO signal the overall performance of this designed receiver is overall acceptable.

Acknowledgement

Foremost, I would like to express my sincere gratitude to my advisor Prof. Ichiro Yoshikawa for continuous support on various field during my master class, for offering countless precious advice on multiple research topic of mine especially during the time of composing this thesis.

Besides my advisor, I would like to thank Lecturer Dr. Kazuo Yoshioka for providing innumerable help in my research and other aspect during my stay in Yoshikawa Lab.

Special and sincere thanks to Mr. Takano and Meiwa Systems.inc for providing priceless helps during the PCB board pattern design, manufacturing and product evaluations stage. Functional circuit and board design could not have been accomplished without their professional guidance and assistance.

My sincere thanks also goes to my labmates in Yoshikawa Lab, University of Tokyo: Mr. Seiya Nishimura, Mrs. Reina Hikida, Mr. Hang Yang, Mr. Fumiharu Suzuki for multiple stimulation discussions, help in multiple research topics, and for the fun during my 2 years' stay in the lab.

Last but not least, I would like to thank my family for priceless supports on almost all the faces during my career in postgraduate research.

Reference

[1] Kuznetsov, V., 2015. Yakov Alpert: Sputnik-1 and the first satellite ionospheric experiment. Advances in Space Research, Volume 55, Issue 22, 2833-2839.

[2] satnews. 2009. Lockheed Martin's NOAA-N Boosted Away. [ONLINE] Available at: http://www.satnews.com/story.php?number=2022104447. [Accessed 1 July 2020].

[3] Schwalb, A., 2020. THE TIROS-N/NOAA A-G SATELLITE SERIES. A Technical Memorandum NESS 95, Volume 95, 1-10.

[4] Gunter's Space Page, (2019), NOAA-1 [ONLINE]. Available at: https://space.skyrocket.de/doc_sdat/noaa_itos-a.htm [Accessed 11 July 2020].

[5] National Oceanic and Atmospheric Administration, 2008. NOAA-N Prime. 1st ed. Suitland, Marynald: National Environmental Satellite Data, and Information Service.

[6] NASA, 1964. NASA Facts B-2-64 TIROS. 1st ed. Washington D.C.: U.S. Government Printing Office.

[7] NOAA satellite and information service. 2020. Celebrating the World's First Meteorological Satellite: TIROS-1. [ONLINE] Available at: https://www.nesdis.noaa.gov/content/celebrating-world%E2%80%99s-first-meteorological-satellite-tiros-1. [Accessed 29 June 2020].

[8] Robel, J., 2014. NOAA KLM USER'S GUIDE with NOAA-N, N Prime, and MetOp SUPPLEMENTS. 1st ed. Asheville, NC: National Oceanic and Atmospheric Administration.

[9] National Oceanic and Atmospheric Administration, (2009), Photo of the AVHRR/3 instrument [ONLINE]. Available at: https://earth.esa.int/image/image_gallery?img_id=189537&t=1338557852270 [Accessed 30 June 2020].

[10]Asnaro Net. 2019. Amplitude modulation wave and AM theory. [ONLINE] Available at: https://e.as76.net/emv/am_mod.php. [Accessed 18 May 2020]

[11] Tetsu, K., 2019. 小型衛星群と柏キャンパス受信アンテナを用いた環境変動、防災に関する情報収集. 1st ed. [ebook] TIA かけはし, p.41. Available at: <https://www.tia-nano.jp/data/doc/1570410823_doc_13_1.pdf> [Accessed 22 May 2020].

[12] Shinichi Nakasuka, "Opening Remarks at the 4th Nano-satellite Symposium," Proceedings of the UN/Japan Workshop and The 4th Nanosatellite Symposium (NSS), Nagoya, Japan, Oct. 10-13, 2012, URL: http://www.nanosat.jp/4th/pdf/Day1-1_OpeningSession1_Nakasuka/Opeining_Prof.Nakasuka.pdf

[13] R.nave Hyperphysics, (2016), Linear Polarization/Circular polarization [ONLINE]. Available at: http://hyperphysics.phy-astr.gsu.edu/hbase/phyopt/polclas.html [Accessed 22 May 2020].

[14] IEEE Standard Letter Designations for Radar-Frequency Bands," in IEEE Std 521-1984 , vol., no., pp.1-8, 30 Nov. 1984, doi:

[15] Radiocommunication Sector ITU (2015). Nomenclature of the frequency and wavelengh bands used in telecommunications. Genève: International Telecommunication Union. p2.

[16] AA, N., 2009. User's Guide for Building and Operating Environmental Satellite Receiving Stations. 4th ed. Silver Spring, Maryland: National Oceanic and Atmospheric Administration/ National Environmental Satellite, Data, and Information Service.

[17] Cola, Tomaso & Marchese, Mario. (2010). Reliable Data Delivery over Deep Space Networks: Benefits of Long Erasure Codes over ARQ Strategies. IEEE Wireless Communications. 17. 57-65. 10.1109/MWC.2010.5450661.

[18] Associazione Radioamatori Italiani Sezione di Bra. 2011. QFH Antenna for VHF and UHF. [ONLINE] Available at: http://www.aribra.it/autocostruzione/qfh/index_e.php. [Accessed 23 May 2020].

[19] Hirobumi, S., 2020. World Fastest Communication from a 50kg Class Satellite. IEICE Communications Society – GLOBAL NEWSLETTER, Vol. 39, No. 2, 2.

[20] The Japan Amateur Radio League. 2010. Attenuation of Coaxial Cable. [ONLINE] Available at: https://www.jarl.org/Japanese/7_Technical/lib1/coax.htm. [Accessed 23 May 2020].

[21] GEORGE H. MILLMAN. (1958). Atmospheric Effects on VHF and UHF Propagation. PROCEEDINGS OF THE IRE. Volume: 46 (8), 1492 - 1501.

[22] National Oceanic and Atmospheric Administration (2004). NOAA-N. Suitland, Maryland: National Environmental Satellite, Data, and Information Service. 3.

[23] US Air Force, VAFB, (2008), NOAA-N Prime Satellite Lifting to Vertical [ONLINE]. Available at: https://www.nasa.gov/images/content/297424main_Going-Vertical-4_web_med.jpg [Accessed 15 July 2020].

[24] ACT Electronics, (2020), ACT 4.9152MHz HC49/U [ONLINE]. Available at: https://www.rapidonline.com/act-4-9152mhz-hc49-u-30-30-4-915200mhz-hc-49-u-crystal-90-0205 [Accessed 15 July 2020].

[25] Circuitcrush, (2020), Inside a crystal [ONLINE]. Available at: https://www.gadgetronicx.com/wp-content/uploads/2020/05/Crystal-Oscillators1.jpg [Accessed 15 July 2020].

[26] Circuits Today. 2011. Class C power amplifier. [ONLINE] Available at: http://www.circuitstoday.com/class-c-power-amplifier. [Accessed 31 May 2020].

[27] J.F, J., 1995. Student's Guide to Fourier Transforms: With Applications in Physics and Engineering. 1st ed. Cambridge, UK: Cambridge University Press.

[28] Stephen.A, M., 2003. Nonlinear Microwave and RF circuits. 2nd ed. 685 Canton Street Norwood, MA 02062: ARTECH HOUSE, INC.

[29] Murata Manufacturing.co.ltd (1998). Ceramic Filter (CERAFIL) for FM receivers SFE 10.7/SFT 10.7 Series. Tokyo: Murata Manufacturing.co.ltd. 3.

[30] Introduction to Naval Weapons Engineering. 1998. Frequency Modulation. [ONLINE] Available at: https://fas.org/man/dod-101/navy/docs/es310/FM.htm. [Accessed 5 June 2020].

[31] Ji. Wang. (2007). Energy Trapping of Thickness-Shear Vibration Modes of Elastic Plates With Functionally Graded Materials. ieee transactions on ultrasonics, ferroelectrics, and frequency control. 54 (3), 687.

[32]Bert Henderson., 2013. Microwave Mixer Technology and Applications. 1st ed. 685 Canton Street Norwood, MA 02062: ARTECH HOUSE, INC.

[33] Krauss, H., 1980. Solid State Radio Engineering. 1st ed. Blacksberg Verginia: John Wiley&Sons.

[34] R. G. Kinsman, "A history of crystal filters," Proceedings of the 1998 IEEE International Frequency Control Symposium (Cat. No.98CH36165), Pasadena, CA, USA, 1998, pp. 563-570, doi: 10.1109/FREQ.1998.717956.

[35] David Heeres. (2016). How to compensate oscilloscope probes. Available: https://www.testandmeasurementtips.com/compensate-oscilloscope-probes/. Last accessed 22 May 2020.

[36] Dr. T.S. Kelso. (2020). NORAD Two-Line Element Sets Current Data. Available: https://www.celestrak.com/NORAD/elements/. Last accessed 12th Jul 2020.

Appendix :

01: Low-pass filter for extracting certain frequency from a square wave

As it is stated in Chapter 5, the signal generator used for injecting unmodulated RF signal into the receiver uses ADF4351 PLL oscillator IC for generating higher frequency signals. The ADF 4351 could generate RF signal from 35MHz to 4400MHz, with its basic frequency range being 2200MHz to 4400MHz. While frequency lower than 2200MHz is generated by its N-divider. Namely, all of its signal with frequency between 35MHz to 2200MHz are square waves.

When trying to use it as a 137MHz signal generator, we do not want any other frequency components except 137MHz thus a band pass filter has to be connected after signal generator (between signal generator and receiver input).

The filter is made referencing a homebrew SSB band-pass filter utilizing IFT (IF transformers) from JG6GTT shown in following figure.

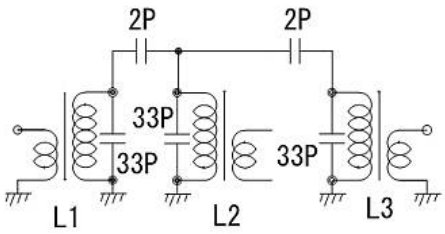

Figure A01.1: Design of BPF utilizing IFT for a HF SSB transmitter referenced for making 137MHz filter in this work (JG6GTT, 2005)

The original design was for 27MHz HF transmitter thus the tank capacitors were changed from 33p into 7p in order to match the 144MHz IFT for this design.

Completed homebrew BPF is shown in Figure A01.2. In fact several attempts of etching a circuit board were made to improve the grounding but none of them saw success, thus a single layer printed circuit board is used.

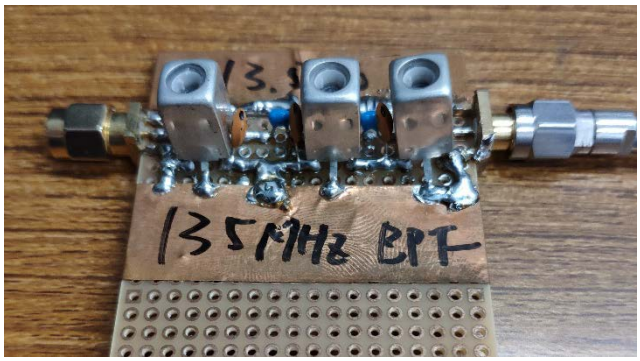

Figure A01.2: Image of Handmade 137MHz BPF

The outcome was in fact rather decent for a handmade filter on roughly grounded circuit board. The central frequency did stay around 135MHz which is close enough for its design application, and the attenuation characteristics on each side (higher and lower frequency sides) are acceptable. Its pass through characteristic does show several sub-peaks on UHF frequency but those peaks do not overlap with any harmonic of 137MHz.

Peak analysis result before and after connecting this BPF are already shown in Figure 5.12a and 5,12b, but A01.3 and A01.4 here shows the measured frequency domain plot of ADF4351 signals before and after connecting this BPF.

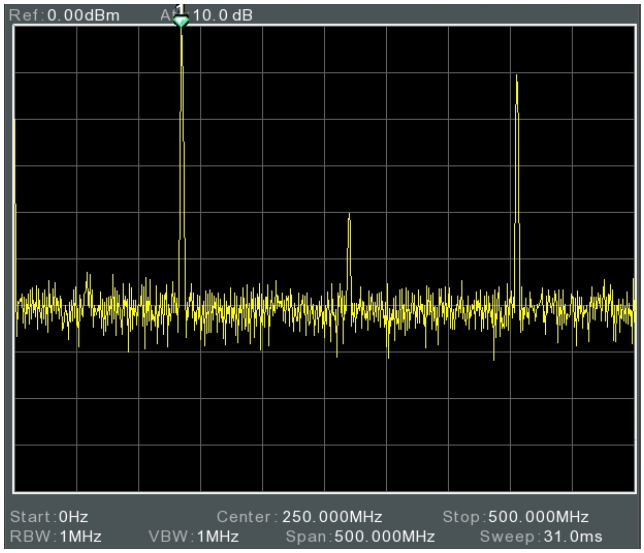

Figure A01.3: Frequency plot of RF signal generated from ADF4351 before connecting BPF

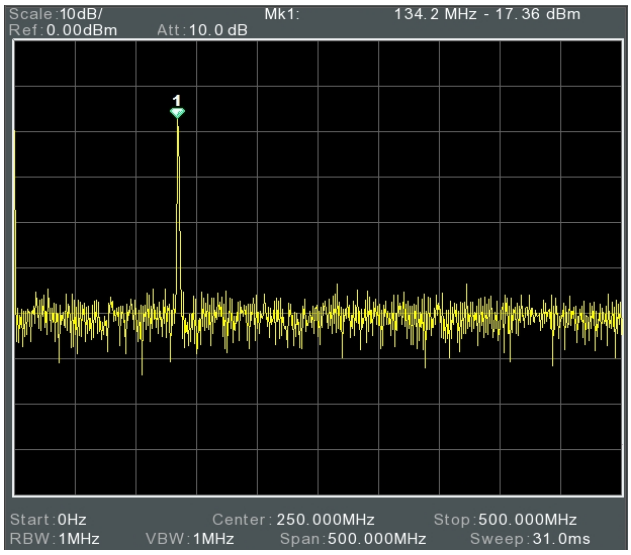

Figure A01.4: Frequency plot of RF signal generated by ADF4351 after connecting BPF

02: Description of several measurement instruments used in experiments.

Spectrum Analyzer

As it is already claimed in Chapter 5, frequency domain image are all obtained from a spectrum analyzer. Spectrum analyzer is basically a FFT (Fast Fourier Transformation) machine which performs Fourier transformation on sampled digital signals and plot them onto the screen.

Here, GSP-9330 digital spectrum analyzer from GW Instek.inc is used for measurement. Figure A02.1 shows the image of this spectrum analyzer used (GW Instek, 2019)

Figure A02.1 Image of GW Instek 9330 Digital Spectrum Analyzer

The result of measurement, coming out as frequency plots shown in Chapter 5 have horizontal axis as frequency and vertical axis as power in this case. The unit of vertical axis, dBm is the power measured in decibel milli-watt. The relationship of power between the unit dBm and W (watt) is given as:

$$P_w = \frac{10^{P_{dbm}/10}}{1000}(w)$$

From figures in Chapter 5, two different reference level could be observed on the top left corner of each figure: 0dbm reference level and -30dbm reference level. These levels were chosen to measure signal with different strengths. For example, the LO signal in Figure 5.9 is measured in 0dbm reference value for the signal strengths are enough that all of the peaks corresponding to frequency components could be clearly shown in the measured plot. On the contrary, signals with substantially lower strength such as those sampled out of a mixer is measured under -30dbm reference so that “dim” peaks could be seen if they’re necessary for explaining anything.

As it is claimed just before Figure 5.6, the amplitude scale is omitted in the measurement here, for the scale itself interferes with peaks under certain span level settings. Thus complementary scales under two different reference used are shown in following figures

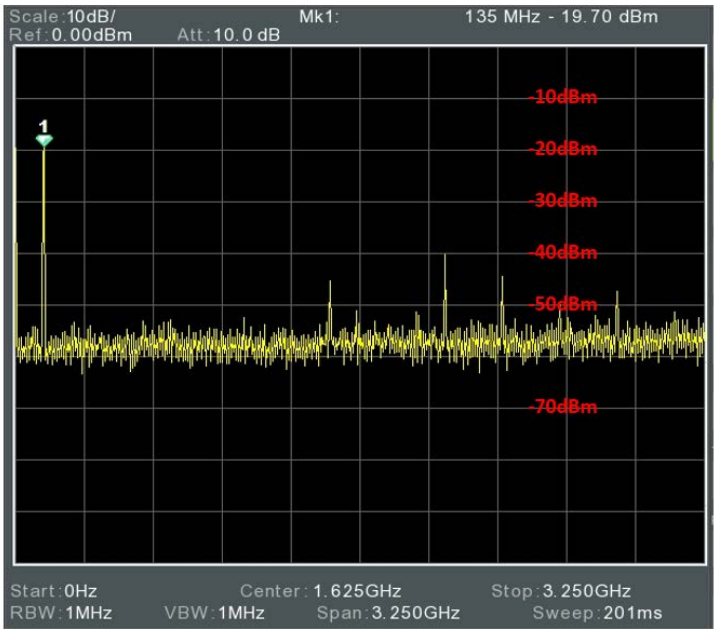

Figure A02.2: Signal strength scale on 0dBm reference level

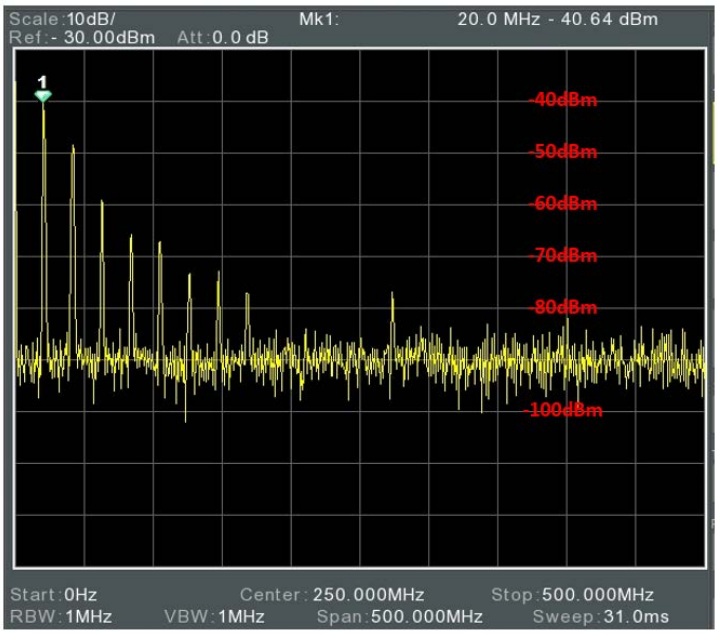

Figure A02.3: Signal strength scale on -30dBm reference level